A Comparison of Oil Weathering Model Equations and Application to Douglas Channel

A. van der Baaren, Y. Wu, and C. Hannah

Bedford Institute of Oceanography
P.O. Box 1006
Dartmouth, Nova Scotia
Canada B2Y 4A2

2018

Canadian Technical Report of
Hydrography and Ocean Sciences 316

Fisheries and Oceans Canada
Pêches et Océans Canada

Canada

Canadian Technical Report of Hydrography and Ocean Sciences

Technical reports contain scientific and technical information of a type that represents a contribution to existing knowledge but which is not normally found in the primary literature. The subject matter is generally related to programs and interests of the Oceans and Science sectors of Fisheries and Oceans Canada.

Technical reports may be cited as full publications. The correct citation appears above the abstract of each report. Each report is abstracted in the data base *Aquatic Sciences and Fisheries Abstracts.*

Technical reports are produced regionally but are numbered nationally. Requests for individual reports will be filled by the issuing establishment listed on the front cover and title page.

Regional and headquarters establishments of Ocean Science and Surveys ceased publication of their various report series as of December 1981. A complete listing of these publications and the last number issued under each title are published in the *Canadian Journal of Fisheries and Aquatic Sciences*, Volume 38: Index to Publications 1981. The current series began with Report Number 1 in January 1982.

Rapport technique canadien sur l'hydrographie et les sciences océaniques

Les rapports techniques contiennent des renseignements scientifiques et techniques qui constituent une contribution aux connaissances actuelles mais que l'on ne trouve pas normalement dans les revues scientifiques. Le sujet est généralement rattaché aux programmes et intérêts des secteurs des Océans et des Sciences de Pêches et Océans Canada.

Les rapports techniques peuvent être cités comme des publications à part entière. Le titre exact figure au-dessus du résumé de chaque rapport. Les rapports techniques sont résumés dans la base de données *Résumés des sciences aquatiques et halieutiques*.

Les rapports techniques sont produits à l'échelon régional, mais numérotés à l'échelon national. Les demandes de rapports seront satisfaites par l'établissement auteur dont le nom figure sur la couverture et la page de titre.

Les établissements de l'ancien secteur des Sciences et Levés océaniques dans les régions et à l'administration centrale ont cessé de publier leurs diverses séries de rapports en décembre 1981. Vous trouverez dans l'index des publications du volume 38 du *Journal canadien des sciences halieutiques et aquatiques*, la liste de ces publications ainsi que le dernier numéro paru dans chaque catégorie. La nouvelle série a commencé avec la publication du rapport numéro 1 en janvier 1982.

Canadian Technical Report of Hydrography and Ocean Sciences 316

2018

A COMPARISON OF OIL WEATHERING MODEL EQUATIONS AND APPLICATION TO DOUGLAS CHANNEL

by

A. van der Baaren[1], Y. Wu[1], and C. Hannah[2]

Ocean and Ecosystem Sciences Division
Maritimes Region
Fisheries and Oceans Canada

Bedford Institute of Oceanography
P.O. Box 1006
Dartmouth, Nova Scotia
Canada, B2Y 4A2

[1] **Bedford Institute of Oceanography, Fisheries and Oceans Canada, Dartmouth, NS**
[2] **Institute of Ocean Sciences, Fisheries and Oceans Canada, Sidney, BC**

Cat. No. Fs97-18/316E ISBN 978-0-660-07093-3 ISSN 1488-5417

Correct citation for this publication:

A. van der Baaren, Y. Wu, and C. Hannah. 2018. A Comparison of Oil Weathering Model Equations and Application to Douglas Channel. Can. Tech. Rep. Hydrogr. Ocean Sci. 316: xi + 113 p.

CONTENTS

TABLE OF FIGURES

ABSTRACT

A. van der Baaren, Y. Wu, and C. Hannah. 2018. A Comparison of Oil Weathering Model Equations and Application to Douglas Channel. Can. Tech. Rep. Hydrogr. Ocean Sci. 316: xi + 113 p.

The purpose of this work was to develop software tools to provide a basis for understanding commonly used oil weathering models. We evaluated computational algorithms that are used by three popular oil weathering models, and similar algorithms that are used by other researchers, to see how sensitive the algorithms/models were to variable environmental conditions and to gather information on whether the models typically produce similar results. We computed the weathering evolution, under constant and variable environmental conditions, of dispersion, release/spreading, evaporation, emulsification (water content), oil density, and oil viscosity for a hypothetical spill, and we compared the results for the different models' algorithms. We applied the algorithms to a second hypothetical spill. The second spill was of Cold Lake Bitumen in Douglas Channel. We found that none of the algorithms produced realistic results when using a time varying wind speed as input probably because they were developed under conditions of constant wind speeds. Finally, this work is not a definitive description of the expected evolution of the properties of diluted bitumen in Douglas Channel.

RÉSUMÉ

A. van der Baaren, Y. Wu, and C. Hannah. 2018. A Comparison of Oil Weathering Model Equations and Application to Douglas Channel. Can. Tech. Rep. Hydrogr. Ocean Sci. 316: xi + 113 p.

Cet ouvrage avait pour objet de mettre au point des outils logiciels pour offrir une base de compréhension des modèles d'altération des hydrocarbures couramment utilisés. Nous avons évalué les algorithmes de calcul utilisés par trois modèles populaires d'altération des hydrocarbures et des algorithmes semblables utilisés par d'autres chercheurs pour déterminer la sensibilité des algorithmes et des modèles aux conditions environnementales variables et pour recueillir de l'information afin de déterminer si les modèles produisent normalement des résultats semblables. Nous avons calculé l'évolution de l'altération, dans des conditions environnementales constantes et variables, de la dispersion, du rejet et de l'épandage, de l'évaporation, de l'émulsification (teneur en eau), de la densité et de la viscosité des hydrocarbures pour un déversement hypothétique, et avons comparé les résultats pour les algorithmes des différents modèles. Nous avons appliqué les algorithmes à un deuxième déversement hypothétique. Le deuxième déversement a été celui de Cold Lake Bitumen dans le chenal Douglas. Nous avons constaté qu'aucun des algorithmes ne produisait de résultats réalistes lorsqu'on utilisait en entrée une vitesse du vent variable dans le temps, sans doute parce qu'ils ont été élaborés dans des conditions de vitesse du vent constante. Enfin, ces travaux ne constituent pas une description définitive de l'évolution prévue des propriétés du bitume dilué dans le chenal Douglas.

PREFACE

Oil tanker and pipeline spills appear in the news almost daily. While most of these occurrences are quickly cleaned up, some, like the Exxon Valdez tanker spill in 1989 in Prince William Sound, are so catastrophic that they become headline news for months, and the impact of the spill on habitat is felt for decades. However, the devastating effects of an oil spill can be reduced if the oil's weathering properties are well-understood.

photo credit: US Coast Guard

On March 24, 1989, the Exxon Valdez spilled 11-38 million US gallons of crude oil into Prince William Sound. Mechanical cleanup began almost immediately with booms, but skimmers were not available for the first 24 hrs. In the end, only 10% of the total oil was actually cleaned. Immediate impacts included the death of at least 100000 seabirds. In 2010, research showed that 23000 US gallons of the crude remained in Alaskan sand and soil (sources: NOAA Office of Response and Restoration http://response.restoration.noaa.gov/; https://en.wikipedia.org/wiki/Exxon_Valdez_oil_spill)

What is Oil Weathering?

Oil weathering includes the evolution of oil emulsion viscosity, oil density, oil water content, evaporation, initial release and spreading, dispersion, dissolution, oxidation, and sediment-oil interactions. Knowing how these weathering properties evolve is essential for accurately estimating the time frame allowed for an effective clean-up response to an oil spill. Under-estimating the weathering time frame, for example, could needlessly waste recovery resources that could be deployed elsewhere, and over-estimating the time could make the spill recovery more difficult due to the oil's sinking or spreading throughout the spill region. Oil weathering models provide step-by-step values for each of these weathering properties for a variety of simulated oil spills.

Oil Weathering Models and Our Application to Hypothetical Spills

In 2005, R. J. Vos, from the Rijkwaterstaat in The Netherlands, reviewed 5 popular modules of oil weathering from oil spill models (Vos, 2005) developed by 3 different agencies: SIMPAR oil module (The Netherlands), MEMW-DREAM (SINTEF, Norway), OWM (SINTEF, Norway), ADIOS-2 (NOAA), and GNOME (NOAA). These models use empirically-derived algorithms to describe the weathering properties in time.

Part 1 of our report evaluates the algorithms used by three of the models that Vos reviewed (SIMPAR, ADIOS-2, and OWM) and similar algorithms used by other researchers. We computed the weathering evolution of dispersion, release/spreading, evaporation, emulsification (water content) for a hypothetical spill. We also computed oil density and oil viscosity. We graphically compare the results for the different models' algorithms and evaluate the algorithms under constant and variable environmental conditions. The computing platform that we used was Matlab®.

Part 2 of our report applies the algorithms to a hypothetical spill in Douglas Channel, on the west coast of British Columbia, Canada. Douglas Channel has been the current focus of much study because of proposed development of an oil pipeline terminus at Kitimat, British Columbia, at the head of the fjord of which Douglas Channel is a part. There is a proposed oil tanker route from Kitimat, through Douglas Channel, to the Pacific Ocean. Should a spill occur somewhere along this route, it is imperative that the response team know where the oil will travel and how much time it has to implement the clean-up before the oil sinks or washes ashore. Fjords are estuaries with unique oceanographic properties so that the response for the open ocean might not be appropriate for such a confined channel. We studied the seasonal differences of oil weathering under various environmental conditions for a hypothetical spill of Cold Lake Bitumen using the weathering algorithms from Part 1.

The weathering algorithms that the computer models used were developed in laboratories under strict constant mean environmental conditions. The problem is that the world outside the laboratory does not function under constant environmental conditions. Water conditions change with the tides and with the wind, and wind speeds and air temperatures can change dramatically within 24 hours. Furthermore, almost as many empirical methods exist as there are laboratories that study oil weathering. While different methods have advantages and disadvantages, determining the most appropriate algorithm or model depends on the type of spill, the type of oil, and, most of all, the environmental conditions at the time of the spill. In the end, the results from our hypothetical cases establishes a rough time scale for oil weathering to guide the development of spill countermeasures in Douglas Channel. Our experiments show how sensitive the three popular computer models are to variable environmental conditions so that an informed choice can be made when considering which weathering model or algorithm to employ for predicting the weathering of oil. This work is presented with the proviso that we are not providing a definitive description of the expected evolution of the properties of the diluted bitumen in Douglas Channel.

1 PART 1: EVALUATION OF OIL WEATHERING MODEL ALGORITHMS USING MATLAB®

1.1 INTRODUCTION

R. J. Vos's 2005 review of Oil Weathering models (Vos, 2005) described five weathering modules used in 5 different oil spill models that were developed by the Rijkswaterstaat, SINTEF of Norway, and NOAA. Although there are many oil weathering modules for oil spill models available globally (e.g. SRLOSM by S. L. Ross Environmental Research of Ottawa), Vos selected models based on two criteria:

1. Those that could be coupled to hydrodynamic programs.
2. Those that were readily available to the Rijkswaterstaat and that were user friendly.

Vos chose:

1. SIMPAR oil weathering module developed by the Rijkswaterstaat
2. MEMW-DREAM ("DREAM", for short) by SINTEF of Norway
3. GNOME by NOAA
4. ADIOS-2 by NOAA
5. OWM by SINTEF of Norway

Points to note about the 5 models:

- Only GNOME and ADIOS-2 are freely downloadable from NOAA's web site.
- SIMPAR has no oil database
- GNOME's weathering module is limited (Vos, 2005), but includes 2D transport of oil spills
- ADIOS-2 has no transport
- DREAM is coupled to both 2D and 3D transport models and the oil weathering module is the same as OWM (Vos, 2005)
- Vos's review is 10 years old and some of these models (e.g. ADIOS and GNOME) have been improved since the review

Vos tested and compared the oil weathering modules for 4 types of oil for 4 weathering processes only:

1. Initial release/spreading
2. Oil dispersion/entrainment
3. Evaporation of floating oil
4. Emulsification

None of the oil spill models are Open Source so we coded our own weathering programs using the weathering equations presented in Vos's review for the 3 weathering modules. In this part of the report, we describe coding the oil weathering equations for four weathering processes into the Matlab® programming language. We used the equations that Vos described in the model review as well as a few variations from other researchers.

To test the programs, we applied the equations using the oil types Ekofisk Exxon, TROLL, and Arabian Heavy as in Vos's review to graphically compare our results with those in the review. Furthermore, we applied the equations to a faux oil spill of Ekofisk Exxon in Douglas Channel using wind and ocean conditions typically found in Douglas Channel, a confined channel on the west coast of British Columbia to test the sensitivity of the algorithms to "real world" conditions.

Testing the validity of our programs required that we use, to the best of our knowledge and ability, the same inputs that Vos used so that we could compare the results from our programs to what Vos presented. When Vos neglected to mention the inputs that were used in the review, we made a best guess from researching the literature.

In this section of our report, we review the tests for each weathering process for:

1. constant inputs (e.g. density and viscosity are constant and not coupled to evaporation/emulsification/dispersion),
2. variable inputs and coupled oil density and oil viscosity (water properties and wind vary, and oil density and oil viscosity are coupled to evaporation/emulsification/dispersion),
3. variable "realistic" inputs from Douglas Channel using real wind and ocean data.

Vos noted that none of the models actually directly coupled evaporation with emulsification, so we did not test that coupling process.

Our ultimate goal was to develop a weathering program that computed three to five weathering processes (e.g. % evaporated, water uptake, and emulsification) using the algorithm that gives the most realistic results for each process.

The version of Matlab® that we used was r2012a.

1.1 SET-UP OF OUR TESTS

Vos set up test simulations using the following crude oils:

Oil types:

- Troll Crude Oil (Troll in OWM, but not in ADIOS-2)
- Ekofisk Exxon (Ekofisk Blend in OWM)
- Arabian Heavy (Exxon in ADIOS-2)

We used Troll and Ekofisk Exxon in most of our tests, but mostly we used Ekofisk Exxon. Figures in Part 1 of this report are results for Ekofisk Exxon unless otherwise noted.

Vos states that GNOME's oil weathering module was too limited to bother testing, and DREAM and OWM used essentially the same equations. This left only three models for us to examine so we tested equations from the following models only:

- SIMPAR
- ADIOS-2

- OWM

Constant parameters used by Vos:

- wind speed = 8.0 ms^{-1}
- water temperature = 15^{o}C
- ρ water = 1030 kgm^{-3} in SIMPAR and ADIOS-2 (~40 psu at 0 dbar, computed using an online water density calculator (http://www.csgnetwork.com/water_density_calculator.html, accessed 14 June 2015)
- ρ water = 1025 kgm^{-3} in OWM
- release = 1000 tonnes (metric); instantaneous = 10^6 kg
- volume = 1100 m^3
- oil temperature = 15^{o}C

Tables 4, 5, 6, and 7 in Vos (2005) contain input parameters for the different oils and models that Vos used.

Because ADIOS-2 is freely available, we downloaded the model to rerun the tests that Vos performed for that model. However, additional inputs were needed to run ADIOS-2 so we could not check the results against Vos's for correctness. We used the following additional inputs to run ADIOS-2:

- 0 gm^{-3} for sediment load
- 1 ms^{-1} current speed with 0^{o} current direction
- 0^{o} wind direction for the proposed 8 ms^{-1} wind speed
- wave height computed from the wind speed

The Oil Database

We used oil parameters from an oil database from the freely available oil spill model, Medslik II (www.medslikii.bo.ingv.it, accessed 16 November 2015; De Dominicis et al., 2013a, b). We imported the Medslik II database into MS Excel, and we added entries for Troll, Ekofisk Exxon, and Arabian Heavy using Vos's values for oil density, oil viscosity, etc. The MS Excel file is called oilbase.xlsx[3]. The Matlab® function that we wrote to read the database is *read_oil_data_xlsx.m*.

1.2 INITIAL RELEASE/SPREADING

Matlab® function: *release.m*

The initial release (or spreading) in the models is represented by a length scale. Two length scales were defined in the models. ADIOS-2 and SIMPAR assume that the spill is

[3] The original "Medslik II + Vos additions" file is oilbase_original.xlsx in which we discovered a few errors that we had to correct. The corrected file is oilbase.xlsx and this is the file that is read by the Matlab® routines.

circular so their release modules computed radii, and OWM/DREAM computes a simple length scale.

ADIOS-2 and SIMPAR assume an instantaneous release. They use the same formula to compute the initial release (or spreading) of the oil slick. The formula returns a radius which presupposes that the slick is circular. The radius is used to compute the evaporation for these two models. Equation 3.1 in Vos estimates the spreading in SIMPAR and ADIOS-2:

$$R = \frac{k_2^2}{k_1}\left(\frac{V_{oil}^5 g(\rho_w - \rho_{oil})/\rho_w}{v_w^2}\right)^{1/12}$$

- g = 9.80665 ms^{-2}
- ρ_w = density of water = 1030 kgm^{-3}
- ρ_{oil} = density of the oil with units, kgm^{-3}
- v_w = kinematic viscosity of water in m^2s^{-1} (computed using the Matlab® seawater function, *sw_Kviscosity.m* (CSIRO, accessed 18 November 2015), with constant water temperature = 15ºC and constant salinity = 40)
- k_1 = 1.15
- k_2= 1.45
- *Voil* = volume of the oil spill = 1100 m^3

OWM, on the other hand, computes a length scale that is the equilibrium length of the oil layer. This is the formula for the length scale found in the SINTEF technical manual for OWM/DREAM; Equation 4 in their manual (SINTEF, 2005, accessed August 10, 2015). We used this length scale for the evaporation module from the OWM model.

$$X = \left[\frac{3}{2}\frac{V_{oil}^2 \rho_{oil} g'}{B^2}\right]^{\frac{2}{5}} (\rho_w \mu_w)^{\frac{-1}{5}} U_{H2O}^{\frac{-3}{5}}$$

OWM/DREAM calls *U* the spreading velocity that we assumed to be the water current, U_{H2O}. *B* is the channel width.

$$g' = g(\rho_w - \rho_{oil})/\rho_w \quad \text{and} \quad \mu_w = v_w \rho_w$$

DREAM/OWM also allows for a slow release of the oil over time so that it can vary with time, however we did not program this variation because SIMPAR and ADIOS-2, according to Vos, only allow for instantaneous releases.

Which length scale to use depends on the algorithm being used in the Evaporation module.

Vos did not present any results for the release of crude oil for the weathering models so we could not compare any results.

1.3 NATURAL DISPERSION OF OIL/ENTRAINMENT OF OIL DROPLETS

Matlab® function: *dispersion.m*

The rate at which oil droplets are taken up by the surrounding sea (dispersed) depends on the distribution of the droplets and the sea state. Large droplets tend to rejoin the oil slick and smaller droplets tend to mix with the water column.

Vos notes that oil dispersion is defined slightly differently between SIMPAR and ADIOS-2 and completely differently in DREAM and OWM. While both base their algorithms on Delvigne and Sweeney ("D&S", 1988), the difference lies in how oil droplet size is defined and used.

The original D&S (1988) equation:

$$Q(d_0) = C_0 D_{ba}^{0.57} d_o^{0.7} \Delta d$$ Equation 8 in Delvigne and Sweeney (1988)

where

- $Q(d_0)$ is the entrained mass of oil droplets
- d_o is the oil droplet diameter in m
- Δd is an interval that surrounds d_0 per unit surface area per breaking event
- D_{ba} is the dissipative breaking wave energy per unit surface area
- C_0 is a proportionality constant

Vos states that integration over droplet size is used in SIMPAR and ADIOS-2. The integration of Vos's Equation 3.4 yields Equation 3.10:

$$\frac{\partial Q}{\partial d}\Big)_{d_0} = C_0 D_{ba}^{0.57} F_{wc} S_{cov} d_o^{0.7}$$ Equation 3.4 in Vos (2005); when the equation is integrated over all droplet classes from minimal to maximal droplet diameter, Equation 3.4 gives Equation 3.10

$$Q = \frac{d_{max}^{1.7}}{1.7} \times C_0 D_{ba}^{0.57} F_{wc} S_{cov}$$ Equation 3.10 in Vos

In these formulae, S_{cov} is the sea coverage factor of the oil spill. Vos defines it as 1.0 for a closed patch. F_{wc} is the fraction of the sea surface covered by breaking waves (s^{-1}).

Equation 3.10 in Vos gives the total entrainment rate Q of the oil per square meter. Equation 3.10 is similar to the original D&S (1988) equation, but D&S (D&S, 1988) presented what they described as "a more practical version" for describing oil on the sea surface using the entire droplet size distribution. This is the algorithm used in OWM/DREAM. This is Equation 16 in the SINTEF manual (SINTEF, 2005). Delvigne used this practical variation in a 1993 publication (Delvigne, 1993):

$$Q(d) = C_0 D^{0.57} d_o^{0.7} \Delta d S_{cov} F_{wc}$$ Equations 11 and 2 in D&S (1988) and Delvigne (1993), respectively

In that algorithm, the number of oil droplets has the mean, d_o, in the range defined by $d_o \pm 0.5\Delta d$ (D&S, 1988). The droplet size needs to be expressed in metres for the definition and the D&S formula to be valid. C_0 is a proportionality constant.

ADIOS-2 and SIMPAR integrate over the droplet size to compute the dispersion. These two models use a minimum droplet diameter of 0 µm and a maximum droplet diameter of 70 µm according to Vos. However, Payne *et al*. (1987) cited two sources for minimum droplet size values of 50 µm (Payne *et al*. citing Milgram, 1978) and 1 µm (Payne *et al*. citing Shaw, 1977). We noted that a report on the weathering properties of diluted bitumen described oil droplets of diluted bitumen having diameters between 30 µm and 70 µm (Government of Canada, 2013). This fact was relevant to our application tests in Douglas Channel where we felt that it was reasonable, in that case, to have a maximum droplet diameter as 70 µm in the dispersion algorithm.

Vos stated that OWM/DREAM uses the following empirical relation (Vos's Equation 3.9) to determine the droplet diameter:

$$d_o = \frac{Cv^{0.34}}{\sqrt{e}} \qquad \text{Equation 3.9 in Vos}$$

where

- C is a parameter that varies between 500 and 3400
- v is the oil viscosity
- e is the rate of energy dissipation = 1000 $Jm^{-3}s$

Vos described another relation (Equation 3.8) from which d_o can be determined although we do not use it:

$$N_d = N_o d_o^{-2.3} \qquad \text{Equation 3.8 in Vos}$$

N_o is a normalization factor that we set to 1 and N_d is the number of droplets per diameter, d_o. We programmed this equation as an option for finding d_o for SIMPAR and ADIOS-2. We did not use this option because we defined d_{max}=70 µm for those models and did not compute any droplet sizes for either of the two models.

In either algorithm for computing entrainment rates, C_o is an oil dispersion parameter related to oil viscosity. The relationship between C_o and viscosity for ADIOS-2 and SIMPAR is given in Vos's Equation 3.11. Viscosity needed to be in cSt (centistoke; 1 cSt = 1 x 10^{-6} m^2s^{-1}). In our Matlab® code, viscosity was in m^2s^{-1} so we converted it within the function. The relation for C_0 in DREAM was given in Vos's Equation 3.12 and defined in Equation 17 in the SINTEF manual.

1.4 PROGRAMMING AND TESTING THE DISPERSION

We programmed Vos's Equation 3.10 (essentially the D&S 1988 Equation 11) to compute the entrainment rate for all SIMPAR/ADIOS-2:

```
Matlab®: Q = ((dmax^1.7)/1.7)*C0*Dba^0.57)*Scov*Fwc;          % Equation 3.10
```

and

Equation 16 in the SINTEF manual for DREAM/OWM:

```
Matlab®: Q = C0*(Dba^0.57)*Scov*Fwc*dmean^(0.7)*deltad;
```

Dba, the dissipative wave energy, is computed using Equation 3.7 in Vos:

- $D_{ba} = 0.0034\rho_w\, g\, \left(\frac{H_0}{\sqrt{2}}\right)^2$ Equation 3.7 in Vos
- $H_0 = \frac{0.243\, U_w^2}{g}$ also included in Equation 3.7 in Vos

with

- ρ_w as the density of water in kgm^{-3}
- g = 9.80665 ms^{-2}
- U_w is the wind speed in ms^{-1} (@10 m)

The fraction of the sea surface hit by breaking waves was computed according to Holthuijsen and Herbers (1986) for SIMPAR and ADIOS-2, as cited by Vos in Equation 3.5:

$$F_{wc} = \frac{0.032\, \max(U_w - 5.0; 0.0)}{T_w} \qquad \text{Equation 3.5 in Vos}$$

where

- F_{wc} is per unit time
- T_w is the wave period

In DREAM/OWM, however, F_{wc}, is computed with Equation 3.6, which is from Monahan and O'Muircheartaigh (1980) and cited by Vos:

$$F_{wc} = 3 \times 10^{-6}\, U_w^{3.5} \qquad \text{Equation 3.6 in Vos}$$

In the original publication by Monahan and O'Muircheartaigh, the relation is $F_{wc} = 2.95 \times 10^{-6}\, U_w^{3.52}$. We used Vos's equation. U_w is the wind speed measured at 10 m above the sea surface.

We differentiated the models in the Matlab® code by how F_{wc} was calculated. The wind speed, U_w, is constant. It is easy to see that when the wind speed varies, so too will the energy of the wave breaking in the both algorithms.

The models also compute the proportionality constant, C_0, differently. DREAM/OWM used $C_0 = 4450\nu^{-0.4}$ (Equation 3.12 in Vos). For SIMPAR, Vos cited Delvigne and Hulsen (1994) as the source for C_0 values:

For $\nu < 125$; $C_0 = 1827\nu^{-0.04658}$ and if $\nu > 125$; $C_0 = 1827\nu^{-1.1951}$ where ν is in cSt

We used the SIMPAR algorithm for both SIMPAR and ADIOS-2. OWM and DREAM use essentially the same algorithms. We computed the proportionality constant, C_o, and compared the result from the *dispersion.m* function (**Figure 1**) with what Vos's Figure 3.1. Vos used viscosities directly in cSt within the computation and included 125 cSt, but we used a vector of viscosities in m^{2}s^{-1} for 1e-6 to 1 and converted the input viscosities to cSt within *dispersion.m*. Vos does not say what C_0 should be if ν= 125 cSt.

The following figure is our figure of C_0 vs viscosity:

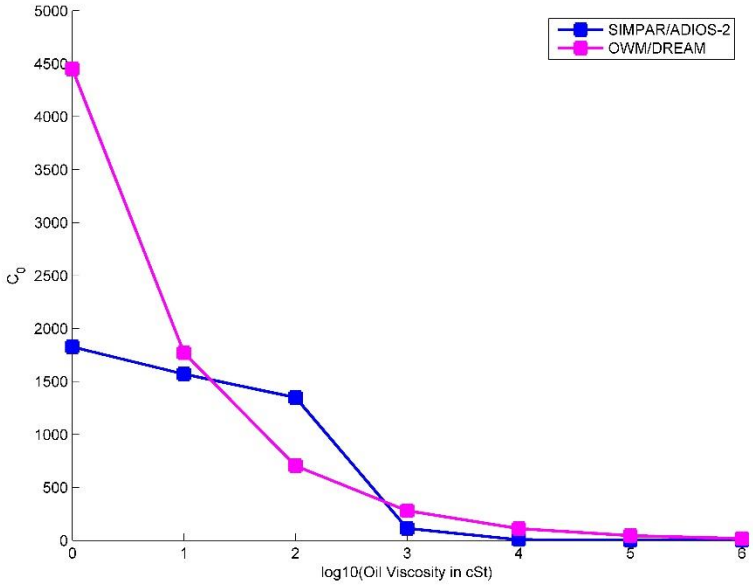

Figure 1 Our version of Vos's Figure 3.1, viscosity vs. the constant of proportionality that we used to compute oil entrainment rates.

SIMPAR and ADIOS-2 defined the droplet diameters as d_{min}= 0 and d_{max}=70 µm (70×10^{-6}m). Lehr (2001) stated that the maximum droplet size that would not be expected to refloat is 50-70 µm so defining d_{max}=70 µm for the SIMPAR and ADIOS-2 algorithms seems reasonable.

For the DREAM/OWM algorithm, we computed the mean droplet diameter using Vos's Equation 3.9 where we arbitrarily defined C=1000, and we assigned the computed maximum of d_o to be d_{max}. We defined the half-range of the droplet size, Δd in SINTEF Equation 16, as 50 µm. **Figure 2** shows the maximum droplet sizes, d_{max}, as a function of different viscosities.

One thing that was not clear from Vos's text for the DREAM/OWM algorithm was if Equation 3.9 required the viscosity to be in cSt or m^2s^{-1}. We converted viscosity to cSt using the assumption that D&S worked in cSt for their 1988 paper.

Droplet diameter needed to be converted to metres from microns. We noted that this somewhat arbitrary method for determining the droplet diameter would vary with the oil viscosity, and not in a good way. If viscosity increased, then the size would increase. In addition, Vos noted that having a fixed energy dissipation rate, *e*, is not correct for non-turbulent environments so Vos's Equation 3.8 (for droplet size distributions), might not have been correctly applied to reveal Equation 3.9.

When it came time to test the dispersion equation itself (computing the entrainment rate of the oil droplets, *Q*), we called *dispersion.m* with constant wind and a constant oil viscosity. For now, we defined the oil viscosity as 1×10^{-6} regardless of the type of oil. We

defined the density of sea water as 1030 kgm^{-3} and 1025 kgm^{-3}, for SIMPAR/ADIOS-2 and DREAM/OWM, respectively. These were the same values that Vos used. The wave period was defined as 1, but Vos did not specify a value for T_w in the review. We also arbitrarily defined S_{cov} = 1, so that the spill was an enclosed patch. Vos's review did not say what S_{cov} was used.

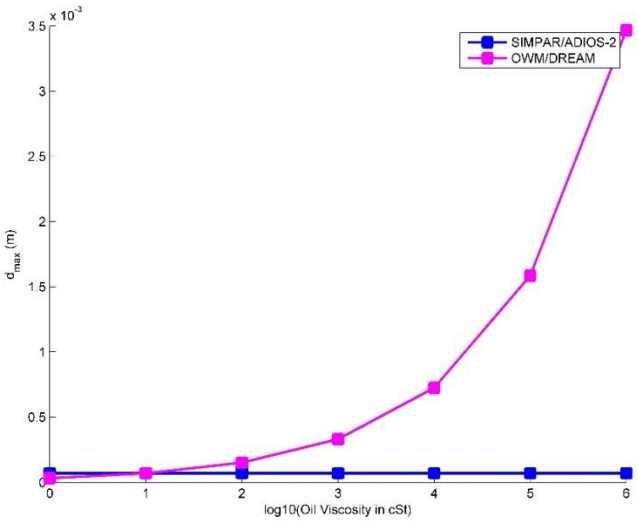

Figure 2 d_{max} as a function of different viscosities

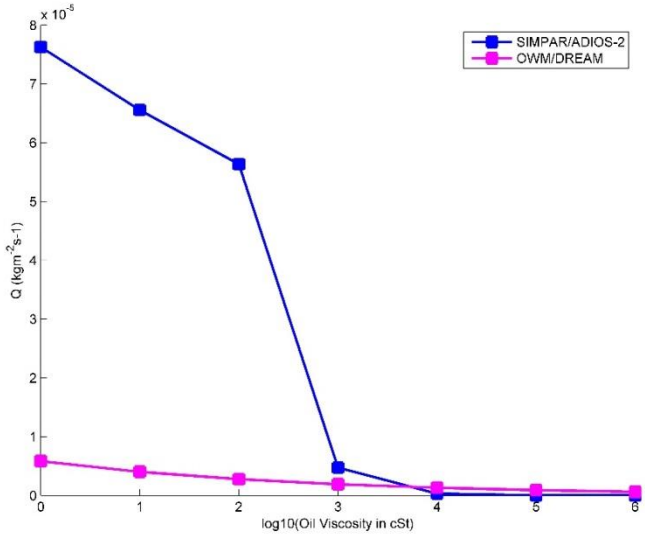

Figure 3 Entrainment rate, Q, as a function of different viscosities

Figure 3 shows the different entrainment rates computed using different viscosities for SIMPAR/ADIOS-2 and DREAM/OWM. Vos does not plot viscosity vs entrainment, but D&S (1988) do. From their Figure 13 (D&S, 1988), entrainment decreases with increasing viscosity as would be expected (larger droplets refloat according to D&S).

1.5 EVAPORATION

Matlab® function: *evaporation.m*

Evaporation theory for oil weathering has been reviewed several times by Fingas (1995, 2011, and 2013). Vos described three implementations of oil evaporation theory:

1. first order decay with a fixed constant
2. using a single fraction model of oil composition following MacKay and Matsugu (1983) or Stiver and MacKay's (1984) semi-empirical distillation theory
3. using a multi-fraction (a.k.a. as a pseudo-component) model of oil composition based on Reijnhardt and Rose (1982) and Jones (1997)

Vos presented the single and multi-fraction (pseudo-component) models for SIMPAR (both) and OWM/DREAM (multi-fraction model only). This produced the SIMPAR and OWM/DREAM results depicted in Vos's Figures 3.2 and 3.3. The essential difference between the SIMPAR and OWM/DREAM multi-component algorithms is the definition of the mass transfer coefficient. In SIMPAR, the mass transfer coefficient follows MacKay and Matsugu (1973). However, OWM/DREAM uses a definition with a drag coefficient. The SINTEF manual also states specifically that the evaporation algorithm used in OWM/DREAM is based on a distillation curve presented by Reijnhart and Rose. For ADIOS-1, Vos presented evaporation computed by the semi-distillation theory based on Stiver and MacKay (1984; hereafter called "S&M"). However, the more recent ADIOS-2 model uses the pseudo-component model based on Jones (1997) (Lehr, 2002).

Fingas (2011, 2013) stated that Bobra (1992) found that the S&M algorithm could reliably predict evaporation for the first 8 hours, but that it overestimated the evaporative loss after 24 hours. In his reviews of oil evaporation, Fingas (2011, 2013) presented evaporation equations that were derived from distillation data.

The evaporation module that we developed was difficult to test because Vos did not provide all the test values that were needed to replicate the results in the review paper, nor did we have the evaporation algorithms for all the models. We first tried to recreate Vos's Figures 3.2 and 3.3, but without certain input values, we could only guess what they should be. We tested the SIMPAR, ADIOS-2, and OWM evaporation equations described in Vos for Ekofisk Exxon and Troll crudes, but we only present results for Ekofisk Exxon.

To compute evaporation, we first ran *release.m* to obtain:

1. the radius of an assumed round spill used by SIMPAR and ADIOS-2
2. the equilibrium length used by OWM's

We used the output from *release.m* as input for our evaporation function.

We tried computing evaporation with the algorithms provided in Vos's review, but we eventually computed evaporation using algorithms that we found in the literature:

1. We used a version of the single fraction model that we found in Fingas (1995; 2011; and 2013).

2. We used versions of S&M given in Fingas (2013) for the ADIOS-2 inputs, and in Short (2013) for the SIMPAR and OWM inputs.
3. For all the models, we used a version of S&M found in Buchanan and Hurford (1988)'
4. For all the models, we used the empirical equation found in Fingas (2013) in Table 2 for Ekofisk (as representative of Ekofisk Exxon in our test)

We compared the original model algorithms and the ones from outside literature using plots of the percent evaporated of Ekofisk Exxon over 24 hours presented in **Figure 4** and **Figure 5**.

These are the inputs that we used, some of which are what Vos used:

- `T_oil = 15; % oil temperature in deg C`
- `Tair = 15; % air temperature in deg C`
- `B = 1000; % channel width in metres`
- `U_H2O = 0.01; % current speed in m/s`
- `Uw = 8; % constant wind speed in m/s`
- `V_oil = 1100; % initial volume of the spill m^3`
- `Area = V_oil/thickness; % area of oil slick in m*m`
- `thickness = 0.001; % 1 mm release thickness`
- `hours = 0:24; % time in hours for which to track the spill`

```
visc_H2O = SW_Kviscosity(15,'C',40,'ppt'); % compute the water velocity in m*m/s
using water temperature = 15 deg C and salinity = 40 ppt
```

The function, *SW_Kviscosity.m* (CSIRO, accessed 18 November 2015), computes the sea water kinematic viscosity. It is from the Matlab® sea water toolbox package written at CSIRO and is readily downloadable (www.cmar.csiro.au/datacentre/ext_docs/seawater.htm).

Oil viscosities were 6.9 and 27.0 cSt, respectively, for Ekofisk Exxon and Troll at 15°C. Evaporation requires the computation of the oil spill length scale so we had to call our initial release module, *release.m*. The initial release length scale computation uses the density of the oil at release. The code reads the Ekofisk-Exxon and Troll values from the oil database.

The next few sections briefly describe the algorithms that compute evaporation in the three models and those that other researchers used, and the algorithms that we eventually used with the length scales computed by the release algorithms associated with each model. Each model also had different equations for various parameters (vapour pressure, mass transfer coefficient, and drag coefficient) which we used when we could.

1.5.1 MacKay and Matsugu (1973)

Vos presents Equations 3.14 and 3.15 for the mass rate of evaporation derived by MacKay and Matsugu for a single fraction first order decay.

$$\frac{dm_s}{dt} = -K\frac{P_{vp}A}{RT_{oil}}f_{evap}M_w \qquad \text{Equation 3.14 in Vos}$$

A is the surface area of the oil slick (*A* = spill volume/slick thickness) and M_w is the molecular weight of the oil in g mol^{-1}. *R* is the ideal gas constant = 8.206×10^{-5} atm m^3 mol^{-1}K (from Vos) or 8.31451 Jmol^{-1}K (http:chemistry.about.com/od/chemistryglossary/a/gasconstantdef.htm, accessed 18 November 2015). f_{evap} is the fraction of oil that's been evaporated. m_s is the mass of the slick in grams.

P_{vp}, the vapour pressure

Values for the vapour pressure, P_{vp}, can be looked up in the literature. Many values are in the oil database that we used, in which P_{vp} is given in units of *bars* so we converted the value to *Pa* when we extract P_{vp}. P_{vp} can also be computed by knowing the carbon number, *N*, of the oil compound: $Pvp = e^{(10.94-1.06N)}$ (Equation 11 in Fingas, 2011). Vos used P_{vp} = *2.0e-4* atm in the computation of evaporation using the single fraction algorithm when testing Ekofisk Exxon for SIMPAR. We used Vos's P_{vp} for the SIMPAR test using Ekofisk Exxon.

For ADIOS-2, Vos states that P_{vp} is probably computed according to Stiver and MacKay (1984), but we used the database value for ADIOS-2 and OWM: 0.524. However, later we abandoned the algorithms that used P_{vp}.

T_{oil}, the oil temperature

In Vos's equation, T_{oil} was actually presented as *T* and Vos was not clear whether this was the temperature of the oil or air temperature. The fraction, P_{vp}/RT_{oil} is derived from Henry's constant which is the ratio of the equilibrium concentration of a substance in its vapour state to its liquid state. Because we are talking about oil here, we assumed that *T* from the definition of Henry's constant would be the temperature of the oil. In the absence of an oil temperature value, Lehr (2001) suggested using sea surface temperature.

1.5.1.1 K, the mass transfer coefficient

K is the mass transfer coefficient. Its computation, as defined by MacKay and Matsugu, was presented by Vos in Equation 3.15, and is how *K* is computed in SIMPAR.

$$K = 0.029(3600U_w)^{0.78}D^{-0.11}S_c^{0.067}\sqrt{\frac{M_w+29}{M_w}} \qquad \text{Equation 3.15 in Vos and Equation 60 in Fingas (1995)}$$

D is the diameter of the slick in metres, and we used the radius length scale computed by our Matlab® function, *release.m*. S_c is the Schmidt number, and it is equal to 2.7. Wind speeds were in metres per hours, and we converted the wind speeds to metres per seconds, as in Vos.

Determining the molecular weight of hydrocarbons is not easy and data are not readily available (Schneider, 1998). The value can be found in tables produced by the American Petroleum Institute or by searching through the literature. For our test of Ekofisk-Exxon

and Troll, Vos provided values for M_w. For Ekofisk-Exxon, we used 139 g mol^{-1} and for Troll we used 114 g mol^{-1}. We converted these values to kg mol^{-1} by dividing by 1000.

However, because molecular weight is not always available for all oil types, we used the definition for the mass transfer coefficient found in Fingas (1995), also based on MacKay and Matsugu, rather than the SIMPAR or OWM algorithms:

$$K = 0.029(U_w)^{0.78} D^{-0.11} S_c^{0.067} \qquad \text{Equation 4 in Fingas (1995)}$$

Equation 4 in Fingas (1995) is essentially the same as Vos's equation based on MacKay and Matsugu except Equation 4 ignores the molecular weight. Wind speeds are in ms^{-1} in the Fingas algorithm.

The SINTEF manual defined K as varying with time:

$$K(t) = C_d U_w(t) \qquad \text{Equation 13 in SINTEF (2005)}$$

The SINTEF manual says that its definition of K is according to Amorocho and DeVries (1980). The wind over oil drag coefficient, C_d, is $C_d = \left(\frac{U_w^*}{U_w\,(t)}\right)^2$ (Equation 14 in SINTEF, 2005). Equation 15 in the SINTEF manual defines the special parameter, U_w^*.

$$U_w^* = \begin{cases} CU_w(t) \quad for \quad U_w(t) < u_1 \\ Cu_1 + (Du_2 - Cu_1)\dfrac{U_w(t) - u_1}{u_2 - u_1} \quad for\ u_1 \le U_w(t) \le u_2 \\ DU(t) \quad for \quad U_w(t) > u_2 \end{cases}$$

- C = 0.0323
- D = 0.0474
- u_1 = 7 ms^{-1}
- u_2 = 20 ms^{-1}

Zanier et al. (2014) defined the drag coefficient at 10 m above mean sea level as $C_{10} = (0.8 + 0.065U_w) \times 10^{-3}$. Although we did not use the SINTEF formula for evaporation (SINTEF Equation 12), we did use their definition of K and C_d in the evaporation module for OWM model.

Fingas (2013) described another formula for determining K (Equation 31) that he attributed to Hamoda et al. (1989). This is an empirical formula that describes how API, water temperature, and water salinity influence K.

$$K = 1.68 \times 10^{-5} API^{1.253} T^{1.80} S^{0.1441} \qquad \text{Equation 31 in Fingas (2013)}$$

API is the gravity-a unit of density defined by the American Petroleum Institute (Fingas 2013).

ADIOS-2 used a simpler formula as stated in Janeiro et al. (2008), and the authors cited the formula to be from Buchanan and Hurford (1988):

$$K = 2.5 \times 10^{-3} (U_w)^{0.78}$$

1.5.2 Single Fraction Theory (Fingas, 1995)

While programming and testing the single fraction evaporation algorithm from Vos's Equation 3.14, above, we discovered that replicating Vos's figures would be difficult because of its reliance on molecular weight and decided not to use this algorithm. Fingas (1995, 2011) provided a simpler single-fraction method for determining the percentage evaporated:

$$\frac{x}{x_0} = e^{(-KtPvp/x_0)}$$ Equation 6 in Fingas (1995); Equation 10 in Fingas (2011); Equation 8 in Fingas (2013)

- x is the amount of crude at time, t
- x_0 is the original amount of crude when weathering begins
- t is time in seconds
- Pvp is the vapour pressure
- K is what Fingas calls an "empirical rate coefficient" that we could only assume is the same as the Vos's "mass transfer coefficient"

As mentioned before, P_{vp} can be computed using the carbon number of the oil:

$$Pvp = e^{(10.94-1.06N)}$$

Another way of computing P_{vp} is by using an effective vapour pressure that depends on the amount of substance that has evaporated. This formula is Stiver and MacKay's evaporation for semi-empirical distillation theory where the evaporative exposure term is now replaced by the definition of vapour pressure.

$$Pvp = \frac{RT_{oil}}{\gamma} exp\left(A - \frac{B}{T_{oil}}\left(T_0 + T_g f_{evap}\right)\right)$$ Equation 3.18 in Vos

x/x_0 is the fraction that remains after weathering (Equation 6; Fingas, 1995). We computed K from Equation 4 in Fingas (1995; also Equation 6 in Fingas, 2013), and we described it in the previous section.

```
Matlab®: weathering_fraction = exp((-K*t*Pvp)/x0);
         x = 100*(1 - weathering_fraction);
```

We computed x/x_0 for input from SIMPAR, ADIOS-2, and OWM.

1.5.3 Stiver and MacKay (1984): Semi-Empirical Distillation Theory for a Single Component

Vos said that ADIOS-1, an earlier version of ADIOS-2, computes evaporation using semi-empirical distillation theory following the work of S&M.

$$\frac{df_{evap}}{dt} = exp\left(A - \frac{B}{T_{oil}}\left(T_0 + T_g f_{evap}\right)\right)\frac{d\theta}{dt}$$ Equation 3.16 in Vos

Mackay et al. (1983) suggested A = 6.3 and B = 10.3, which is what ADIOS-1 uses (Vos, 2005).

T_0 and T_g are the initial boiling point (at f_{evap}=0) and a temperature parameter that is related to the gradient of the distillation curve. Both are in degrees Kelvin, as is the oil temperature, T_{oil}. Θ is called the evaporative exposure. $\Theta = K\frac{Area}{V_o}t$ where V_o is the initial spill volume. t is in seconds. Because $Area = V_0/h$, $\Theta = Kt/h$ where h is the slick thickness.

Several researchers have used different variations of the original S&M algorithm. These researchers include Buchanan and Hurford (1988), Bobra (1992) as described by Fingas (2011, 2013), Janeiro et al. (2008), and Short (2013). We briefly describe these variations in chronological order.

1.5.3.1 Buchanan and Hurford (1988)

Buchanan and Hurford used the following algorithm:

$$f_{evap} = \frac{15}{C_2} ln\left[\frac{C_2 U_w^{0.78} t}{6000h} exp\left(16.6 - \frac{C_1}{15}\right) + 1\right]$$

t is in seconds. h is the slick thickness in metres. C_1 and C_2 are distillation constants. We used C_1 = 10.3 and C_2 = 6.3.

1.5.3.2 Bobra (1992) described in Fingas (2011, 2013) Review: Equation 32

Equation 32 in Fingas (2011, 2013) is a version of S&M that Bobra (1992) used:

$$f_{evap} = \ln\left[1 + B\left(\frac{T_G}{T_{oil}}\right)\theta e^{A - B\left(\frac{T_0}{Toil}\right)}\right]\left(\frac{T_{oil}}{BT_G}\right)$$

When we used this formula, we used A = 4.8 and B = 10.3 because Fingas did not give values for these constants. Θ is the evaporative exposure related to K where $\Theta = K*Area*t/V_0$ (Equations A.2 in Vos) as defined in Section 1.6.3.

Fingas stated that it was Bobra who found that S&M's equation predicts oil evaporation well until about 8 hours and that it overestimates the rate. The overestimate can be as much as 10% at 24 hours (Fingas, 2011).

1.5.3.3 Janeiro et al. (2008)

Vos does not give values for T_0 and T_g for computing evaporation so we used formulae that we found in Janeiro et al. (2008):

- T_0 = 532.98 – 3.1295 x API (in ^oK)
- T_g = 985.62 – 13.597 x API (in ^oK)

Janeiro et al. (2008) describe NOAA algorithms from ADIOS-2 that they used to compute oil weathering in their oil spill model. The mass transfer coefficient that they used was:

$$K = 2.5\times10^{-3}U_w^{-0.78}$$

This equation was from Buchanan and Hurford (1988).

The variation of S&M that Janeiro et al. (2008) used was actually:

$$\frac{df_{evap}}{dt} = \frac{KArea}{V_0}\exp\left(A - \frac{B}{T_{oil}}\left(T_0 + T_g f_{evap}\right)\right) \qquad \text{Janeiro et al. (2008)}$$

We did not use this algorithm because it is so similar to the Bobra algorithm that Fingas described. The algorithm used by Janeiro et al. was also used by Mishra and Kumar (2015) in their oil weathering study.

1.5.3.4 Short (2013)

Short described the weathering of diluted bitumen from the Alberta tar sands. Short used MacKay et al.'s (1983) algorithm to compute the evaporation (based on S&M):

$$f_{evap} = \ln\left[1 + \left(\frac{12191}{T_{oil}}\right)\theta e^{8.2-\left(\frac{5239}{T_{oil}}\right)}\right] / \left(\frac{12191}{T_{oil}}\right) \qquad \text{Equation 7 from Short (2013)}$$

Short defines the evaporative exposure, $\Theta = \frac{Kt}{x_0}$, with x_0 as the slick thickness and $K = 0.0015U_w^{0.78}$. This is the option that we used for SIMPAR to compute evaporation when we did not have a molecular weight and used Short's equation to compute the fraction lost with inputs from SIMPAR and OWM.

1.5.4 Empirical Equations (Fingas, 2011 and 2013)

Fingas described generic empirical evaporation equations using distillation data. The empirical equations have several advantages:

1. Users do not need to know geometric dimensions of the spill which are not always available.
2. The empirical equations can handle "diesel-like evaporation".
3. The empirical equations can predict long-term evaporation more accurately than the semi-empirical equations.
4. The empirical equations avoid producing unrealistic evaporation rates common with algorithms that use wind velocities.

His 2011 review gave the logarithmic relation that was empirically developed at 15°C air temperature:

$$f_{evap} = [B + 0.045(T - 15)]\ln(t)$$

where t is time in minutes, and B is an equation parameter that is determined empirically.

Fingas also stated that some oils follow a square root relation rather than a logarithmic one. He listed a large number of empirically derived evaporation relations in a table, and we used the relation given for our Ekofisk Exxon test, and, later, we used the relation for Cold Lake Bitumen for our experiments that we present in Part 2 of this report.

The relation for Ekofisk is

$$f_{evap} = [4.92 + 0.045T]\ln(t)$$

1.5.5 Computing Evaporation

Computing evaporation using Vos's algorithm with molecular weight was not feasible without a database of molecular weights. We decided to try several of the other equations that we found in the literature.

We computed evaporation the following ways for a hypothetical Ekofisk Exxon spill with a constant wind = 8 ms^{-1}:

1. single fraction theory: x/x_0 as reviewed by Fingas (1995) for all models (note that Vos states that only SIMPAR actually uses the single fraction theory)
   - using *K* computed by Equation 3.15 from Vos for SIMPAR; $K=C_dU_w$ for OWM; and *K* computed using the Janeiro et al. (2008) equation for ADIOS-2
   - *Pvp* from the oil database for all models (0.524 bar = 52400 Pa)
2. semi-empirical distillation theory: f_{evap}
   - f_{evap} by Short (2013) for SIMPAR and OWM (*K* from Short and SINTEF (2005), respectively), and f_{evap} for ADIOS-2 using the Bobra equation, Equation 32 in Fingas (2011, 2013), with *K* by Hamoda (1989) as given in Fingas (2013)
   - f_{evap} by Buchanan and Hurford for all models with *K* from Janeiro et al. (2008)
   - f_{evap} computed using the empirical equation

Figure 4 and **Figure 5** show how Ekofisk Exxon evaporated under the constant wind (8 ms^{-1}) using the three weathering models with evaporation computed as described above.

The results for the upper panel of **Figure 4** were computed using Fingas's x/x_0 single fraction formula. "Fingas1995" in the legend means that we used Equation 6 from Fingas's 1995 review. All three models have the oil evaporating 100% within two hours. The different ways of computing *K* didn't make a difference. The different length scales that were used did not seem to have an effect either. The evaporation rate seemed unrealistic; i.e. too fast.

The results for the lower panel of **Figure 4** were computed using the empirical equation for Ekofisk. All the models produced the same results because the same air temperature and time were used for each model.

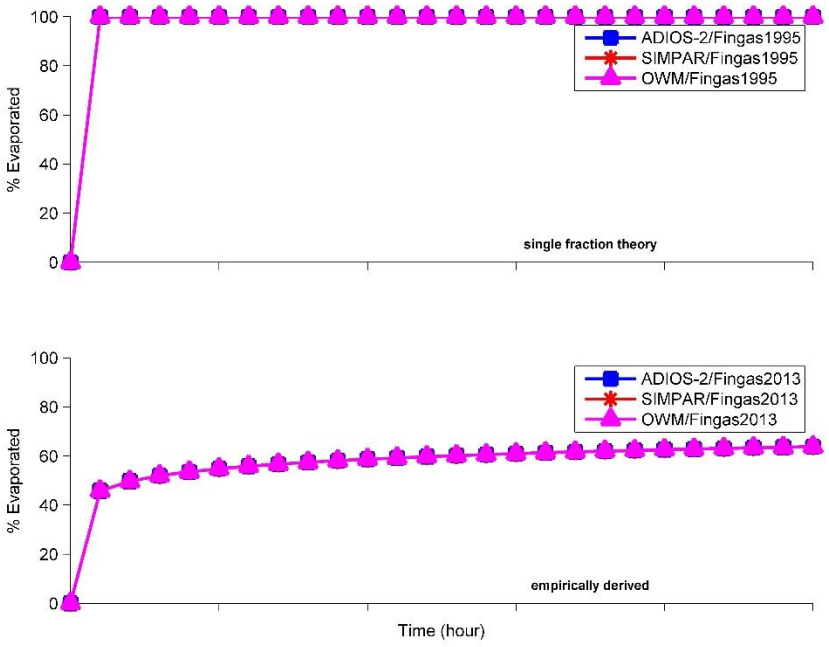

Figure 4 Percent evaporated computed using single fraction theory (Equation 6 in Fingas, 1995) in the top panel for all models and using the empirically derived relation for Ekofisk oil for the 3 models in the bottom panel (Fingas, 2011 and 2013)

For ADIOS-2 inputs using Janeiro et al.'s (2008) S&M equation, and using Short's equation (Short, 2013) for the SIMPAR and OWM weathering model inputs, we used Short's equation for *K* for SIMPAR, and we used the SINTEF equation for *K* for OWM. The different mass transfer coefficients for SIMPAR and OWM did not make a big difference. The evaporation rates represented in the lower panel were much more realistic than those from the upper panel.

The top panel of **Figure 5** shows the % evaporated computations using the three weathering models' inputs, but using the Bobra variation of S&M reviewed in Fingas 2011 and 2013 (Equation 32) for ADIOS-2 with Hamoda's mass transfer coefficient (Fingas 2013), and the variation of S&M from Short (2013) for SIMPAR and OWM, with the length scales and mass transfer coefficients associated with the respective models. The top panel shows the difference between using the Bobra algorithm and the one from Short where the Bobra algorithm appears to be optimistic regarding the % evaporated compared to the bottom panel from **Figure 4**.

The bottom panel of **Figure 5** shows the % evaporated which is computed using the variation of the S&M algorithm outlined in Buchanan and Hurford (B&H, 1988). The results using the B&H algorithm were similar to those that from the empirical equation in **Figure 4**'s bottom panel. B&H presented results in their Fig. 3 where the apparent predicted maximum % evaporated was approximately 45% after 6-8 hours for a constant wind speed of 7.5 ms^{-1} using Ekofisk Exxon crude. B&H's algorithm, however, overestimated the actual data points in their study. The curve for % Evaporated as computed by our ADIOS-2 model algorithm (combined Bobra and Janeiro et al.) for Ekofisk Exxon predicts a far greater loss of volume than Mishra and Kumar predicted for a similar light oil, Statfjord crude, over 24 hours. Their model observed just over 50% evaporated whereas ours produced over 80% loss.

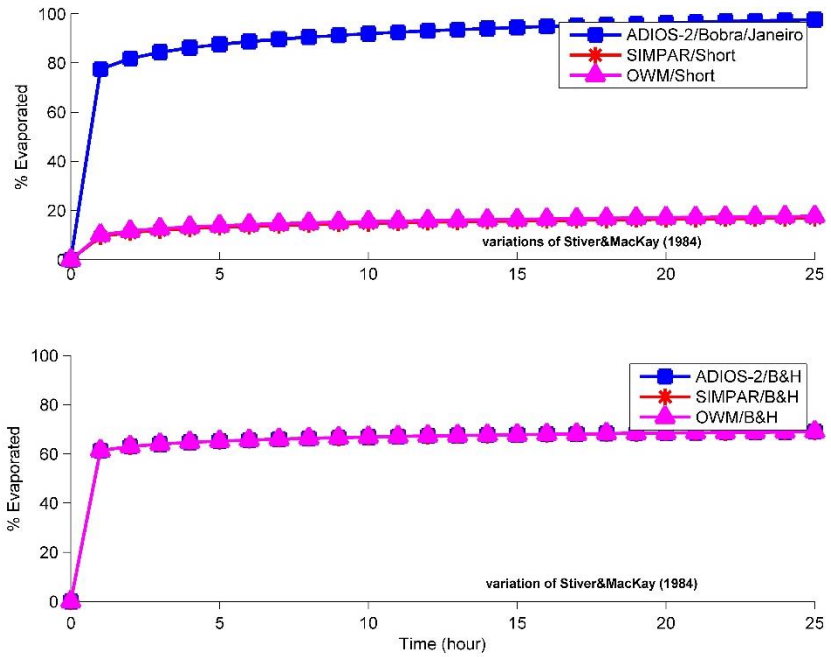

Figure 5 Percent evaporated computed using Bobra's equation (Equation 32 in Fingas, 2011 and 2013) in the top panel for all models, and the algorithm from Buchanan and Hurford (1988) in the bottom panel

1.5.6 Actually Running NOAA's ADIOS-2

Out of interest, we ran NOAA's ADIOS-2 model with the following inputs:

Oil type = Ekofisk Exxon
API = 40.1
Oil density @ 15^{o}C = 0.832 g/cc
Oil viscosity @ 15^{o}C = 11.8 cSt
Uw = 8 m/s @ 0 deg wind direction
Wave height = computed from wind speed
Water temperature = 15^{o}C
Salinity = 40 ppt
Sediment Load = 0gm^{-3}
Water current = 1 ms^{-1}

Amount spilled = 1000 metric tons
You cannot enter values <1 into the ADIOS-2 model (e.g. wind speed = 0.5 ms^{-1} or water current = 0.01 ms^{-1}).

The graph that ADIOS-2 produced for evaporation is shown in **Figure 6**. The evaporation is given as a % evaporated. After 24 hours, ADIOS-2 predicted that about 43% of the oil would be evaporated. This is very different from what we produced with the equations that we programmed. Vos admitted that the differential equations for ADIOS-2 were not available, but speculated that they are based on Jones (1997) and that vapour pressure is computed following S&M (semi-empirical distillation theory). In the absence of the actual ADIOS-2 equations, we substituted the Bobra evaporation algorithm and the

Hamoda definition of mass transfer coefficient. We expect that our choices created the difference between our results and those produced by actually running the ADIOS-2 model.

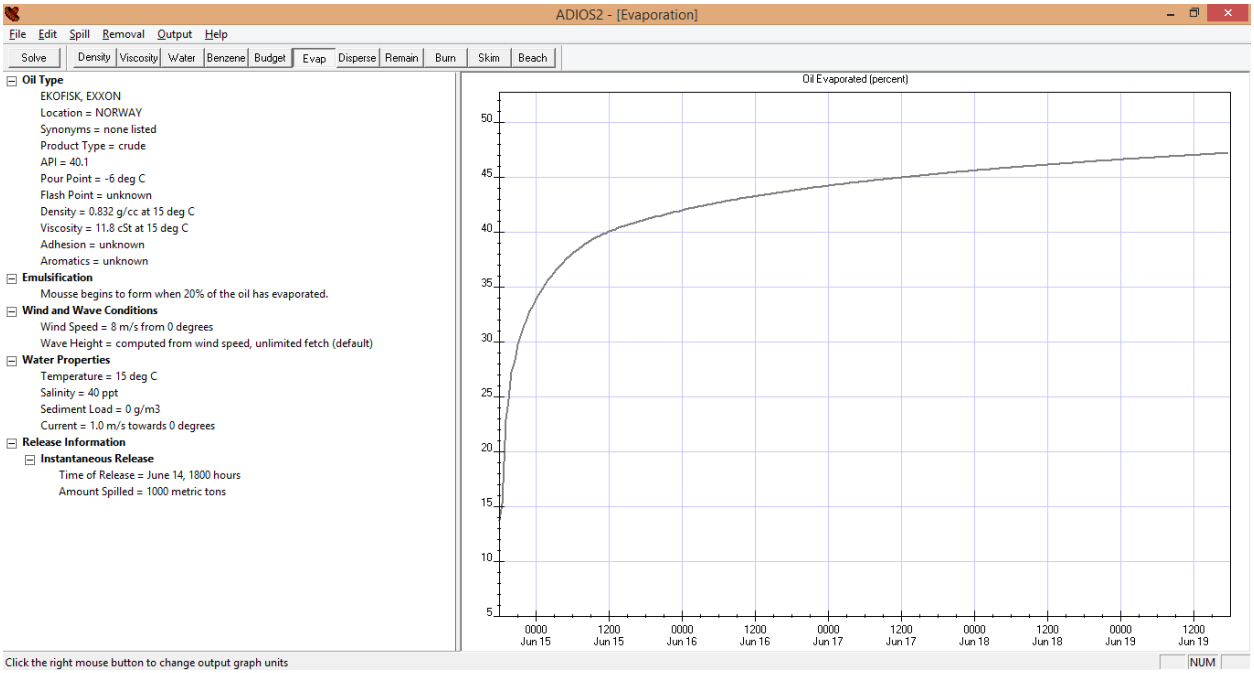

Figure 6 Evaporation rate computed by ADIOS-2 for Ekofisk Exxon

1.5.7 A Brief Comment about Evaporation

None of our tests using the single fraction theory or the semi-empirical distillation theory had evaporation reach ~40 to 50%, which was what Vos's example figures showed after 24 hours for the models. In the end, we think that the empirically derived formulae might be the most practical for our study, but only because we are using oils that are listed in Fingas's tables. Of all the formulae that we used that are based on S&M, Short's variation might give the most realistic results even though they seem underestimated in our test. An advantage of the empirical equations and the S&M formulae is that they do not use the vapour pressure, which is difficult to pin down; we had two very different values of *Pvp* from two different sources. For *K*, either a formula that used the wind or the water temperature and salinity could be used. We do not have an opinion as to which would be better, but would recommend one that did not need molecular weight.

1.6 EMULSIFICATION

Matlab® function: *emulsification.m*

Figure 3.4 in Vos displayed the water content vs time over 336 hours for SIMPAR, OWM, and ADIOS-2 for no wind and with a wind speed = 10 ms^{-1}. The water content of the oil is the amount of water uptake. In all the model algorithms, water content was independent of evaporation and only relied on the wind speed.

Vos stated that, in ADIOS-2 and SIMPAR, the emulsification was modeled according to Eley (1988) where water content was defined as a function of the ratio of interfacial surface area to oil volume.

1.6.1 SIMPAR

For SIMPAR, Vos presented the following three equations that make up Equation 3.26 in the review:

$$y = \frac{x}{(6+x)} \qquad \text{Variation of Equation 3.25 in Vos}$$

$$x = x_{max}\,(1 - e^{-k_s t}) \qquad \text{Equation 3.26 in Vos}$$

$$x_{max} = \frac{6y_{max}}{(1-y_{max})} \qquad \text{Equation 3.26 in Vos}$$

Vos defined the emulsification rate, k_s, in Equation 3.28, but we called it k_y to be consistent with the ADIOS-2 formula. It describes the wind dependency of emulsification.

$$k_y = \frac{k_0}{y_{max}}(U_w + 1)^2 \qquad \text{Equation 3.28 in Vos}$$

y_{max}=1 means maximum water uptake = 100% of the water is gone. y_{max} is the "stable water content of the emulsion" and it is typically 0.7-0.8 (Zanier et al., 2014). Vos set y_{max}=0.7. k_s is the emulsification rate in s^{-1} and k_0 is the rate for y_{max}=*1* and zero wind. Reed (1989), cited by Vos, used k_0=*2x10*$^{-6}$ s^{-1}, and Zanier et al. (2014) used 2x10^{-6} s^{-1}.

To compute emulsification for the SIMPAR weathering model, we programmed the four equations above (Vos 3.26 and 3.28) to give a value for *y*, the amount of water uptake with y_{max}=0.7, as in Vos:

```
k_s = (k0/y_max) * (Uw+1)^2;  % k_s is the emulsification rate (1/s);
                              Equation 3.28 in Vos
x_max = (6*y_max)/(1-y_max);  % Equation 3.26
x = x_max*(1-exp(-k_s*t));    % Equation 3.26
y = x/(6+x);                  % Equation 3.25 in Vos (solve for x)
```

1.6.2 ADIOS-2

Vos does not know the wind dependency of the emulsifying algorithm used by ADIOS-2, but described an algorithm by MacKay et al. (1980) that is analogous to the Eley algorithm that SIMPAR uses.

$$y = y_{max}\,(1 - e^{-k_y t}) \qquad \text{Equation 3.27 in Vos}$$

$$k_y = \frac{k_0}{y_{max}}(U_w + 1)^2 \qquad \text{Equation 3.27 in Vos}$$

In this case, k_y is the emulsification rate in s^{-1}. k_0 is defined as for SIMPAR. Janeiro et al. (2008), however, used k_0=*1x10*$^{-6}$ s^{-1}. These researchers based their weathering algorithms on the work by NOAA (i.e. ADIOS-1 and ADIOS-2), so we used both 2.0x10^{-6} and 1.0x10^{-6} for k_0 to see what difference it made.

We programmed the MacKay et al. (1980) algorithm to represent the one used by ADIOS-2.

```
k_y = (k0/y_max) * (Uw+1)^2; % k_y is the emulsification rate
                               (1/s); Equation 3.27 in Vos
```

```
y = y_max * (1-exp(-k_y*t)); % Equation 3.27
```

1.6.3 OWM

Vos's description of the algorithm that OWM uses to compute emulsification was ambiguous. We decided to program emulsification according to the SINTEF manual (SINTEF, 2005) rather than follow Vos's description. We programmed Equations 21, 22, and 23 from SINTEF. These equations are duplicated in Vos as Equations 3.31 and 3.32. The algorithm used in OWM uses water content as a function of time so that one can integrate the water content over time (unlike in SIMPAR and ADIOS-2). The one problem with these equations is that one value relies on average half-time values that were found in the laboratory and that were not given in Vos nor in the SINTEF manual. Another issue is that Vos does not give a value of "C" to use. Therefore, we could not test these equations.

Matlab®:

```
Uref = 10; % m/s
t_ref = C*t_lab; % Equation 22 in SINTEF and are empirically
                 % determined
t_half = ((1+Uref)/1+Uw))^2 *t_ref; % Equation 3.32 in Vos
y(t+dt) = y_max(t) - (y_max(t) - y(t)) * 0.5^(dt/t_half); % Equation
                                                         % 3.31 in
                                                         % Vos
```

However, Vos states that the SINTEF approach is based on the MacKay et al. (1980) model displayed in Equations 3.29 and 3.27. Therefore, without the SINTEF lab results to use, we simply changed the code:

```
k0 = 1.0e-6;
k_y = (k0/y_max) * (Uw+1)^2;
if Uw==0,
    t_half = 2.43e5;
else
    t_half = log(2)/k_y; % Equation 3.29
end
y(t+dt) = y_max(t) - (y_max(t) - y(t)) * 0.5^(dt/t_half);
```

y_max is a constant as far as we can see from Vos's explanation for Figure 3.4. Vos's Equation 3.29 describes the half saturation times in rate constants (Vos, 2005, p. 26). It may or may not have anything to do with the half saturation time defined in OWM, but, because we lacked the OWM values, we used Equation 3.29 for our algorithm: $k = \ln 2/t_{half}$ to define t_{half}. That is, $t_{half} = ln2/k_y$ where we defined k_y as the emulsification rate defined by MacKay et al. (1980), as for ADIOS-2. When there is no wind, $t_{half} = 2.43x10^5$ (from Vos's Figure 3.4 inputs).

1.6.4 Zaneiro et al. (2014)

Zaneiro et al. (2014) also based their emulsification algorithm on MacKay et al. (1980):

$$y(t) = y_{max}\left[1 - \exp\left(\frac{-k_0}{y_{max}}(1 + U_w^2 t)\right)\right]$$

It is slightly different than what Vos described in that in Zaneiro et al.'s formula, only the wind speed is squared, not the binomial sum of wind speed and "1". Also, the negative

sign in front of k_0 is not in Vos's equations. We programmed Zaneiro et al.'s algorithm to see what the difference in water content would be.

1.6.5 Computing Emulsification

In this subsection, we present figures of the water content computed by the four emulsification algorithms. The SIMPAR model computation used the Eley formula described in Vos, and it is represented by "Eley/SIMPAR". The ADIOS-2 algorithm is represented in the legend by "MacKay/Vos". We computed water content for the OWM model according to the SINTEF manual and Eley, and the results are represented in the legend by "OWM". The last blue line is water content that we computed as described in Zaneiro et al. (2014) following MacKay ("MacKay/Zaneiro et al.")

1.6.5.1 No Wind

For the first figure, we used $k_0=2x10^{-6}\ s^{-1}$ (**Figure 7**) and $k_0=1x10^{-6}\ s^{-1}$ (**Figure 8**) under conditions of no wind. The curves have shapes similar to Vos's Figure 3.4 except ours appear more linear. The different values of k_0 had little effect.

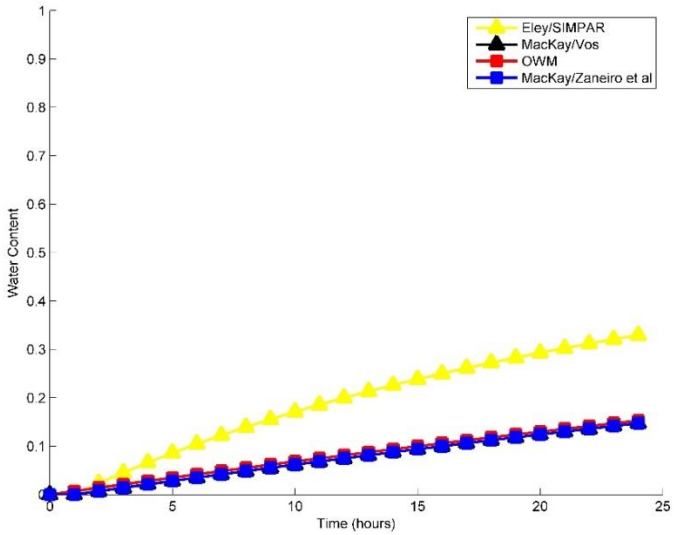

Figure 7 Water content computed using 4 different algorithms with $k_0=2x10^{-6}$ and no wind: $U_w=0\ ms^{-1}$

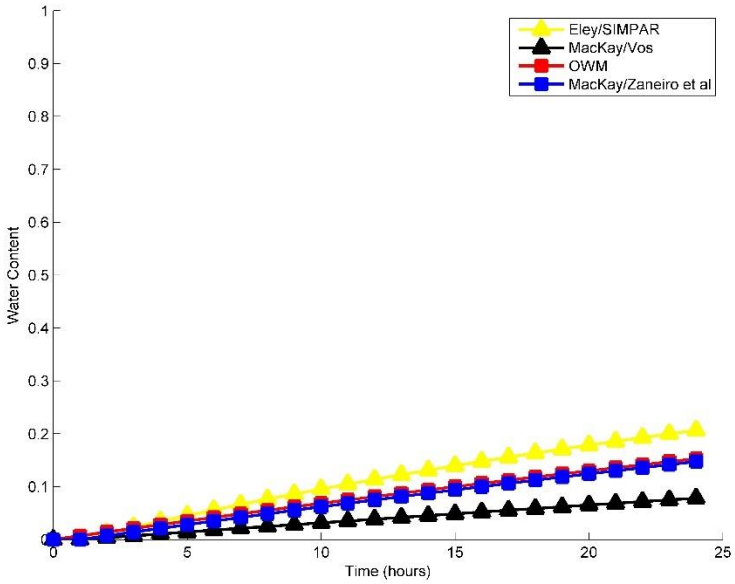

Figure 8 Water content computed using 4 different algorithms with k_0=1x10^{-6} and no wind: U_w=0 ms^{-1}

1.6.5.2 With Wind

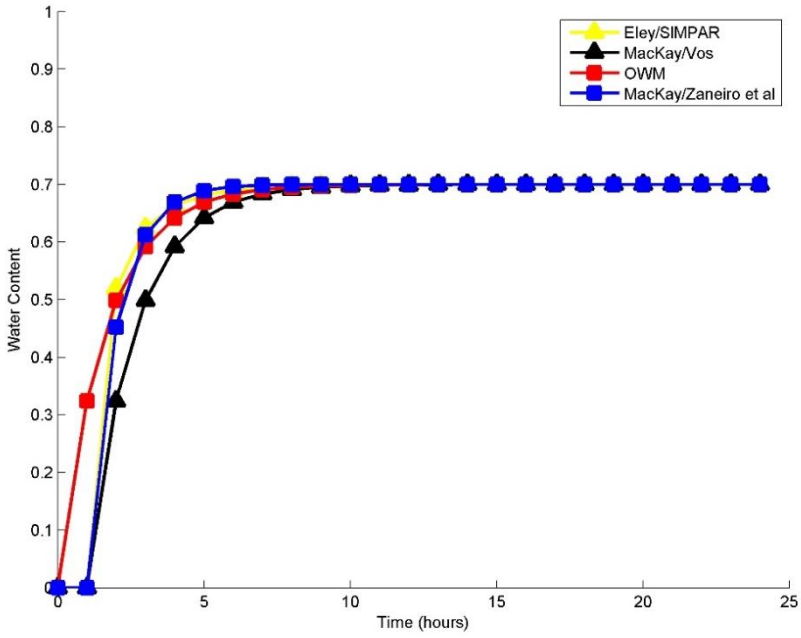

Figure 9 and

Figure 10 show the water content computed by the four algorithms under conditions of U_w=10 ms^{-1} for k_0=2x10^{-6} s^{-1} (**Figure 9**) and k_0=1x10^{-6} s^{-1} (**Figure 10**). Buchanan and Hurford ("B&H",1988) used the MacKay et al. (1980) algorithm that we programmed as the ADIOS-2 algorithm; however, they used k_0=-4.5x10^{-6} s^{-1}. The B&H curve for water content of surface Statfjord crude in their Fig. 8 showed that water uptake occurred much

more rapidly than what we are showing for Ekofisk Exxon. However, B&H's model results did overestimate the water content when compared to real data.

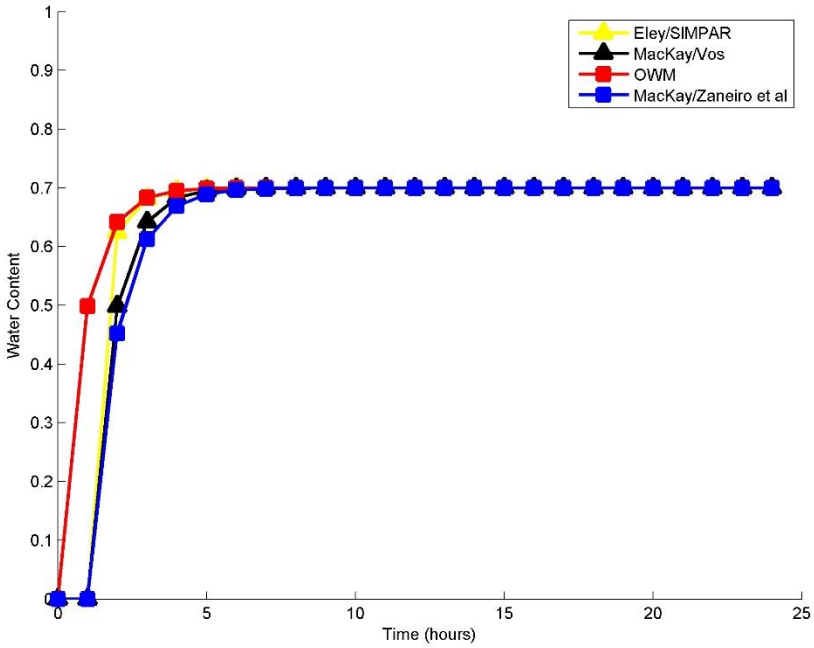

Figure 9 Water content computed using 4 different algorithms with k_0=2x10^{-6} and U_w=10 ms^{-1}

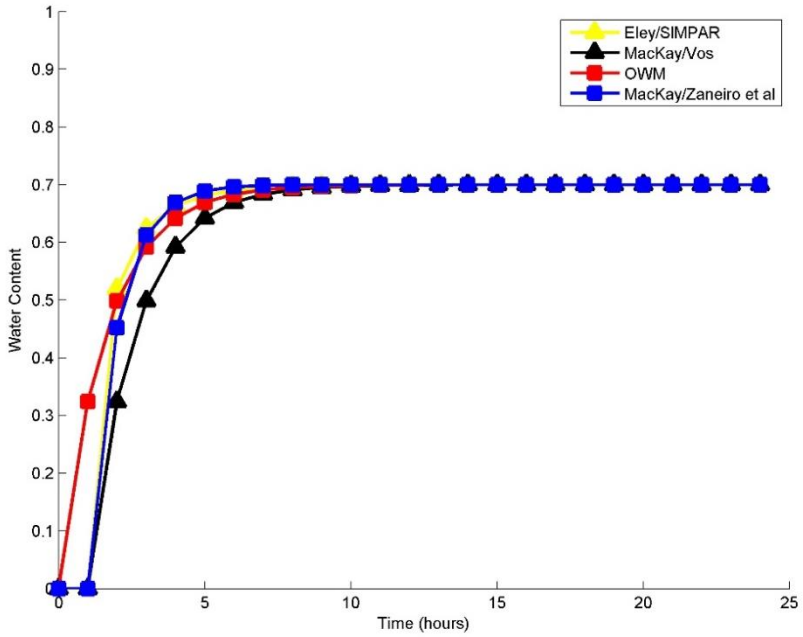

Figure 10 Water content computed using 4 different algorithms with k_0=1x10^{-6} and U_w=10 ms^{-1}

1.7 OIL WEATHERING WITH VARIABLE WIND SPEED

To this point, we explored oil weathering algorithms under no wind or constant wind conditions. In this section, we present the results with randomly generated and variable U_w. We redrew the graphs for those modules where wind was a factor. We used a 5 hour and a 25 hour sample of random data. Vos did not test any weathering processes for variable wind so we cannot compare our graphs with those in the review, but we can compare our results with the NOAA ADIOS-2 model results for Evaporation using a variable wind in NOAA'S ADIOS-2. Also, we noted that none of the theory that we explored has tested weathering for continually varying wind speeds. Most literature only reports results at different constant wind speeds.

The five hours of variable wind data were, for speed and direction (The actual NOAA ADIOS-2 model asks for wind direction data.):

hour 1 = 2 m/s ; 10 deg
hour 2 = 2 m/s ; 10 deg
hour 3 = 1 m/s ; 19 deg
hour 4 = 3 m/s ; 4 deg
hour 5 = 5 m/s ; 12 deg

Figure 11 is a simple plot of the test variable wind speeds for 5 hrs and 25 hrs.

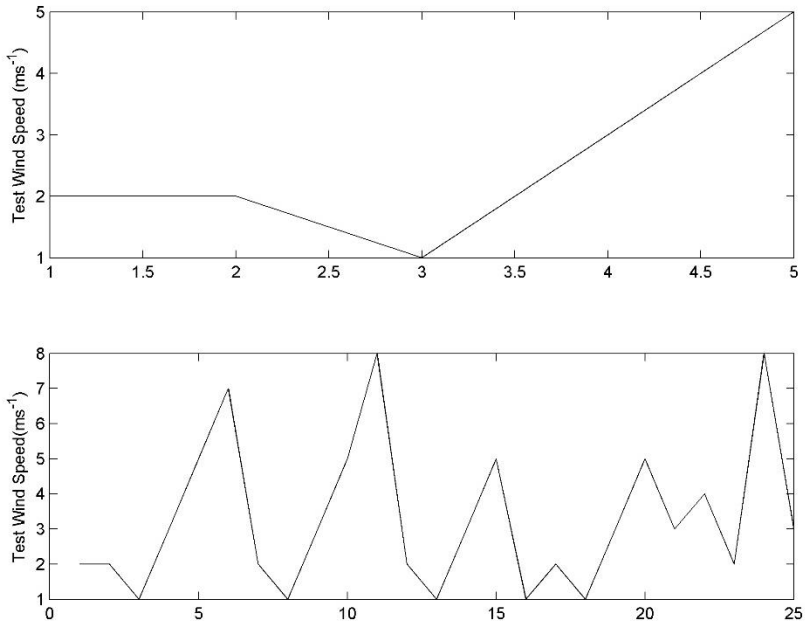

Figure 11 Random variable wind speed (ms^{-1}) used for testing oil weathering algorithms models

1.7.1 Dispersion with Variable Wind

Figure 12 to **Figure 15** are plots for H_0, the dissipative wave energy (D_{ba}), the fraction of the sea surface affected by breaking waves (F_{wc}), and the entrainment rate as a function of time, modeled for the three weathering models under 5 hours of variable wind. The droplet diameter is not a function of wind speed so we did not plot it.

5 hours of variable wind data

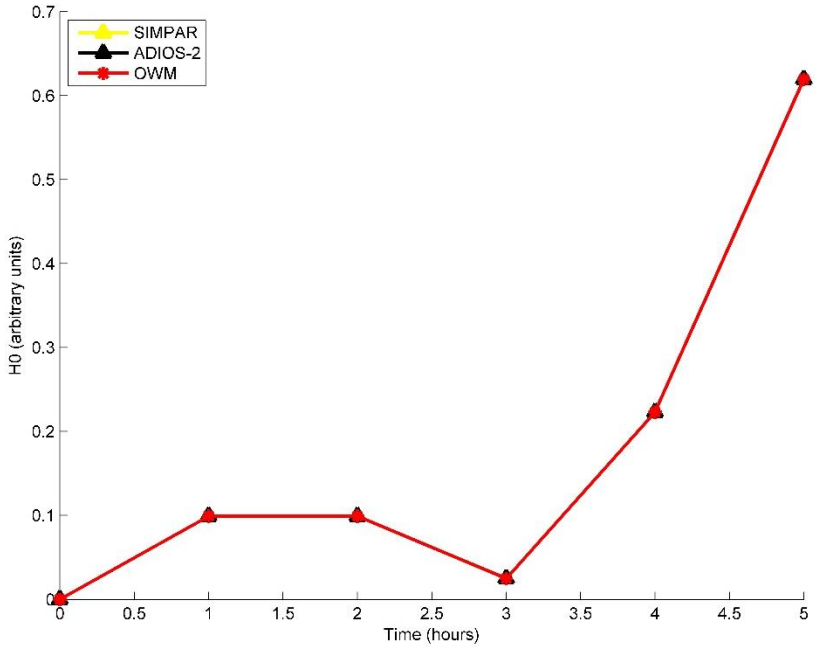

Figure 12 H_0 as a function of time with variable wind for 5 hours

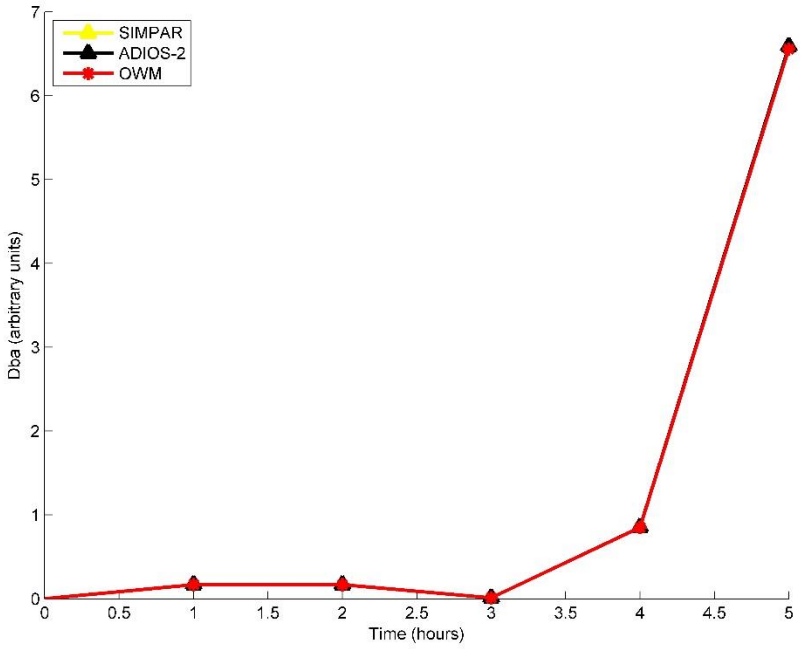

Figure 13 Dissipative wave energy as a function of time with variable wind for 5 hours

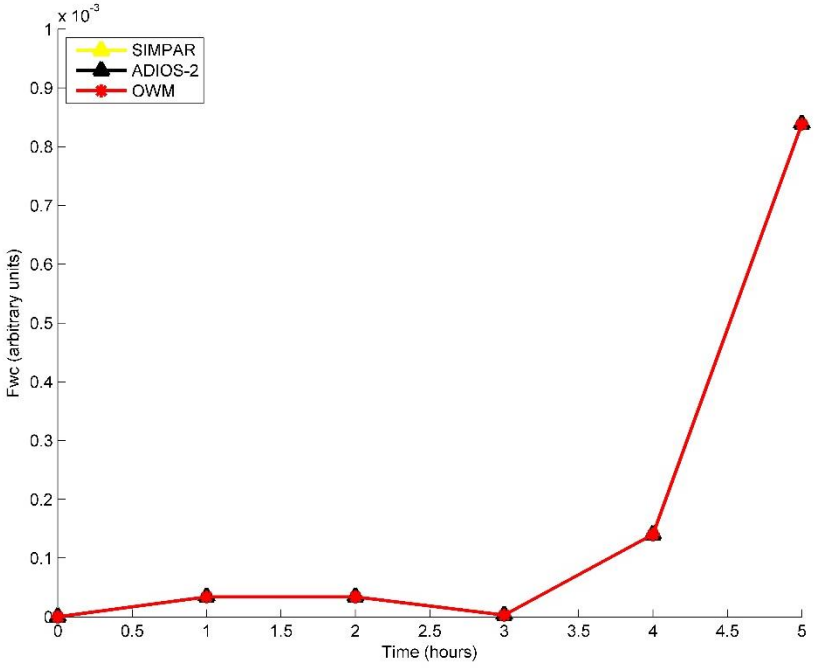

Figure 14 F_{wc} as a function of time with variable wind for 5 hours

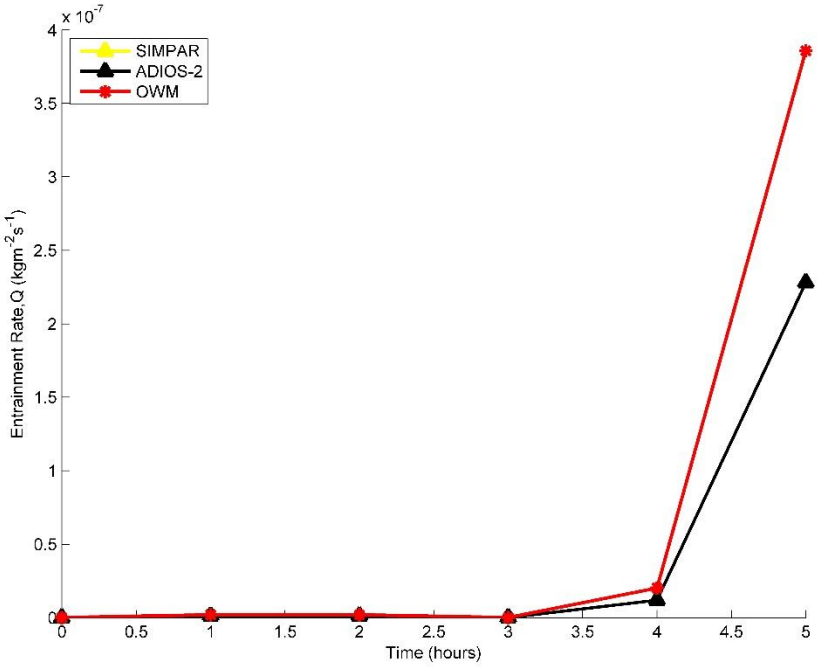

Figure 15 Entrainment rate as a function of time with variable wind for 5 hours

25 hours of variable wind data

Figure 12 to **Figure 19** are plots of H_0, the dissipative wave energy (D_{ba}), the fraction of the sea surface affected by breaking waves (F_{wc}), and the entrainment rate as a function of time, modeled for the three weathering models under 25 hours of variable wind. In these figures, the lines for SIMPAR are hidden by the lines that represent ADIOS-2.

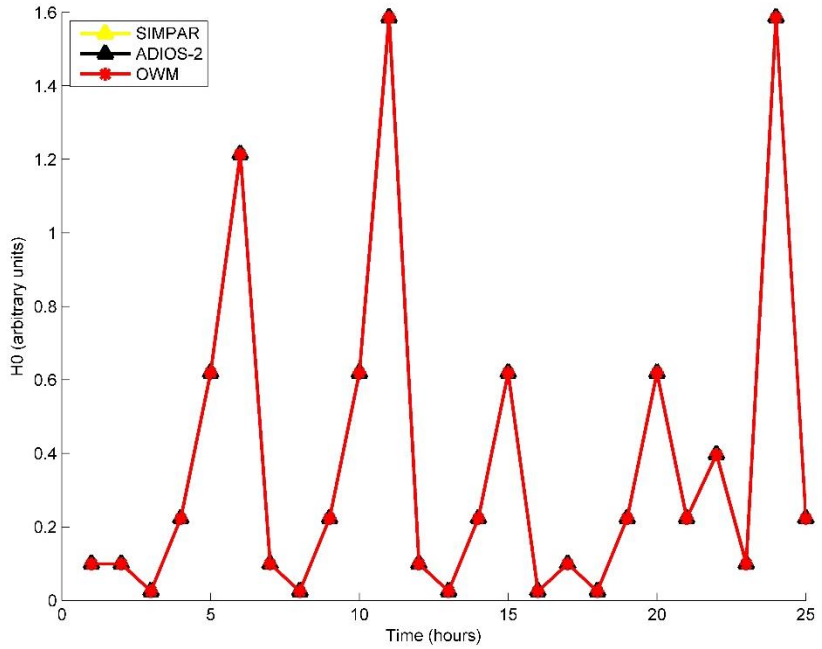

Figure 16 H_0 as a function of time with variable wind for 25 hours

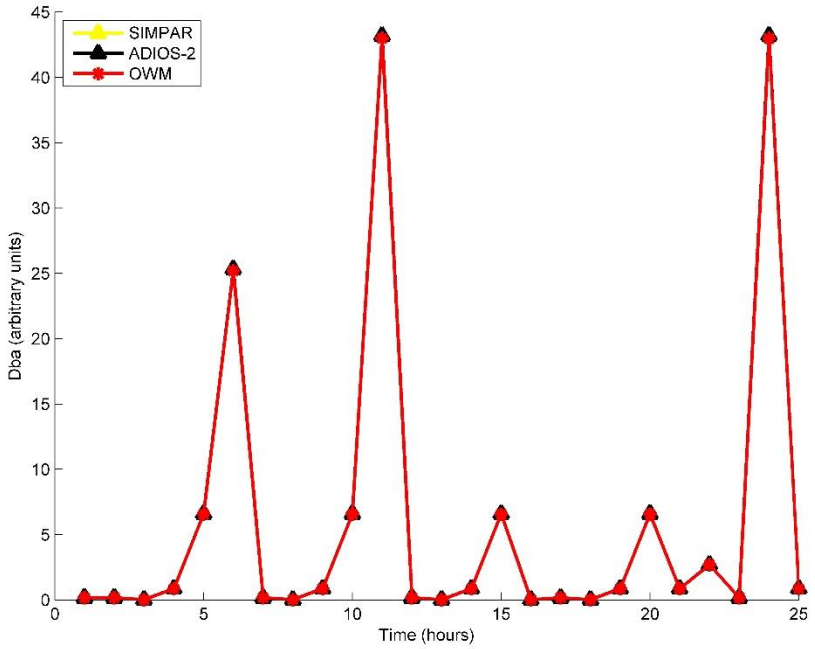

Figure 17 Dissipative wave energy as a function of time with variable wind for 25 hours

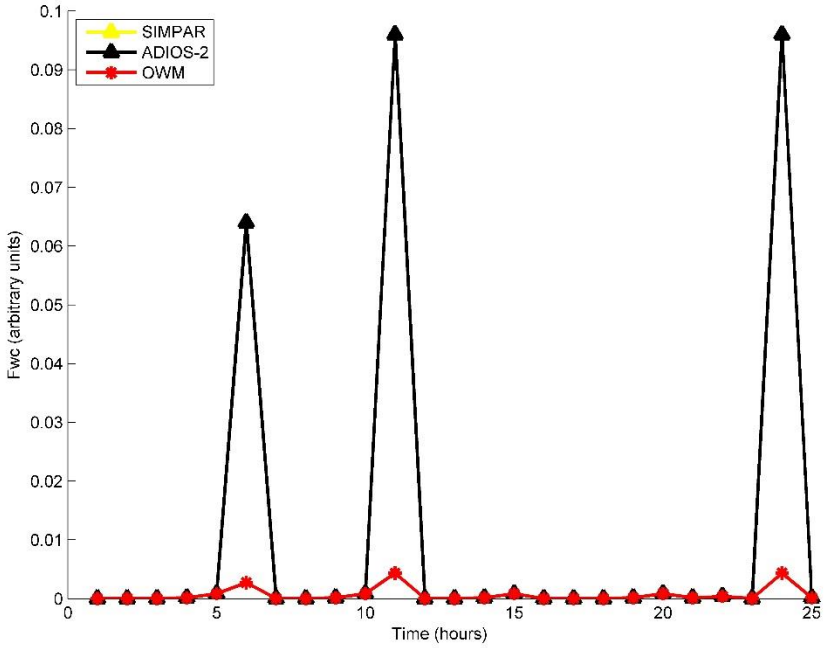

Figure 18 F_{wc} as a function of time with variable wind for 25 hours

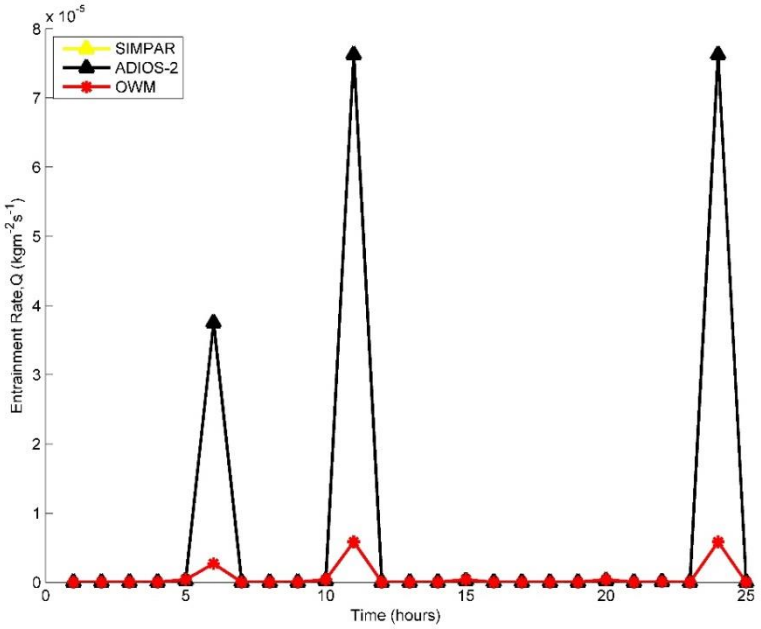

Figure 19 Entrainment rate as a function of time with variable wind for 25 hours

1.7.2 Evaporation with Variable Wind

We tested the Evaporation algorithms with the variable wind data, for 5 hours and 25 hours. For these figures, we used a computed P_{vp} for the Fingas (1995) algorithm. The results are in **Figure 20** and **Figure 21** for the computation under 5 hours of variable wind. The results are in **Figure 23** and **Figure 24** for the computation under 25 hours of variable wind.

Figure 22 shows the % evaporated computed by ADIOS-2 directly. The algorithms for evaporation were all developed empirically under conditions of constant wind. That's why we see evaporation decrease when the wind decreases; this behaviour is despite the fact that the computation is iterative, depending on the value of the previous time step. The Buchanan and Hurford algorithm was least affected by the variable wind, but this algorithm also produced the fastest evaporation.

5 hours of varying wind

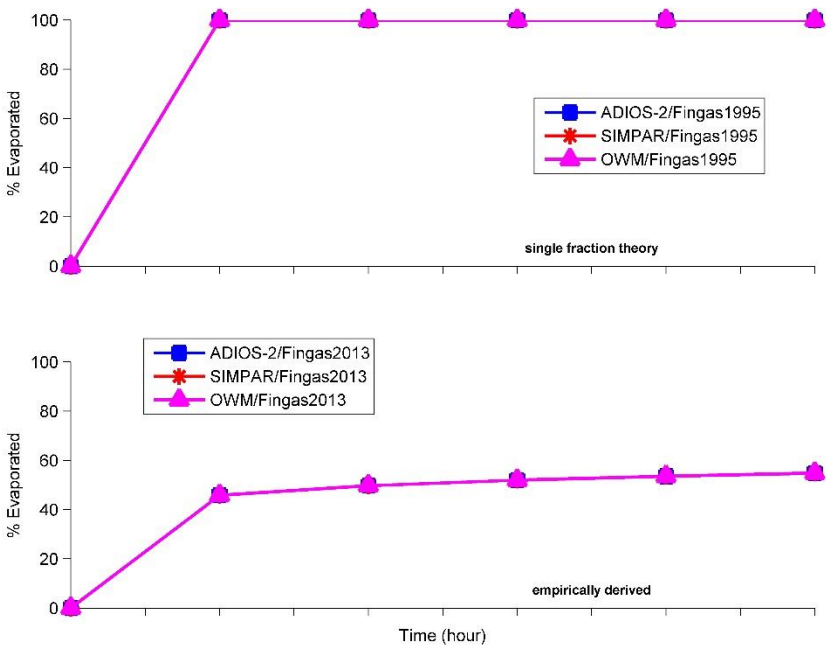

Figure 20 Percent evaporated computed with 5 hours of variable wind and single fraction theory (Equation 6 in Fingas, 1995) in the top panel for all models and using the empirically derived relation for Ekofisk oil for the 3 models in the bottom panel (Fingas, 2011 and 2013)

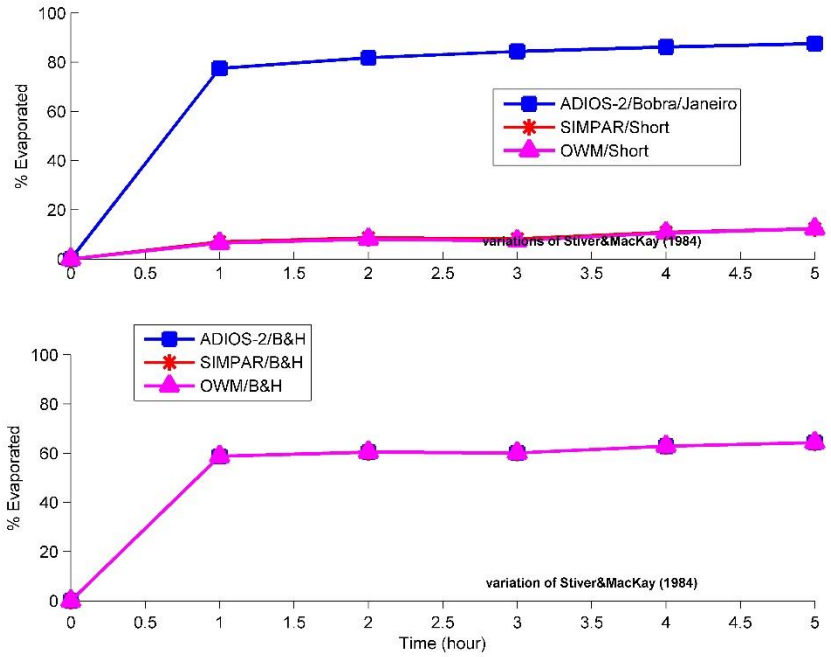

Figure 21 Percent evaporated computed with 5 hours of variable wind and using Bobra's equation (Equation 32 in Fingas, 2011 and 2013) in the top panel for all models, and the algorithm from Buchanan and Hurford (1988) in the bottom panel

Figure 22 is the graph for Evaporation that NOAA's ADIOS-2 produced with five hours of variable wind for Ekofisk Exxon oil. We manually entered each wind datum into the model. This is why we only used five hours of wind. The graph does not resemble our graphs at all (**Figure 20** and **Figure 21**). The Bobra/Janeiro algorithm that we used to represent the ADIOS-2 model algorithm seems to overestimate the actual computed NOAA ADIOS-2 evaporation. It is interesting to see that Evaporation is affected by the decrease in wind with NOAA's ADIOS-2 model. The variation in evaporation will directly affect viscosity due to the oil emulsification that depends on the evaporated fraction of the oil.

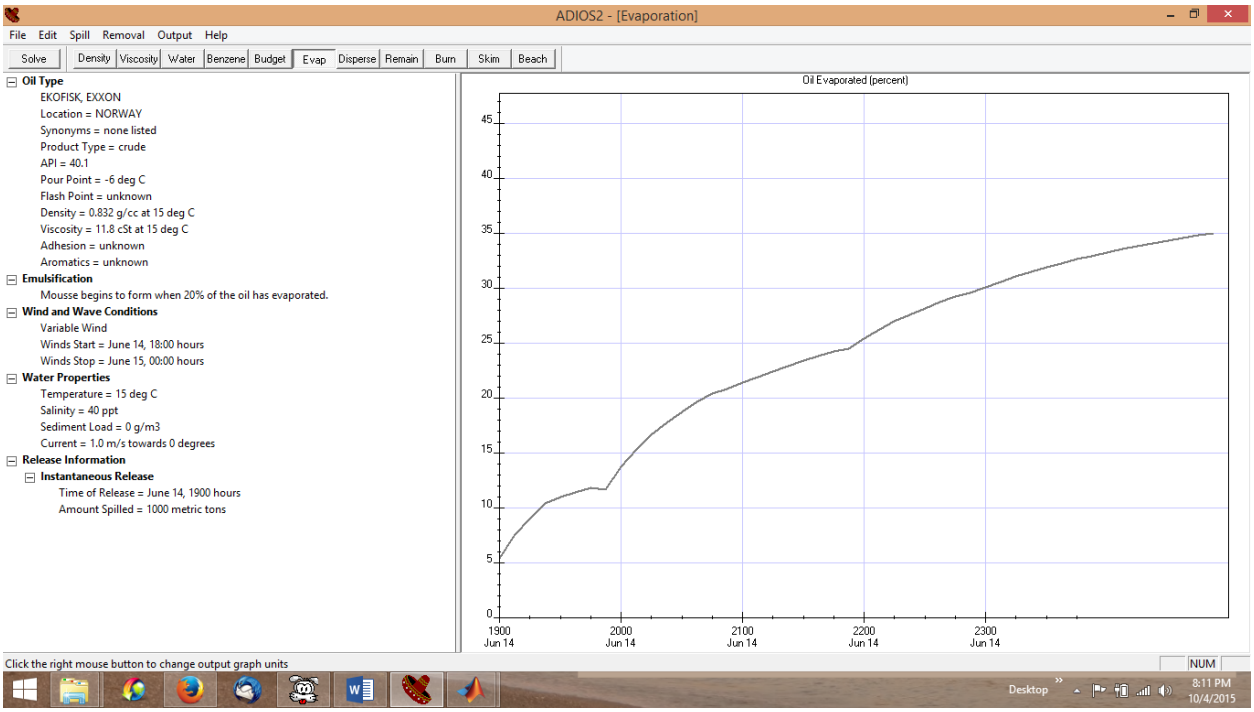

Figure 22 Percent evaporated computed with 5 hours of variable wind produced by NOAA's ADIO-2 weathering model

25 hours of varying wind

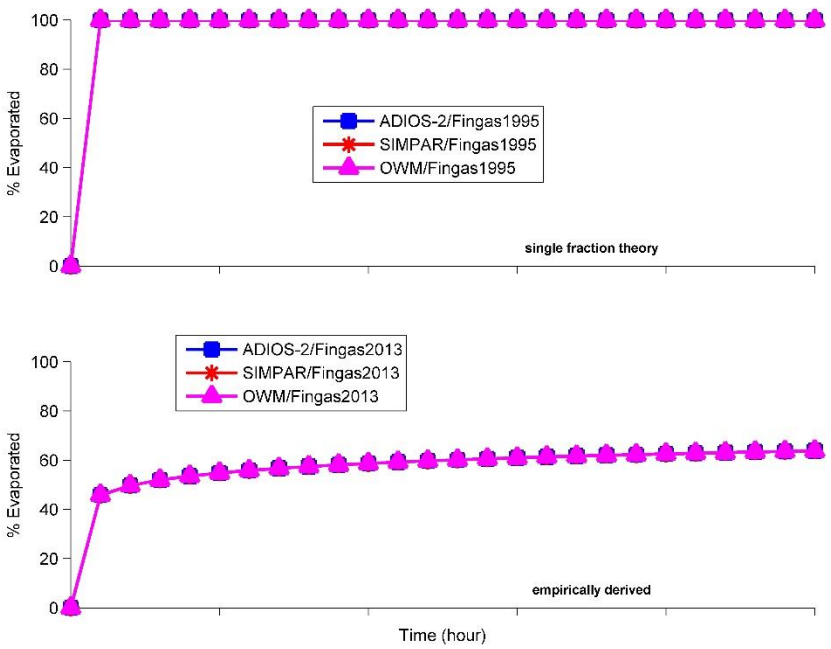

Figure 23 Percent evaporated computed with 25 hours of variable wind and single fraction theory (Equation 6 in Fingas, 1995) in the top panel for all models and using the empirically derived relation for Ekofisk oil for the 3 models in the bottom panel (Fingas, 2011 and 2013)

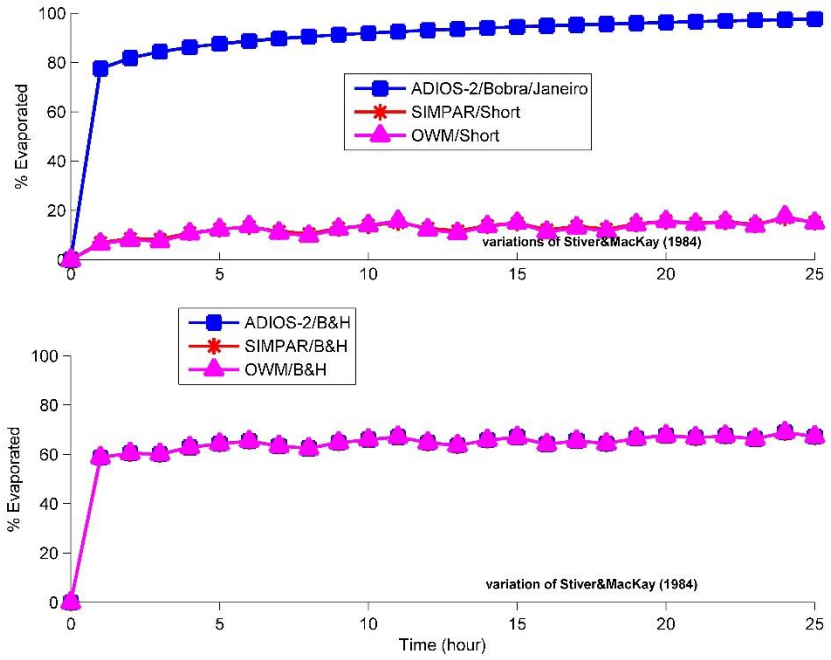

Figure 24 Percent evaporated computed with 25 hours of variable wind and using Bobra's equation (Equation 32 in Fingas, 2011 and 2013) in the top panel for all models, and the algorithm from Buchanan and Hurford (1988) in the bottom panel

1.7.3 Emulsification with Variable Wind

The test of the emulsification algorithms using a variable wind produced the results that are plotted below for the five hours of wind data and the 25 hours of wind data. Similar to evaporation, the emulsification algorithms were developed empirically under conditions of constant wind and the behaviour of the models with the changing wind conditions reflects that.

```
k_y = (k0/y_max) * (Uw+1)^2
```

One solution would be to only allow the function to run until a maximum water content were reached; e.g. y_{max} = 0.7, which is what we did.

For these computations, we used $k_0=2.0x10^{-6}\ s^{-1}$ following Reed (1989), as suggested by Vos. The algorithms that we used were the same four that we used for the constant wind computations of emulsification.

Figure 25 shows the results for five hours of variable wind data, and the **Figure 26** shows the results for 25 hours of variable wind data. Only OWM produced results that were physically realistic.

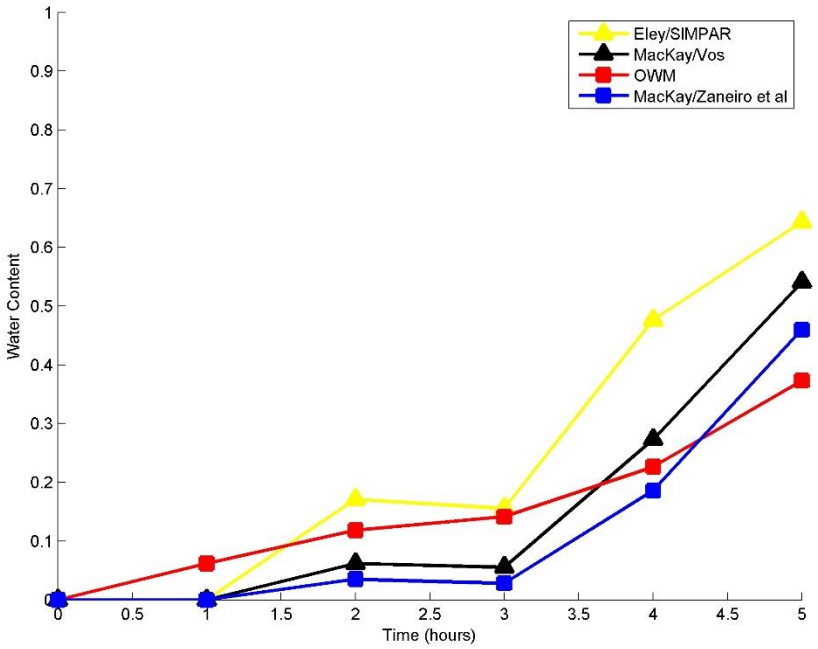

Figure 25 Water content computed under conditions of 5 hours of variable wind for 4 different algorithms

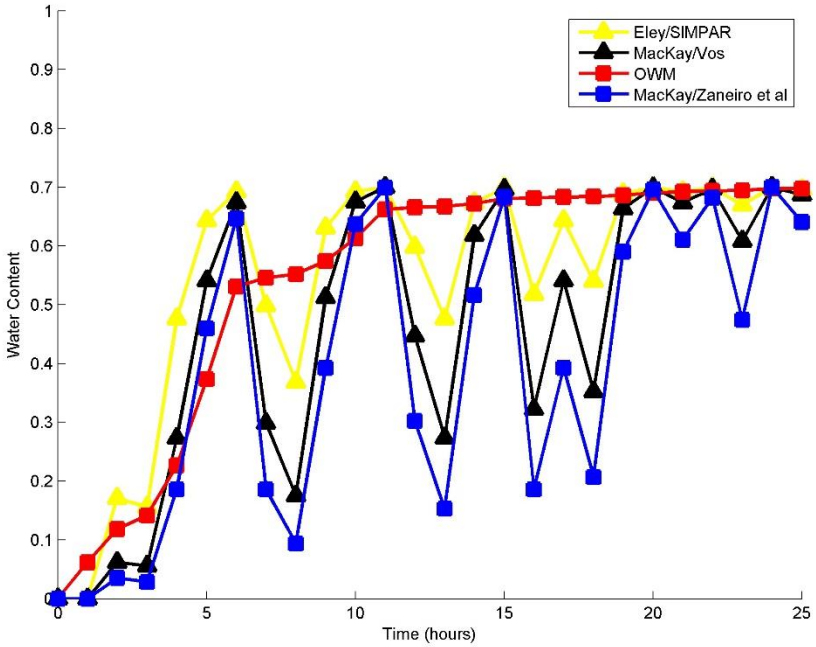

Figure 26 Water content computed under conditions of 25 hours of variable wind for 4 different algorithms

1.8 COMPUTING VARIABLE OIL DENSITY AND OIL VISCOSITY

The computation of oil emulsion viscosity, oil density, evaporation, and water content is a coupled process. None of the properties can be computed without knowledge of the other three; therefore, all four properties are computed simultaneously. The key to predict when or if oil will sink, or how it will spread, is to know the oil's density and viscosity. If the oil becomes heavier than the seawater, it will sink. If the oil thickens too much, then its tendency to spread reduces, and it might readily sink because the density generally increases with viscosity.

1.8.1 Oil Density

Matlab® routine: *oil_density.m*

Vos defined the computation of oil density according to the algorithm used by ADIOS-2 (Vos's Equation 3.20). The algorithm demonstrates density dependence on water content, temperature, and evaporative effects.

$$\rho_{oil}(y, T_{oil}) = y\rho_w + (1-y)\rho_0(0, T_{ref})[1 - c_1(T_{oil} - T_{ref})(1 + c_2 f_{evap})]$$

y is water content. T_{oil} is oil temperature in either ^oC or ^oK. T_{ref} is a reference oil temperature in either ^oC or ^oK. c_1 and c_2 are oil dependent constants. All three models used this algorithm, but Vos admitted that, due to lack of information, he/she used $c_1 = 0$, $c_2=0$ for $T_{ref} = 20^oC$. In Janeiro et al. (2008), c_1 and c_2 were renamed C_{DT} and C_{DE},

respectively. Janeiro et al. stated that C_{DE} = 0.18 and C_{DT} = $8x10^{-4}$ according to NOAA (cited by Janeiro et al. as NOAA, 1994). We used the Janeiro et al. values for ADIOS-2 (C_1 = $8x10^{-4}$ and C_2 = 0.18). We assumed that oil temperature was the sea surface temperature (Lehr, 2001).

f_{evap} and y are the fraction of evaporated oil and water content, respectively. The emulsification module provides the water content, and f_{evap} is computed in the evaporation module. However, if the oil dependent constants, c_1 and c_2, were both 0, then oil density would depend only on water content. ρ_0 is a reference oil density (at time = 0 with the reference T_0 and water content at time = 0; that is, the time of the spill). Water density (ρ_w) was constant in both SIMPAR and DREAM/OWM and was 1025 kgm^{-3} and 1030 kgm^{-3}, respectively, according to Vos's tests. In ADIOS-2, the water density is dependent on water temperature and salinity so we defined the these as 15°C and 25, respectively, and we computed water density using the equation of state.

We tested the density algorithm, coupled to emulsification and evaporation, for the three weathering models (using constant water density and variable water density) for constant wind and the variable wind data for five hours and 25 hours (as before). We held the viscosity constant at 1×10^{-6}. We did not have any results from Vos with which to compare our test results. We used Ekofisk Exxon as our test oil blend. Our computations of evaporation and emulsification were for constant water parameters and oil viscosity.

The computation of evaporation for SIMPAR and OWM had no effect because c_1=0 and c_2=0 for these models, whereas we used the Janeiro et al. values for the constants for ADIOS-2. f_{evap} for ADIOS-2 was computed using the S&M variation initially reported by Bobra (1992) and described by Fingas (2011, 2013). We used Short's (2013) algorithm to compute f_{evap} for SIMPAR and OWM.

We used Eley (1988), as reported by Vos, to compute water content for SIMPAR, Vos's version of MacKay (1980) to compute water content for ADIOS-2, and Vos's version of the SINTEF algorithm, combined with MacKay (1980) to compute water content for OWM.

1.8.1.1 Oil Density with No Wind

In the case of no wind, the two models, ADIOS-2 and OWM, have similar rates of increasing density, and density computed with the SIMPAR algorithm increased the fastest (**Figure 27**).

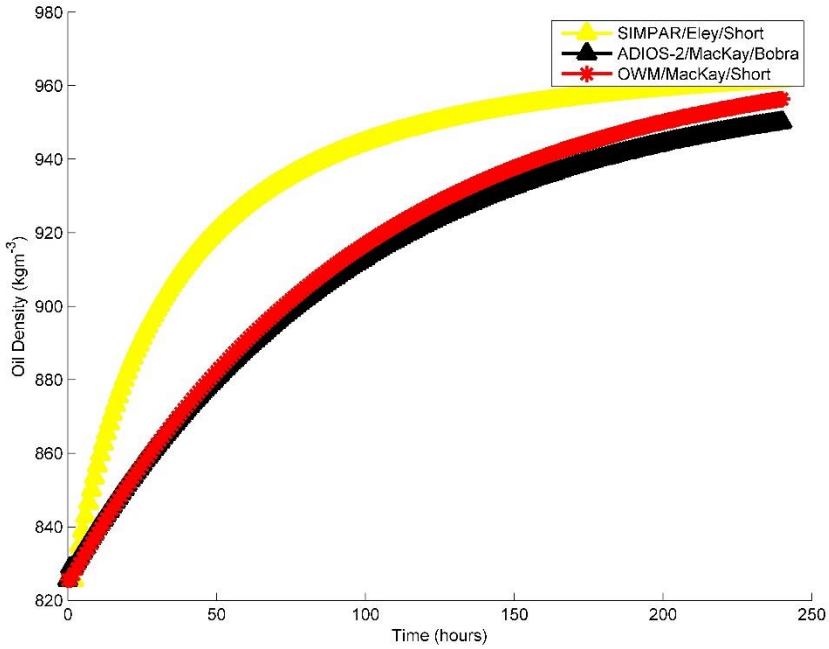

Figure 27 Oil density was computed using 3 model algorithms with no wind effects. Emulsion was computed using Eley (1988) for SIMPAR, MacKay (1980) for ADIOS-2 (Vos, 2005), and a combination of SINTEF (2005) and MacKay (1980) for OWM.

1.8.1.2 Oil Density with Constant Wind = 8 ms^{-1}

A plot of oil density for constant wind is shown in **Figure 28**. In **Figure 28**, all the models show density increasing similarly. The density that we computed with the ADIOS-2 algorithms did not achieve the maxima of the other two models.

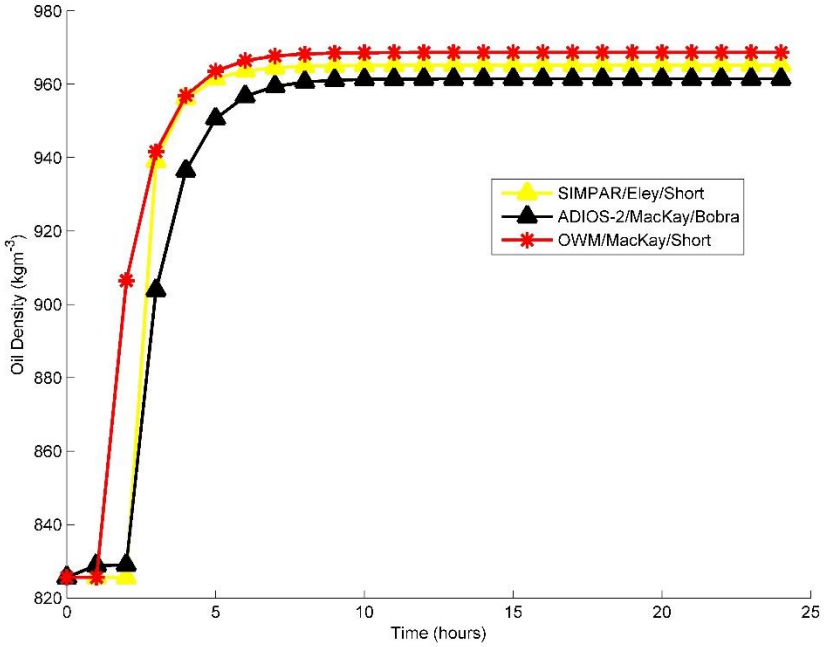

Figure 28 Computed oil density using constant wind = 8 ms^{-1}

1.8.1.3 Oil Density with Variable Wind, Constant Water Parameters

Below is a plot of oil density for the variable wind speed for 5 and 25 hours. The wind influence on the water content affects the oil density more than the evaporation rate of the oil slick. Only the OWM algorithms produced a physically realistic oil density.

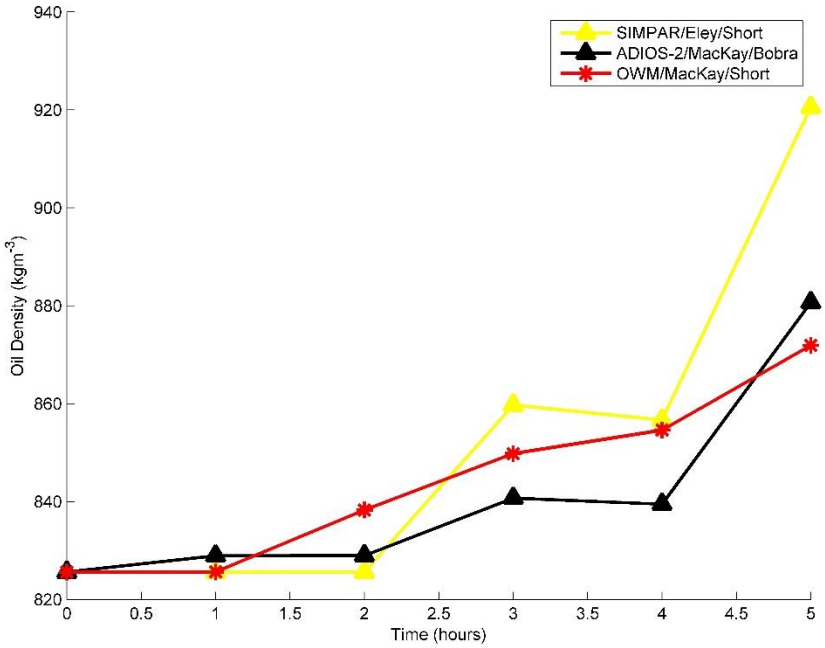

Figure 29 Computed oil density using variable wind for 5 hours using 3 model algorithms

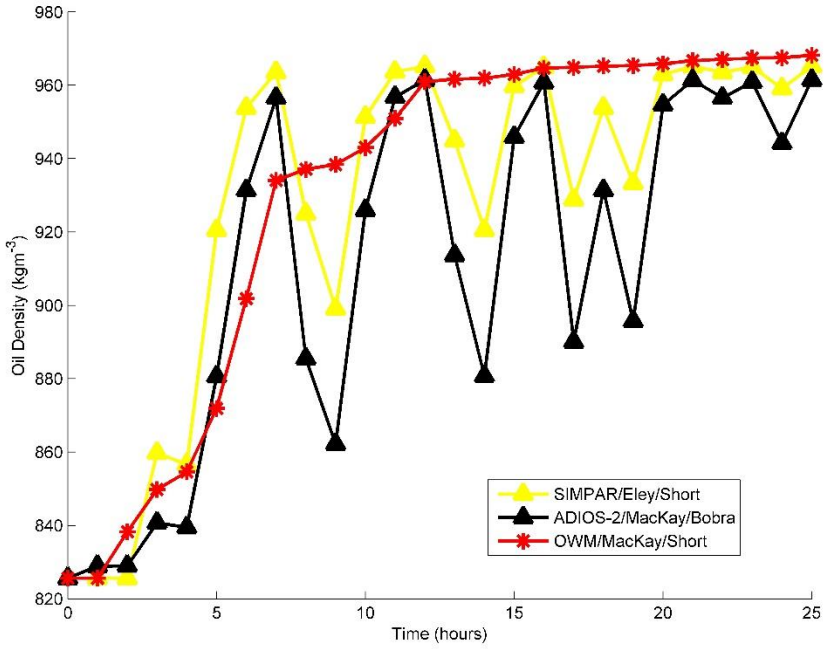

Figure 30 Computed oil density using variable wind for 25 hrs

1.8.1.4 Oil Density with No Wind, Constant Wind, and Variable Wind using empirical equation from Fingas (2013) for evaporation

For this section, we computed the oil density using the empirically derived evaporation equation for Ekofisk described by Fingas (2013). All the models used the same evaporation value computed with this equation, and therefore the results highlight the difference that the emulsion algorithms make to the commonly computed density. The only difference between the model computations of density were the two water densities that we used for SIMPAR/ADIOS-2 and OWM (1025 kgm^{-3} and 1030 kgm^{-3}, respectively). The resulting oil density time series are shown in **Figure 30** to **Figure 33** for computations with no wind, a constant wind speed, and 25 hrs of variable wind speed. The most noticeable difference between these results and the earlier ones is that now the density provided by the ADIOS-2 model algorithm for water content is more in line with SIMPAR. In addition, we can see that using a variable wind speed as input into any of the models is felt most by the emulsification algorithm.

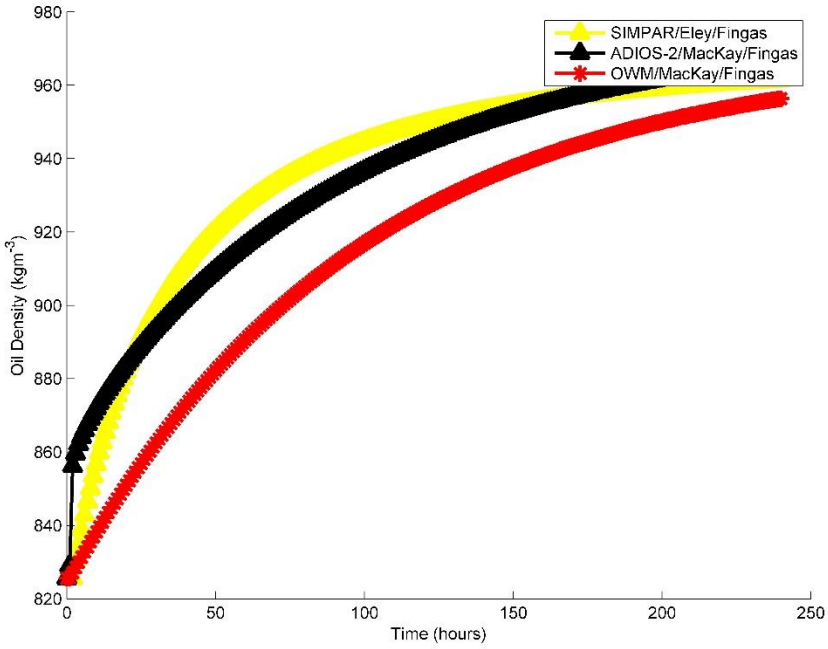

Figure 31 Computed oil density using no wind, but using the empirical equation for Ekofisk described in Fingas (2013) for the evaporation computations

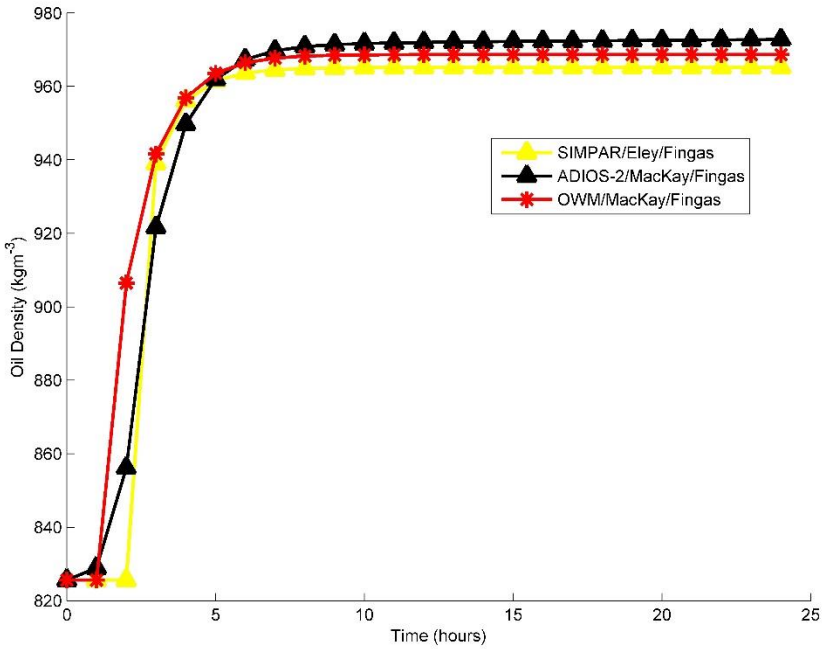

Figure 32 Computed oil density using constant wind speed = 8 ms^{-1}, but using the empirical equation for Ekofisk described in Fingas (2013) for the evaporation computations

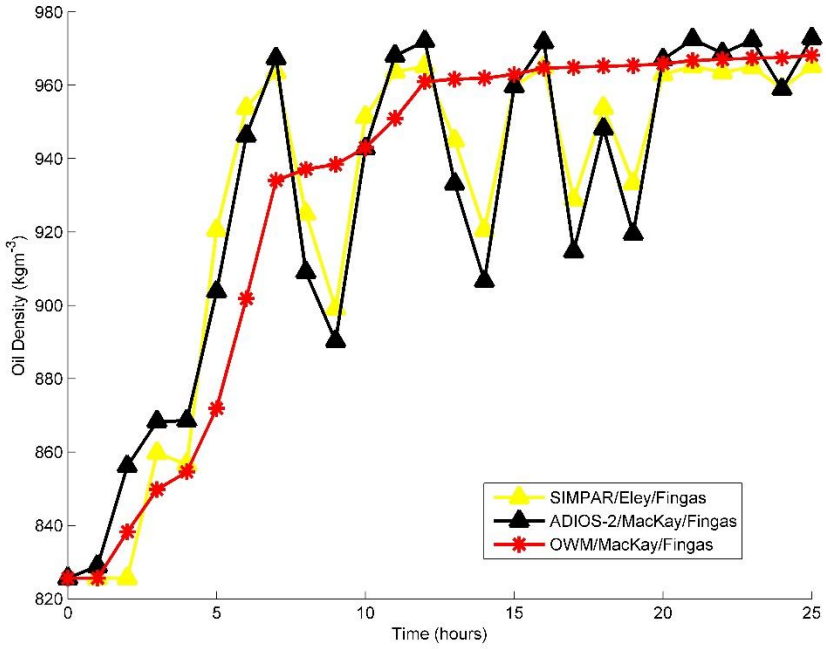

Figure 33 Computed oil density using variable wind speed for 25 hours, but using the empirical equation for Ekofisk described in Fingas (2013) for the evaporation computations

1.8.2 Oil Kinematic Viscosity

Matlab® routine: *oil_viscosity.m*

Vos described the computation of kinematic viscosity of oil as the combination of evaporative effects, water content, and temperature effects. We computed oil viscosity using four different algorithms for each of the three weathering models. The first algorithm only considers the effects of emulsification on viscosity (Mooney, 1951), and the second algorithm considers emulsification and evaporation (Guo and Wang, 2009). The last two algorithms consider emulsification, oil temperature, and evaporation (Janeiro et al., 2008; Vos, 2005). Vos presented relations based on Mooney, and those used in OWM, plus another found in Perry's Chemical Engineering Handbook (1973).

1.8.2.1 Mooney (1951)

We used Mooney's algorithm to compute the oil emulsion viscosity. This algorithm is defined as Equation 3.21 in Vos and Equation 6 in Lehr (2001):

for

- *a=2.5*
- *b=0.654*

$$\nu(t) = \nu_0 \exp\left(\frac{ay(t)}{1-by(t)}\right)$$ Equation 3.21 in Vos

- *y* is the water content
- ν_0 is the reference/initial oil viscosity.

We used the oil viscosity given by our oil database for ν_0.

1.8.2.2 Guo and Wang (2009)

Guo and Wang coupled the oil emulsion viscosity with evaporative exposure.

$$\nu(t) = \nu_0 \exp(K_c f_{evap}) \exp(\frac{ay(t)}{1-by(t)})$$ Guo and Wang, Equation 26

K_c is an oil dependent constant that is between 1 and 10 (Guo and Wang, 2009). Guo and Wang used $K_c=1$, which they based on MacKay et al. (1980); however, Wang et al. (2005) had $K_c=1x10^4$. We used $K_c=4$ because it gave a more realistic result than Guo and Wang's and Wang et al.'s different values.

1.8.2.3 Vos

Vos gave two different algorithms for computing oil viscosity with time. SIMPAR and ADIOS-2 used the same algorithm and OWM used the second algorithm.

According to Vos, SIMPAR and ADIOS-2 used a combination of Mooney to give the water content component, MacKay et al. (1983) for evaporative effects, and Perry's handbook for temperature effects:

with $c_b=5$,

$$\nu(t) = \nu_0 \exp(c_b(f_{evap}(0) - f_{evap}(t))) \exp(\frac{ay(t)}{1-by(t)}) \exp(\frac{c_T}{T_{oil}} - \frac{c_T}{T_0})$$ Equations 3.21, 3.22, and 3.24 in Vos

We defined the coefficient, cT = 5, and we used the same *a* and b as in the original Mooney equation (*a=2.5*; *b = 0.654*).

OWM's algorithm was similar to the one for SIMPAR and ADIOS-2, but the effects of water content on viscosity were computed slightly differently, and the evaporative effects are dependent on empirical constants. For OWM, we programmed a combination of the Mooney algorithm defined in the SINTEF manual (Equation 29 from the manual) and the MacKay et al. (1983) algorithm for evaporative effects defined by Vos in Equation 3.23 of the review. Vos stated that in OWM the effects of temperature on oil viscosity were ignored.

$$\nu(t) = \nu_0 \exp(a_\nu + b_\nu f_{evap}(t))) \exp(\frac{ay(t)}{100 + by(t)})$$

However, from the SINTEF manual, we used a=5 and b=0.9, and we used $a_\nu = c_b f_{evap}(0)$ and $b_\nu = -c_b$ because a_ν and b_ν are regression factors that were not given in either Vos or the SINTEF manual. We let $c_b=5$ as for SIMPAR and ADIOS-2. The SINTEF manual actually cited Mooney to compute the emulsion viscosity, but Vos says that DREAM/OWM used Mooney and evaporative exposure to compute oil viscosity, so we used a combination algorithm for OWM, but used SINTEF's version of Mooney to describe the effects of emulsification. The SINTEF manual also stated that, from least squares regressions, *a* ranged from -10 to 5, and *b* ranged from -2 and 0.9. We arbitrarily chose

a=5 and *b=-2* for our test of Ekofisk Exxon, but we tried the entire range and saw that the results did not differ regardless of the values that we chose for *a* and *b*.

In Vos's review, Vos stated that OWM used the same Mooney algorithm as SIMPAR and ADIOS-2, but in the SINTEF manual, the Mooney algorithm is slightly different. The different versions of Mooney are highlighted by grey boxes in the above viscosity equations. Later, we noted that the algorithm given in the SINTEF manual gave viscosity values for OWM that were inconsistent with the other models.

1.8.2.4 Janeiro et al. (2008)

Janeiro et al. used a slightly different algorithm that included a variation of Mackay et al.'s (1980) empirical constant.

If $\nu_0 > 38$, then c_e*=10*. Otherwise, $c_e = -0.0059{\nu_0}^2 + 0.4461\nu_0 + 1.413$ where ν_0 is the oil viscosity at 15°C. This empirical constant is used as a multiplier for the evaporative effects on the viscosity.

$$\nu(t) = \nu_0 \exp(c_e f_{evap}(t)) \exp(\frac{ay(t)}{1 - by(t)}) \exp(\frac{c_T}{T_{oil}} - \frac{c_T}{T_0})$$

We tested the four viscosity algorithms by computing the changing kinematic viscosity of each with no wind effects, a constant wind speed, and variable wind speed.

1.8.2.5 Computing Oil Viscosity with No Wind

Figure 34 to **Figure 37** present the oil viscosities that we computed using the inputs that Vos used associated with each of the three weathering models, but computed using the four different viscosity algorithms that we have outlined. Each model used different inputs according to previous computations and empirical constants of water content, evaporated fraction, and oil density and the different water densities, but viscosity was computed four times with the same algorithms for each model. If all weathering algorithms were the same and all models used the same inputs, then all the viscosities should be identical regardless of the model.

In this subsection, we used zero wind speed to compute the kinematic viscosity. In the computation, we simultaneously had to compute density, emulsification, and evaporation because water content, the fraction evaporated, and oil density were needed as inputs into the viscosity module. Evaporation was computed using the two variations of the S&M algorithm: Bobra (1992) presented in Fingas (2011, 2013) and Short (2013). The viscosities are shown in **Figure 34** and **Figure 35**. Then we recomputed viscosity with evaporation computed using the empirical equation for Ekofisk in Fingas (2013). These viscosities are shown in **Figure 36** and **Figure 37**.

Figure 34 shows that the evaporative effects from Bobra's algorithm (Fingas, 2011 & 2013) used for ADIOS-2 were very different from those from Short's S&M variation used for SIMPAR and OWM, and the G&W algorithm for computing viscosity was very sensitive to the evaporation algorithm being used. When only emulsification effects were considered in the computation of the viscosity (Mooney's algorithm for emulsion viscosity), all the models produced the expected similar viscosity magnitudes.

Figure 35 reveals that there was definitely a problem interpreting the algorithm for OWM given by Vos/SINTEF. We discovered that it was the Mooney emulsion viscosity algorithm that caused the OWM values to depart from the other models' results. What isn't visible is that the Janeiro algorithm for OWM and the Vos algorithm for ADIOS-2 produced the same result. The thicker black line for ADIOS-2 is covering the thinner red line for OWM. **Figure 35** also reveals that the temperature effects reduced the rate of the kinematic viscosity increase computed by ADIOS-2 from what was shown in **Figure 34** for ADIOS-2 and the G&W algorithm. However, the algorithms that we used for ADIOS-2 to compute evaporation, produced a more rapid increase in viscosity with the G&W algorithm than that algorithm produced for the other two models.

Figure 36 shows once more that the G&W algorithm for computing viscosity is very sensitive to evaporative effects. This figure was produced using the empirical equation for Ekofisk for all models to compute the fraction evaporated.

Figure 37 shows that the algorithm for OWM that computes viscosity, described by Vos, really does not work for that model. The viscosities that OWM produced are so much smaller than those produced by the other algorithms that the plot appears as a flat line in **Figure 37.** The Janeiro et al. algorithm, however, produces reasonable results for all the models when combined with Fingas's empirical equation for computing the fraction evaporated, and the viscosity result computed with the Vos algorithm is similar to those that are shown in **Figure 35**. The viscosity algorithms that account for evaporative effects, water content, and temperature effects are not as sensitive to the evaporation algorithm as the G&W algorithm that does not use temperature effects.

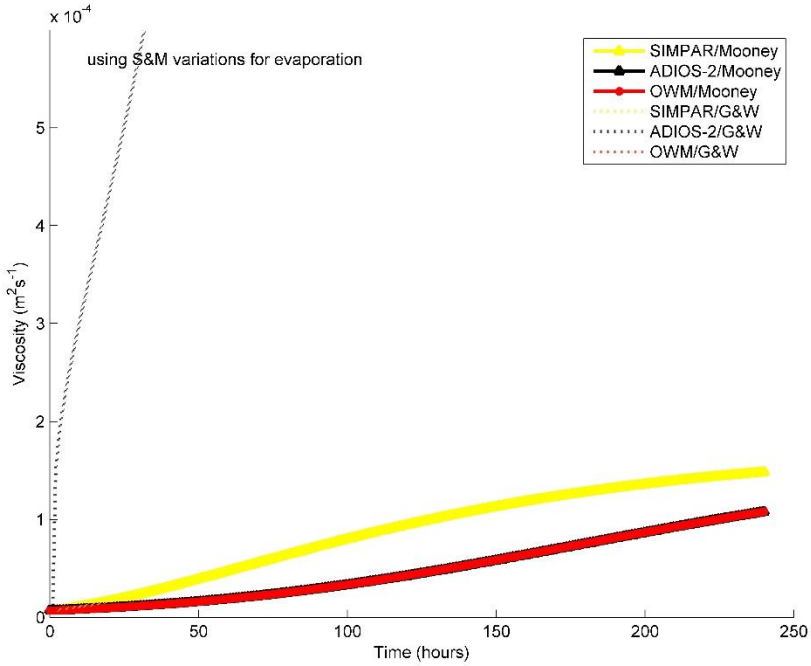

Figure 34 Computed oil viscosity with no wind and using algorithms by Mooney (1951) and Guo and Wang (2009) to compute the viscosity and evaporation algorithms from Bobra (Fingas, 2011 & 2013) for ADIOS-2 and Short (2013) for SIMPAR and OWM

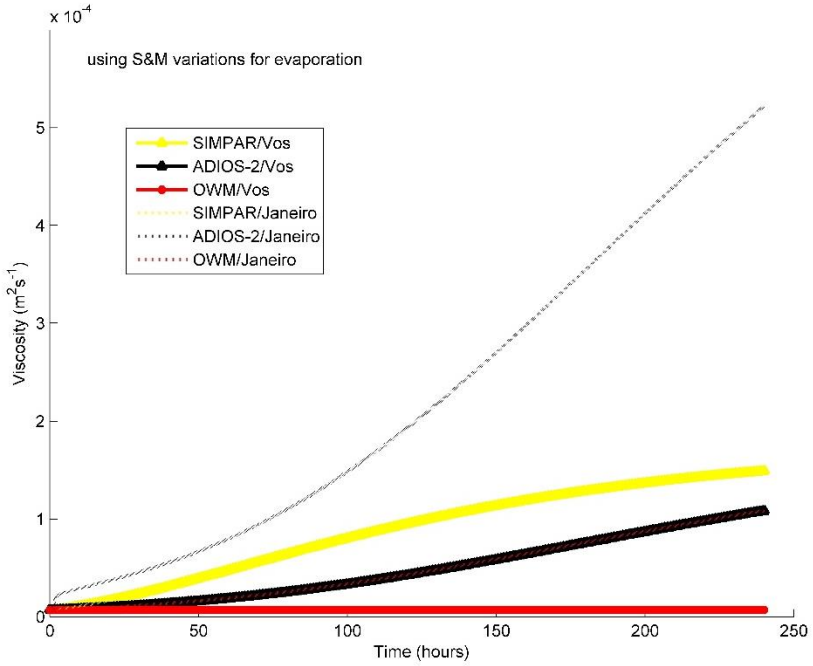

Figure 35 Computed oil viscosity with no wind and using algorithms described in Vos (2005) and Janeiro et al. (2008) to compute viscosity and evaporation algorithms from Bobra (Fingas, 2011 & 2013) for ADIOS-2 and Short (2013) for SIMPAR and OWM

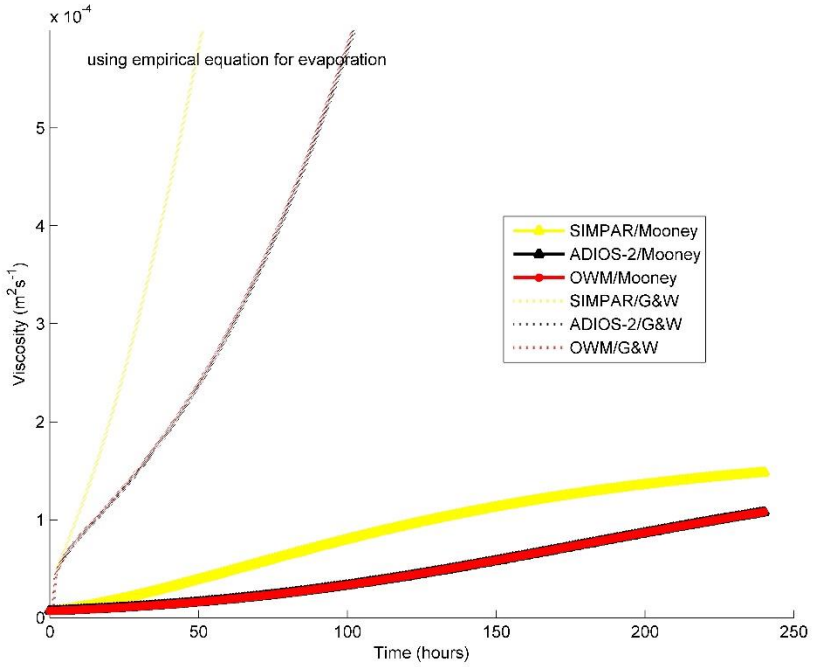

Figure 36 Computed oil viscosity with no wind and using algorithms by Mooney (1951) and Guo and Wang (2009) and evaporation computed with the empirical equation for Ekofisk described in Fingas (2013)

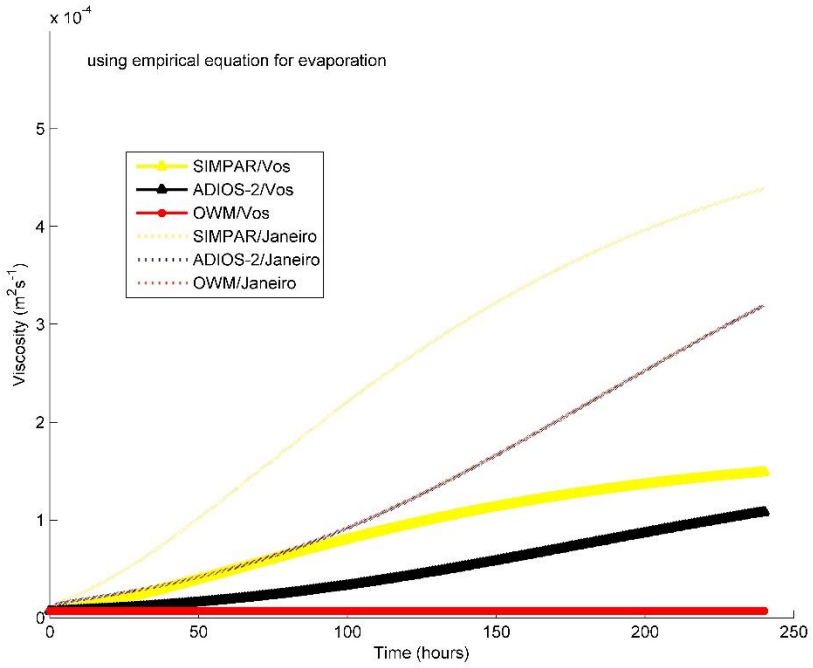

Figure 37 Computed oil viscosity with no wind and using algorithms by Vos (2005) and Janeiro et al. (2008) and evaporation computed with the empirical equation for Ekofisk described in Fingas (2013)

1.8.2.6 Computing Oil Viscosity with a Constant Wind

Figure 38 to **Figure 41** present the oil viscosities that we computed using the inputs that Vos used for the three weathering models and a constant wind speed of 8 ms^{-1}. We computed the viscosities using the four different viscosity algorithms that we have outlined.

Figure 38 presents the viscosities computed using a constant wind and Mooney's and G&W's algorithms for viscosity and variations of the S&M algorithm for evaporation: Short (2013) for SIMPAR and OWM and Bobra's algorithm (Fingas, 2013) for ADIOS-2. With the constant wind speed, the G&W algorithm produces the expected larger viscosities via the evaporative effects with the constant wind speed than without it. However, it is clear that the Bobra algorithm that we used for ADIOS-2 is producing evaporative effects that are causing the G&W algorithm to produce viscosities that are much greater than what the other models produced.

Figure 39 reveals, once more, that larger viscosities result when temperature effects are ignored. This fact is really highlighted in **Figure 40** and **Figure 41**. In **Figure 40**, the viscosities produced from the G&W algorithm were much larger when we computed evaporation with the empirical equation for Ekofisk (Fingas, 2013) than when we used the S&M algorithms to compute evaporation. **Figure 41** shows that when the effect of temperature on viscosity is included in the algorithm, despite the evaporation that depends on air temperature, the oil viscosity values decrease and reach more expected values.

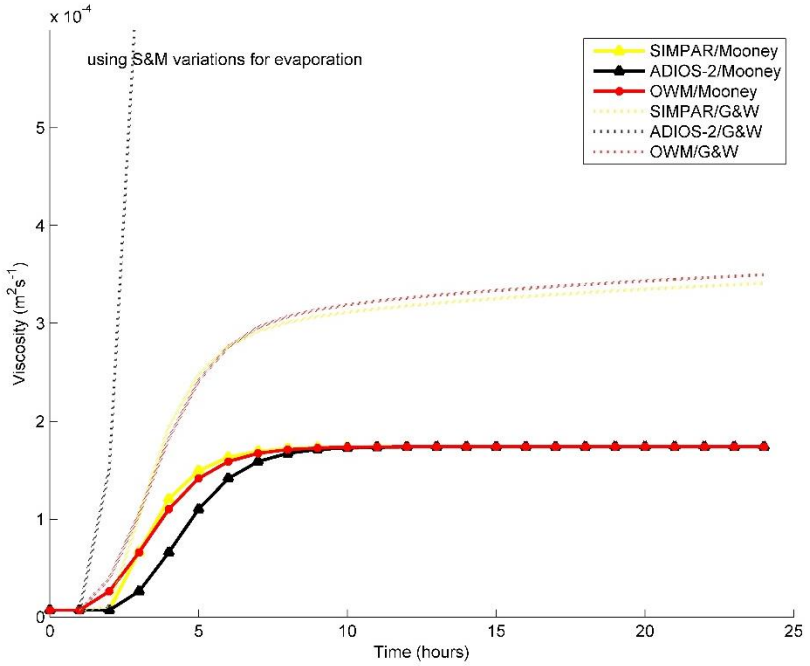

Figure 38 Computed oil viscosity computed with constant wind (= 8 ms^{-1}) using algorithms by Mooney (1951) and Guo and Wang (2009) for the 3 oil spill weathering models and evaporation algorithms from Bobra (Fingas, 2011 & 2013) for ADIOS-2 and Short (2013) for SIMPAR and OWM

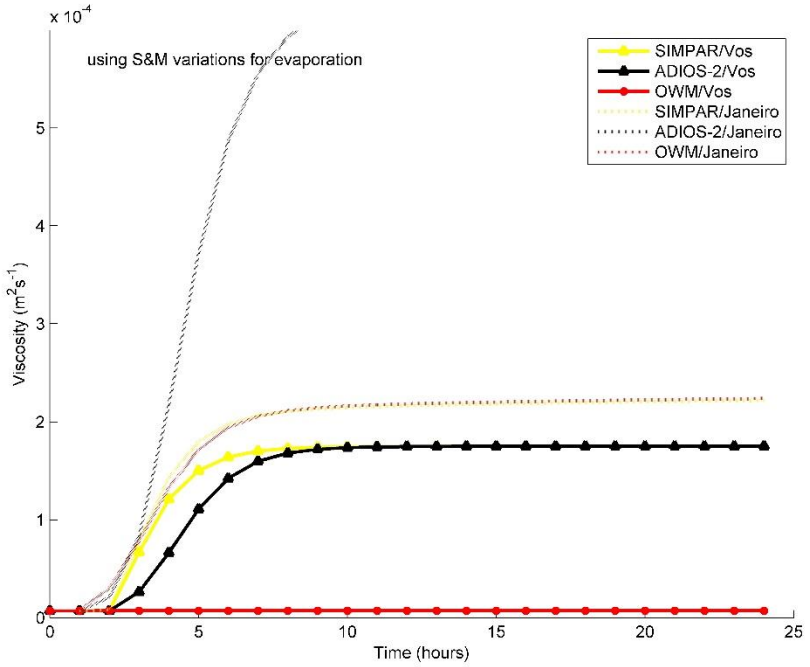

Figure 39 Computed oil viscosity computed with constant wind (= 8 ms^{-1}) using algorithms described in Vos (2005) and Janeiro et al. (2008) for the 3 oil spill weathering models and evaporation algorithms from Bobra (Fingas, 2011 & 2013) for ADIOS-2 and Short (2013) for SIMPAR and OWM

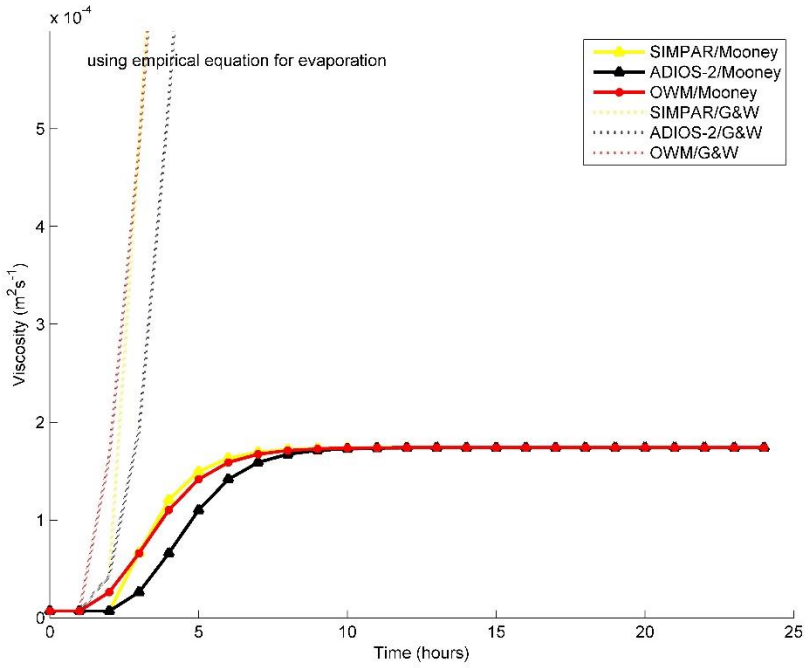

Figure 40 Computed oil viscosity computed with constant wind (= 8 ms^{-1}) using algorithms by Mooney (1951) and Guo and Wang (2009) for the 3 oil spill weathering models and evaporation computed with the empirical equation for Ekofisk described in Fingas (2013)

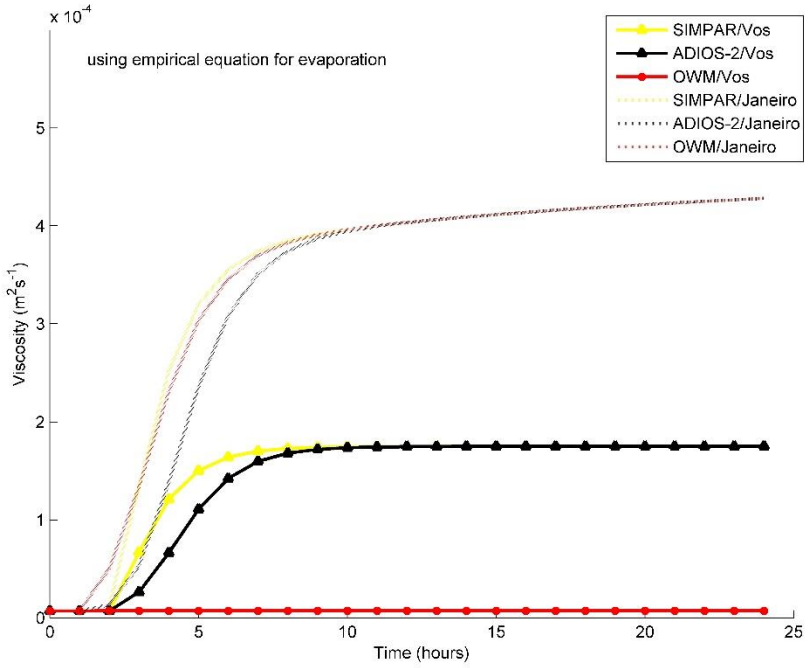

Figure 41 Computed oil viscosity computed with constant wind (= 8 ms^{-1}) using algorithms by Vos (2005) and Janeiro et al. (2008) for the 3 oil spill weathering models and evaporation computed with the empirical equation for Ekofisk described in Fingas (2013)

1.8.2.7 Computing Oil Viscosity with 25 Hours of Variable Wind

In this section, we computed viscosities using 25 hours of variable wind in the computations.

Figure 42 to **Figure 45** show the results of the viscosity computations that we made using 25 hours of variable wind speed. The OWM model appears to be the most insensitive to having the wind speed change every hour when only water content was considered (Mooney viscosity algorithm in **Figure 42** and **Figure 44**). The combination of the OWM model inputs, the Janeiro et al. viscosity algorithm, and Fingas's empirical equation for evaporation of Ekofisk was insensitive to the variable wind speed (**Figure 43** and **Figure 45**). Once more, we saw that the OWM algorithm presented in Vos produced viscosities that were unrealistic compared to the other algorithms (**Figure 43** and **Figure 45**).

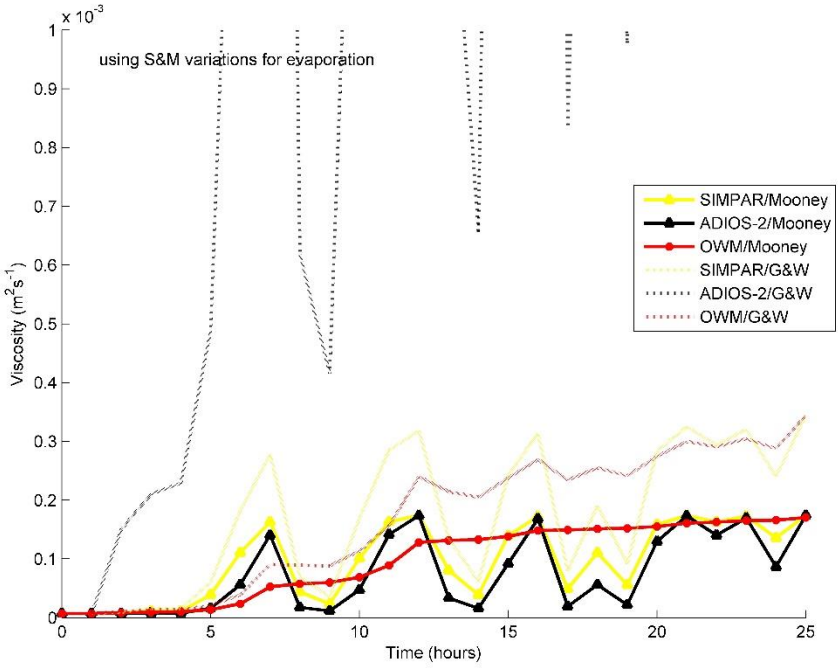

Figure 42 Computed oil viscosity using 25 hours of variable wind and algorithms by Mooney (1951) and Guo and Wang (2009) for the 3 oil spill weathering models and evaporation algorithms from Bobra (Fingas, 2011 & 2013) for ADIOS-2 and Short (2013) for SIMPAR and OWM

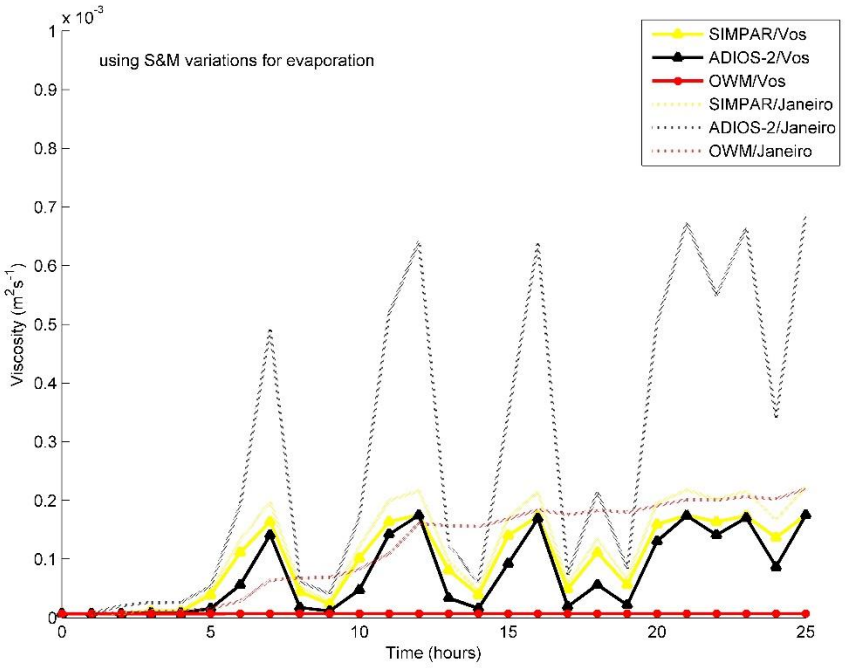

Figure 43 Computed oil viscosity using 25 hours of variable wind and algorithms described in Vos (2005) and Janeiro et al. (2008) for the 3 oil spill weathering models and evaporation algorithms from Bobra (Fingas, 2011 & 2013) for ADIOS-2 and Short (2013) for SIMPAR and OWM

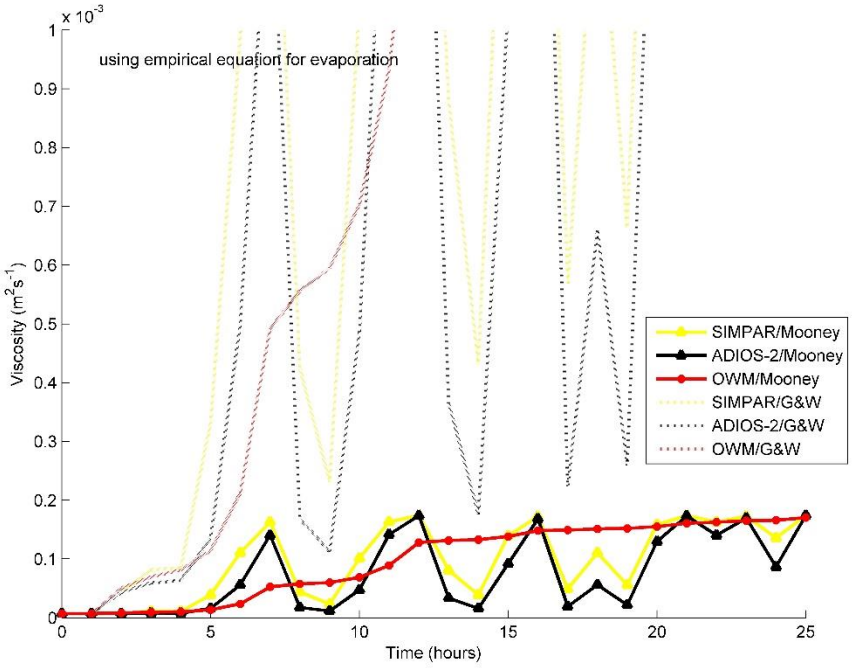

Figure 44 Computed oil viscosity using 25 hours of variable winds and algorithms by Mooney (1951) and Guo and Wang (2009) for the 3 oil spill weathering models and evaporation computed with the empirical equation for Ekofisk described in Fingas (2013)

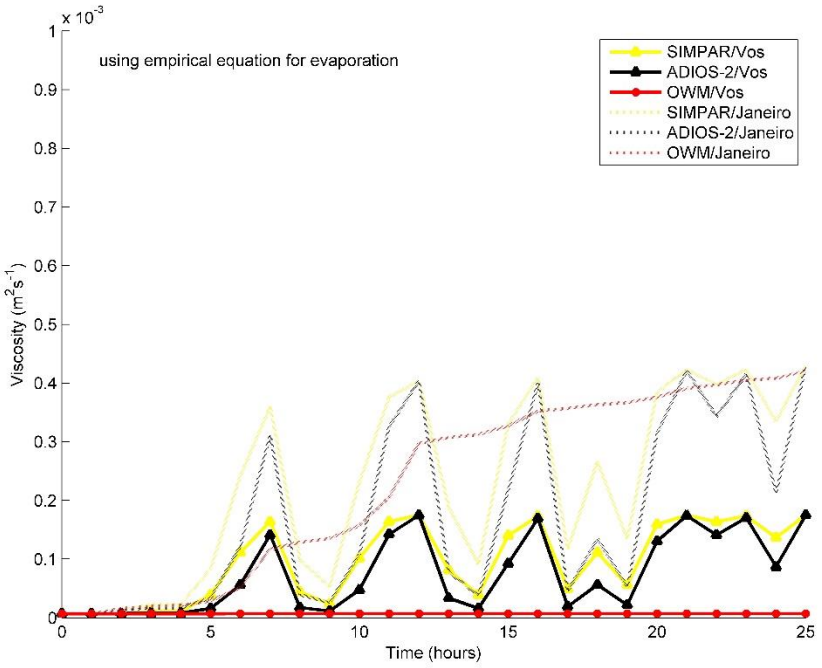

Figure 45 Computed oil viscosity using 25 hours of variable wind and algorithms described in Vos (2005) and Janeiro et al. (2008) for the 3 oil spill weathering models and evaporation computed with the empirical equation for Ekofisk described in Fingas (2013)

1.9 SUMMARY OF PART 1

In Part 1 of this study, we explored oil weathering algorithms that were presented by Vos (2005) in a review of popular oil weathering models. We found that three models described by Vos were sensitive to the inputs used to compute the various weathering process parameters. This was especially true for evaporation, oil emulsification, and for the oil viscosity. Then, when looking through the literature, we noticed that different researchers used algorithms, with slight variations, based on the same theory; for example, evaporation and the work of Stiver and Mackay was a popular form of evaporation theory, yet some researchers had equations that were variations of the theory that were specific to their problems. Applying these variations to our testing, gave different results for each of the inputs associated with the three models described by Vos. Having so many choices for algorithms made it difficult for us to decide on a single algorithm to test so we continued to use several formulae in Part 2 of our study.

We found that all the algorithms that used wind speed to compute the weathering properties were very sensitive to a varying wind. This was likely because these algorithms were developed in laboratory experiments under conditions of constant wind speed. The algorithm that was most insensitive to a time varying wind speed was the one used by OWM for computing oil viscosity over time.

For the rest of the summary of Part 1, we describe the Matlab® functions that we wrote to compute the weathering process parameters described in Vos and elsewhere: initial release/spreading, dispersion (entrainment), evaporation (evaporated fraction), emulsification (water content), oil density, and oil viscosity. There is a summary table of all the equations that we explored in the Appendix at the end of the report.

1.9.1 The Oil Database

Before running any of the modules, it was necessary to read the oil database.

1.9.1.1 Matlab® call

```
oildata = read_oil_data_xlsx
```

1.9.2 Release/Initial Spreading

There are two equations that we used to compute the initial spill release.

1. SIMPAR and ADIOS-2 (based on Fay and Hoult, 1971)

$$R = \frac{k_2^2}{k_1}\left(\frac{V_{oil}^5 g(\rho_w - \rho_{oil})/\rho_w}{v_w^2}\right)^{1/12}$$

2. OWM/DREAM (based on Reed, 2001)

$$X = \left[\frac{3}{2}\frac{V_{oil}^2 \rho_{oil} g'}{B^2}\right]^{\frac{2}{5}} (\rho_w \mu_w)^{\frac{-1}{5}} U_{H2O}^{\frac{-3}{5}}$$

1.9.2.1 Matlab® call

```
[R,X,V] =
release(which_model,h,V_oil,rho_oil,rho_H2O,visc_H2O,B,U_H2O,xmin,xmax)
```

1.9.2.2 Inputs

- which_model: 'simpar','adios', or 'owm'
- rho_oil: ρ_{oil} density of the oil (kgm^{-3})
- V_oil: V_{oil} total mass of the spill or the volume of the spill
- rho_H2O: ρ_w density of water (kgm^{-3})
- visc_H2O: ν_w kinematic viscosity of water (m^{2}s^{-1})
- xmin: time minimum for integral; used for OWM/DREAM model only
- xmax: time maximum for integral; used for OWM/DREAM model only
- h: oil film thickness (m)

1.9.2.3 Outputs

- R = radius (m) of the spill (Equation 3.1 for SIMPAR & ADIOS)
- X = length scale (m) of the oil slick (Equation 3.2 for OWM/DREAM)
- V = volume (m^3) of the oil slick approximated by uniform thickness, Vos p. 14 footnote

V is equal to the input oil volume of the spill for SIMPAR and ADIOS-2, but V is computed by OWM using the oil thickness and the length scale, X. It is an iterative process in OWM, but we only computed the one iteration because the release only occurs once.

1.9.2.4 Defined parameters:

- g = 9.80665 in ms^{-2}
- k_1 = 1.15
- k_2 = 1.45

1.9.3 Dispersion

The dispersion module uses the oil viscosity in its computation so that it is connected to evaporation. The computation uses wind speed and wave energy.

1.9.3.1 SIMPAR and ADIOS-2

$$Q = \frac{d_{max}^{1.7}}{1.7} \times C_0 D_{ba}^{0.57} F_{wc} S_{cov}$$ Equation 3.10 in Vos

where

- *Q* is the entrainment rate of the of oil droplets
- d_{max} is the maximum oil droplet diameter in m, and we defined d_{max}=70 µm
- D_{ba} is the dissipative breaking wave energy per unit surface area
- C_0 is a proportionality constant
- S_{cov} is the fraction of the sea surface covered by oil (=1.0 for closed patches)

Dba, the dissipative wave energy, is defined using Equation 3.7 in Vos:

$$D_{ba} = 0.0034 \rho_w \, g \left(\frac{H_0}{\sqrt{2}}\right)^2$$ Equation 3.7 in Vos

$$H_0 = \frac{0.243 \, U_w^2}{g}$$ also included in Equation 3.7 in Vos (significant wave height)

with

- ρ_w as the density of water
- g = 9.80665 ms^{-2}
- U_w is the wind speed in ms^{-1} (@10 m)

We computed the fraction of the sea surface hit by breaking waves according to Holthuijsen and Herbers (1986) for SIMPAR and ADIOS-2, as cited by Vos in Equation 3.5:

$$F_{wc} = \frac{0.032 \max(U_w - 5.0; 0.0)}{T_w}$$ Equation 3.5 in Vos

where

- F_{wc} is per unit time
- T_w is the wave period in s^{-1}

For v< 125; C_0 = $1827v^{-0.04658}$ and if v> 125; C_0 = $1827v^{-1.1951}$ where v is in cSt

1.9.3.2 OWM/DREAM

$$Q(d) = C_0 D_{ba}^{0.57} d_o^{0.7} \Delta d S_{cov} F_{wc}$$ Equation 11 and 2 in D&S (1988) and Delvigne (1993), respectively (also in the SINTEF manual)

$$d_o = \frac{C\nu^{0.34}}{\sqrt{e}}$$ Equation 3.9 in Vos

where

- *C* is a parameter that varies between 500 and 3400; we used *C=1000*.
- *v* is the oil viscosity
- *e* is the rate of energy dissipation = 1000 $Jm^{-3}s$
- Δd is a particle diameter interval in m
- C_0 is an empirically derived entrainment coefficient

DREAM/OWM, however, computes F_{wc} with Equation 3.6, which is from Monahan and O'Muircheartaigh (1980) and cited by Vos:

$F_{wc} = 3 \times 10^{-6} U_w^{3.5}$ Equation 3.6 in Vos

$C_0 = 4450v^{0.4}$ Equation 3.12 in Vos

1.9.3.3 Matlab® call

```
[C0,Q,H0,Dba,dmax,Fwc] =
dispersion(which_model,N0,Nd,visc,Scov,Uw,rho_water,Tw)
```

1.9.3.4 Inputs

- `which_model: 'simpar','adios', or 'owm'`
- `Scov: sea coverage factor of oil (=1.0); if not enclosed then sea_coverage must be decreased`
- `N0 normalization factor for determining oil droplet diameter (m); never actually used but defined = 1`
- `Nd # droplets per diameter (d0); never actually used but defined = 1`
- `Uw: wind speed (m/s)`
- `rho_water: density of water (computed)`
- `visc: viscosity of oil (computed; please note the units (m²s⁻¹))`
- `C = parameter varying from 500-3400 (=1000)`
- `Tw = wave period (s^-1) (=1)`

1.9.3.5 Outputs

- C_0: proportionality constant
- Q: entrainment rate of oil droplets per unit surface area (kg/s/m^2)
- H_0: significant wave height
- D_{ba}: dissipative wave energy
- d_{max}: maximum diameter of oil droplets (=70µm for SIMPAR and ADIOS; computed for OWM)
- F_{wc}: fraction of the sea surface hit by the waves (computed)

1.9.3.6 Defined Parameters

- g = 9.80665 in ms^{-2}

1.9.4 Evaporation

We computed evaporation several ways. Some algorithms are what Vos had in the model review and a few were found in the literature. We started with the single fraction theory described in Fingas (1995) and continued with four variations of Stiver and MacKay's (1984) semi-empirical distillation theory that accounts for temperature effects on the evaporation process.

1.9.4.1 Single Fraction Theory

In the end, we abandoned using this formula for single fraction theory, but we left it in the code as an option.

$$\frac{x}{x_0} = e^{(-KtPvp/x_0)}$$

- x is the amount of crude at time, t.
- x_0 is the original amount of crude when weathering begins.
- t is time in seconds.
- Pvp is the vapour pressure.
- K is the mass transfer coefficient.

$$K = 0.029(U_w)^{0.78} D^{-0.11} S_c^{0.067}$$ Equation 4 in Fingas (1995)

- *D* is the slick diameter in m.
- S_c is the Schmidt number.

1.9.4.2 Semi-empirical Distillation Theory

Stiver and MacKay (1984) is the basis of the four evaporation algorithms that we used.

For SIMPAR and OWM: Short (2013)

$$f_{evap} = \ln\left[1 + \left(\frac{12191}{T_{oil}}\right)\theta e^{8.2-\left(\frac{5239}{T_{oil}}\right)}\right] / \left(\frac{12191}{T_{oil}}\right)$$

where

$$\theta = K\frac{Area}{V_o}t$$

with

$K = 0.0015U_w^{0.78}$ for SIMPAR

$K(t) = C_d U_w(t)$ for OWM (note that U_w is meant to vary with time)

where $C_d = \left(\frac{U_w^*}{U_w(t)}\right)^2$ and $U_w^* = \begin{cases} CU_w(t) & for \quad U_w(t) < u_1 \\ Cu_1 + (Du_2 - Cu_1)\frac{U_w(t)-u_1}{u_2-u_1} & for\ u_1 \le U_w(t) \le u_2 \\ DU(t) & for \quad U_w(t) > u_2 \end{cases}$

- C = 0.0323
- D = 0.0474
- u_1 = 7 ms^{-1}
- u_2 = 20 ms^{-1}

For ADIOS-2: Bobra (1992) and Hamoda (1989) as described by Fingas (2011, 2013)

$$f_{evap} = \ln\left[\quad 1 + B\left(\frac{T_G}{T_{oil}}\right)\theta e^{A-B\left(\frac{T_0}{Toil}\right)}\right]\left(\frac{T_{oil}}{BT_G}\right)$$

- T_0 is the initial boiling point.

- T_G is the distillation curve gradient.

where

$$\Theta = K\frac{Area}{V_o}t$$

with

$K = 1.68 \times 10^{-5} API^{1.253} T^{1.80} S^{0.1441}$ Hamoda (Equation 31 in Fingas (2013))

- T is the sea surface temperature.
- S is the sea surface salinity.

1.9.4.3 Empirical Equations for all models from Fingas (2013)

For Ekofisk (Ekofisk Exxon in our tests):

$$f_{evap} = [4.92 + 0.045T]\ln(t)$$

For Troll (used in our tests, but results not shown in this report):

$$f_{evap} = [2.26 + 0.045T]\ln(t)$$

For Cold Lake Bitumen (used later):

$$f_{evap} = [-0.16 + 0.013T]/\mathrm{t}$$

- T is the air temperature.

Buchanan and Hurford (1988)

We tested this equation, but abandoned it. However, we left the code intact.

$$f_{evap} = \frac{15}{C_2} ln\left[\frac{C_2 U_w^{0.78} t}{6000h} exp\left(16.6 - \frac{C_1}{15}\right) + 1\right]$$

C_1 = 10.3 and C_2 = 6.3

SIMPAR with known molecular weight (Vos, 2005)

We abandoned this formula because we only knew the molecular weight for oils that Vos used.

$$K = 0.029(3600U_w)^{0.78} D^{-0.11} S_c^{0.067} \sqrt{\frac{M_w+29}{M_w}}$$

- D is the diameter of the slick (m); use the radius length scale.
- S_c is the Schmidt number of cumene (= 2.7).
- U_w is wind speed in metres per hour, but converted to metres per second with Vos's multiplication of 3600.
- M_w is the molecular weight of the oil.

1.9.4.4 Matlab® call

```
[ x,Pvp,f_evap,Fe ] = evaporation(which_model,oil_type,Toil,S,API,...
    Tair,Uw,x0,X,V_oil,Area,h,oildata,t,visc_oil,f_evap_old,x_old)
```

1.9.4.5 Inputs

- which_model: 'simpar','adios', or 'owm'
- oil_type: type of oil that was spilled; use what is in the oil database
- Toil: oil temperature (deg K); use sea surface temperature
- Tair: air temperatue (deg K)
- S: water salinity in ppt
- API: API of the spilled oil (from oil database)
- Uw: wind speed in ms^{-1}
- x0: amount of a particular component of a crude oil at t=0 (time); for computing single fraction theory (= V_oil)
- X: spill length scale determined from *release.m*
- V_oil: volume of oil spilled in m^3
- Area: areal size of the oil spill in m^2
- h: thickness of the oil slick in m
- oildata: oil database input (*read_oil_data_xlsx.m*)
- t: time in hours (converted to seconds within the function)
- visc_oil: viscosity of oil (computed; please note the units (m^2s^{-1}))
- f_evap_old: f_evap from the previous time step (@ t-1); this is where we store the S&M semi-empirical distillation theory results
- x_old: x_old from the previous time step (@ t-1); this is where we store the single fraction theory result

This function calls several other functions:

- *f_evap = get_evaporated_fraction*(which_model, oil_type,Toil,Tair,S,API,Uw,h,t,V0,Area,f_evap_old,oildata) – to compute the evaporated fraction using semi-distillation theory (S&M variations) or empirical equations
- *Cd = get_air_sea_drag_coefficient(which_model,Uw)* – called from within *get_evaporated fraction.m* to compute the drag coefficient (used to compute *K* for OWM)
- *Pvp = find_oil_data('Pvp',oil_type,oildata)* – to get the vapour pressure from the database

1.9.4.6 Outputs

- x: amount of oil evaporated from single fraction theory
- Pvp: vapour pressure (from the database)
- f_evap: fraction evaporated computed using the different semi-empirical distillation theories
- Fe: fraction evaporated computed using Buchanan and Hurford

1.9.4.7 Defined Parameters

- R = 8.31451 is the ideal gas constant; no longer used, but was used to compute *K*
- Sc = 2.7 is the Schmidt number used in the single fraction theory computation

1.9.5 Emulsification

We computed emulsification three different ways with a maximum water content = 0.7 (y_{max} = *0.7*). The water content only relied on wind speed, and the process is not connected to any other weathering process.

1.9.5.1 SIMPAR

Emulsification for SIMPAR is based on Eley (1988).

$y = \frac{x}{(6+x)}$ variation of Equation 3.25 in Vos

$x = x_{max}\,(1 - e^{-k_s t})$ Equation 3.26 in Vos

$x_{max} = \frac{6y_{max}}{(1-y_{max})}$ Equation 3.26 in Vos

$k_y = \frac{k_0}{y_{max}}(U_w + 1)^2$ emulsification rate (Equation 3.28 in Vos)

1.9.5.2 ADIOS-2

Emulsification for ADIOS-2 is based on MacKay et al. (1980) .

$y = y_{max}\,(1 - e^{-k_y t})$ Equation 3.27 in Vos

$k_y = \frac{k_0}{y_{max}}(U_w + 1)^2$ emulsification rate Equation 3.27 in Vos

$k_0 = 1x10^{-6}\ s^{-1}$

1.9.5.3 OWM

We used a combination of equations from Vos and from SINTEF, and coded the computation for OWM as follows:

```
k0 = 1.0e-6;
k_y = (k0/y_max) * (Uw+1)^2;
if Uw==0,
    t_half = 2.43e5;
else
    t_half = log(2)/k_y; % Equation 3.29
end
y(t+dt) = y_max(t) - (y_max(t) - y(t)) * 0.5^(dt/t_half);


Uref = 10; % m/s
t_ref = C*t_lab; % Equation 22 in SINTEF and are empirically
                 % determined
t_half = ((1+Uref)/1+Uw))^2 *t_ref; % Equation 3.32 in Vos
y(t+dt) = y_max(t) - (y_max(t) - y(t)) * 0.5^(dt/t_half); % Equation
                                                          % 3.31 in
                                                          % Vos
```

1.9.5.4 Matlab® call

```
y = emulsification(which_model,Uw,t,dt,y_old)
```

1.9.5.5 Inputs

- `which_model: 'simpar','adios', or 'owm'`
- `Uw: wind speed in ms-1`

- t: time in hours (converted to seconds within the function)
- dt: time step (= 1 hr so dt=1)
- y_old: value of y at the previous time step (t-1)

1.9.5.6 Outputs

y: water content (*0<y<1*)

1.9.5.7 Defined Parameters

- ymax = 0.7; maximum water content
- k0 = 1e-6; in s^{-1}; from Reed (1989)

1.9.6 Oil Density

Oil density is a function of the water content and oil temperature, and it is affected by evaporation. We computed oil density for all three models with the following equation:

$$\rho_{oil}(y, T_{oil}) = y\rho_w + (1-y)\rho_0(0, T_{ref})[1 - c_1(T_{oil} - T_{ref})(1 + c_2 f_{evap})]$$

- T_{oil} is oil temperature in either ºC or ºK.
- T_{ref} is a reference oil temperature in either ºC or ºK.
- c_1 and c_2 are oil dependent constants.
- ρ_0 is a reference oil density (at time = 0)

1.9.6.1 Matlab® call

```
rho_oil = oil_density(y,rho_H2O,rho_ref,T0,T,f_evap,c1,c2)
```

1.9.6.2 Inputs

- y: water content
- rho_H2O: water density; computed depending on water temperature and salinity
- rho_ref: oil density at t=0; from the database
- T0: refenrence temperature; sea water temperature at t=0
- T: oil temperature; set to be the sea water temperature
- f_evap: fraction of evaporated oil; output from *evaporation.m*
- c1: supplied oil dependent constant
- c2: supplied oil dependent constant

1.9.6.3 Outputs

rho_oil: density of oil at time, t (time varying)

1.9.6.4 Defined Parameters

The oil dependent constants need to be supplied. We defined them before calling *oil_density.m*. The code could be easily changed to include these within *oil_density.m*, but, for now, we have chosen not to do so.

- c1 = 8e-4 (Janeiro et al., 2008)
- c2 = 0.18 (Janeiro et al., 2008)

1.9.7 Oil Viscosity

Oil viscosity is influenced by water content, evaporation, and oil temperature. We computed oil viscosity using four different algorithms for the three models.

1.9.7.1 Mooney (1951)

Mooney did not include evaporative effects.

$\nu(t) = \nu_0 \exp(\frac{ay(t)}{1-by(t)})$ Equation 3.21 in Vos

- *a=2.5*
- *b=0.654*
- *y* is the water content
- ν_0 is the reference/initial oil viscosity

1.9.7.2 Guo and Wang (2009)

Guo and Wang coupled the oil emulsion viscosity with evaporative exposure.

$\nu(t) = \nu_0 \exp(K_c f_{evap}) \exp(\frac{ay(t)}{1-by(t)})$ Guo and Wang, Equation 26

K_c is an oil dependent constant that is between 1 and 10. We used K_c*=4*.

- *a=2.5*
- *b=0.654*

1.9.7.3 Vos

Vos gave two different algorithms for computing oil viscosity with time. One algorithm was for SIMPAR and ADIOS-2 and the other was for OWM.

1.9.7.4 SIMPAR and ADIOS-2

We computed oil viscosity as a combination of Mooney and MacKay et al. (1983). We initially used the component attributed to Perry's handbook (Perry, 1973), but later abandoned it. Currently, we do not use the Perry component although the code still exists in the function.

$\nu(t) = \nu_0 \exp(c_b(f_{evap}(0) - f_{evap}(t))) \exp(\frac{ay(t)}{1-by(t)}) \exp(\frac{c_T}{T_{oil}} - \frac{c_T}{T_0})$

c_b*=5*

- *a=2.5*
- *b=0.654*

1.9.7.5 OWM

$\nu(t) = \nu_0 \exp(c_b(f_{evap}(0) - f_{evap}(t))) \exp(\frac{ay(t)}{100+by(t)}) \exp(\frac{c_T}{T_{oil}} - \frac{c_T}{T_0})$

- a=5
- b=-2

1.9.7.6 Janerio et al. (2008)

Janeiro et al. used a variation/combination of Mooney and MacKay.

$$\nu(t) = \nu_0 \exp(c_e f_{evap}(t)) \exp(\frac{ay(t)}{1-by(t)}) \exp(\frac{c_T}{T_{oil}} - \frac{c_T}{T_0})$$

If $\nu_0 > 38$, then c_e*=10*

Otherwise, $c_e = -0.0059\nu_0^2 + 0.4461\nu_0 + 1.413$ where ν_0 is the oil viscosity at 15°C.

- *a=2.5*
- *b=0.654*

- C_T=5
- T_0 is the boiling point defined in the oil database

1.9.7.7 Matlab® call

```
mu = oil_viscosity(which_model,which_method,y,f_evap,mu0,T,T0)
```

1.9.7.8 Inputs

- which_model: 'simpar','adios', or 'owm'
- which_method: 'mooney','guo&wang','vos', or 'janeiro'
- y: water content; obtained from *emulsification.m*
- f_evap: fraction of evaporated oil; output from *evaporation.m*
- mu0: oil viscosity at t=0; obtained from the database
- T0: boiling point of the oil; obtained from the database
- T_{oil}: oil temperature in Celsius (converted to Kelvin within the function)
- c1: supplied oil dependent constant
- c2: supplied oil dependent constant

1.9.7.9 Outputs

mu: oil viscosity at time, t (time varying) in m^2s^{-1}

1.9.7.10 Defined Parameters

```
a = 2.5 for SIMPAR and ADIOS-2; a = 5 for OWM
b = 0.654 for SIMPAR and ADIOS-2; b = -2 for OWM
cT = 5 (for Janeiro and Vos; used only in Vos if the 'Perry' option is used)
Kc = 4 (for Guo and Wang)
cb = 5 (for Vos)
ce = 10 or is computed (for Janeiro)
```

2 PART 2: USING REAL DATA FROM DOUGLAS CHANNEL

We tested the weathering algorithms with real meteorological data and real water temperature and salinity data that were measured in Douglas Channel in summer 2013 and winter 2014 at ~16 m depth. The meteorological data that we used were measured at Emilia Island as described by Stronach et al. (2010) and were provided by Environment Canada. The Institute of Ocean Sciences (IOS, Fisheries and Oceans Canada) provided the *in situ* water temperature and salinity data. These *in situ* data are detailed in Wright et al. (2015).

The objectives of the tests in Part 2 were

1. to see how the algorithms dealt with "real" data, especially time varying data, and
2. to see if there would be a difference between summer and winter weathering.

We were interested in the magnitude of the results and the timing of the initial or largest response. We compared our results with weathering model tests and experiments performed by other researchers. From these tests, we hoped to further refine our Matlab® tools so that we would have a foundation for understanding the properties of spilled oil as it weathers and the sensitivity of the commonly used algorithms to environmental conditions.

In our first test, we used no wind data, but constant air temperature and constant water properties: temperature and salinity. The values for the constant mean water temperature and water salinity were from Short's report (2013). Short synthesized results from Fissel et al. (2010). The water temperatures that Short used were measured at 1.5 m depth.

In our second test, we used a steady wind speed, constant air temperature, constant water temperature, and constant water salinity for 100 weathering hours. We used the same seasonal air temperature, sea surface temperature, and salinity as in the first test. The values for the constant mean wind speed were also from Short's report (2013). Wind speed measurements in Short's report were from Nanakwa Shoal station which is near Emilia Island in Douglas Channel. The mean wind speed did not change much from winter to summer as reported in either Short or Belore. The mean conditions reported in Short were similar to the mean seasonal conditions for Emilia Island reported in Belore (2010).

Our third test used 100 hours of variable wind speed and computed constant mean seasonal air temperatures and sea surface temperatures, and seasonal mean salinity from Short (2013) as in the previous two tests. We computed the mean air temperatures and sea surface temperatures from the meteorological data.

Our final test used variable wind speed, air, and water properties. The wind speed, air temperature, and sea surface temperature data were measured at Emilia Island and the *in situ* water property data provided by IOS were measured in Douglas Channel at a single

station. Meteorological and sea surface temperature data were measured by a GEM meteorological station at Emilia Island as reported in Stronach et al., (2010)

We ran the weathering tests using Cold Lake Bitumen as the test oil for the hypothetical spill. The oil database has several types of Alberta or Canadian crude: Alberta Mix, Bow River Heavy, Cold Lake (i.e. Cold Lake Bitumen), Fosterton, Gulf Alberta L & M, Interprovincial, Leduc Woodbend, Lloyd Minister, Pembina, Rainbow L & M, Redwater, and Wainwright Kinsella. If we had wanted to test an oil not in the database, we could manually supply the initial values that we needed; e. g. oil density, oil viscosity, API, etc.

Other “real” data that we could have used, but whose values we arbitrarily chose, were the channel width at the spill site and the wave period.

We used the mean near-surface current at 5 m that Fissel et al. (2010) measured for the surface current. The mean surface current that they reported was 28.4 cm s^{-1}. We also programmed the option of using the minimum or maximum surface current reported by Fissel et al. The surface current is only relevant in the release module that computes the length scale to use in the evaporation module. We only computed the initial release value; that is, we didn’t iterate the computation over time because we assumed that the release was instantaneous.

There were four different tests that had constant water properties. The tests with constant water properties used average water properties for Test 1 and Test 3 and both mean and minimum water properties for Test 3; i.e. Test 3 had 2 parts. Test 3 also used a mean wind speed and a maximum 1 h sustained wind speed.

1. no wind, constant sea surface temperature and salinity, constant air temperature
    a. average water properties, mean seasonal air temperatures, and 0 ms^{-1} wind speed
2. constant wind speed, constant air temperature, constant sea surface temperature and salinity
    a. average water properties and mean wind speed and air temperature
    b. minimum water properties, mean air temperature, and maximum 1 h sustained wind speeds (Short, 2013)
3. variable wind speed, constant air temperature, and constant water parameters
    a. average water properties
4. variable wind speed, air temperature, and water parameters

In the tests, we had to define several parameters that included oil type, initial oil density, oil API, the boiling point, etc. These values are read from the oil database that we originally accessed from the MedSLIK II oil spill/weathering model (De Dominicis, M. et al., 2013a, b). Whenever we used constant wind and water parameters, we used input values from Short (2013).

For all tests, we made the oil temperature equal to the water temperature. ADIOS-2 does the same thing (Lehr, 2002). For all tests, we initialized other parameters as follows:

Initial Definitions for all Test Runs

- type of oil: Cold Lake Bitumen

- initial oil density: 903 kgm^{-3} (from oil database)
- API: 25.20 (from database)
- oil viscosity: 70.70 (from oil database)
- boiling point: 543.90 = 3.1295*API (computed within the program)
- volume of oil spilled: 1000 m^3 (arbitrary)
- thickness of oil slick: 0.001 m (arbitrary)
- channel width: 1000 m (arbitrary)
- surface water current @ 5m in Douglas Channel: 0.284 ms^{-1} mean; (0.0021 ms^{-1} minimum or 0.913 ms^{-1} maximum; from Fissel et al., 2010)
- wave period: 1 s^{-1} (arbitrary)

Here is the Matlab® code for the initial definitions:

```
oil_type = 'Cold Lake';
rho_ref = find_oil_data('rho_oil',oil_type,oildata);
visc_oil = find_oil_data('visc_oil',oil_type,oildata);
API = find_oil_data('API',oil_type,oildata);
Tboil = 532.98 - 3.1295*API; % in Kelvin and constant value

V_oil = 1000; % initial spill volume in m^3
thickness = 0.001; % 1 mm release/spill thickness
Area = V_oil/thickness; % area of oil slick in m*m
```

We chose the next set of values arbitrarily with the choice of which surface current to use made at run time (input into the test run call: “which_current”. For our tests reported in this part, we used the mean current (0.284 ms^{-1}).

```
B = 1000; % channel width in metres
switch which_current,
    case {'min','minimum'},
        U_H2O = 0.021*ones(size(Uw)); % water velocity in m/s; Fissel et al.
(2010) minimum
    case {'mean'},
        U_H2O = 0.284*ones(size(Uw)); % water velocity in m/s; Fissel et al.
(2010) mean
    case {'max','maximum'},
        U_H2O = 0.913*ones(size(Uw)); % water velocity in m/s; Fissel et al.
(2010) maximum
end
Tw = 1; % wave period in 1/s
```

find_oil_data.m is the Matlab® function that looks up a desired value from the oil database. The oil database needs to be in the Matlab® workspace (*oildata = read_oil_data_xlsx;*).

Evaporation and dispersion depend on the oil viscosity. We computed the oil viscosity using the output from the emulsification module. Variable oil density relied on the output from the evaporation module; i.e. it used the fraction of oil evaporated to compute oil density. The initial oil density and viscosity were read from the oil database. The initial density and viscosity could also be user supplied with small changes to the code. We

computed the boiling point of the oil using the API from the database (or could be supplied).

We noted that Short cited Belore (2010) for properties of Cold Lake Bitumen where @ 15^{o}C, the density is 936 (Table 2, Short, 2013), and an Environment Canada report gives the density as 924.9 @ 15^{o}C (Government of Canada, 2013). Belore reported that the dynamic viscosity in mPas is 368 @ 15^{o}C and the kinematic viscosity is 393.2 (mm^2s^{-1}). Belore used the same evaporation algorithm as Short.

2.1 NO WIND AND CONSTANT AIR TEMPERATURE, WATER TEMPERATURE, AND SALINITY

In this section, we computed parameters of the weathering of the simulated Cold Lake Bitumen spill under zero wind conditions for summer and winter for 100 hrs. We used mean water temperature and salinity conditions (Short, 2013). Mean summer and winter air temperatures are from Belore (2010). Plots are presented for summer and winter oil density, oil viscosity, and water content.

- mean wind speed: 0 ms^{-1}
- air temperature
    - summer: 14.24^{o}C
    - winter: 4.30^{o}C
- mean water temperature
    - July: 13.2^{o}C
    - December: 6.8^{o}C
- mean water salinity
    - July: 17.9
    - December: 30.7

Results showed that in winter the density increased faster towards a higher final density (**Figure 46**), but there was no seasonal difference for the viscosity **(Figure 47**) or water content (**Figure 48**) in the absence of wind.

In the tests in Part 1, the algorithm that we used for computing evaporation in ADIOS-2 did not use wind speed for computing the mass transfer coefficient. This departed from the computation of the mass transfer coefficient used by the actual ADIOS-2 model, but we wanted to see how the S&M algorithm reacted to a non-wind dependent K. The Hamoda expression that we used for K that is described in Fingas (2013), depended on temperature and salinity of seawater. The viscosities computed by ADIOS-2, using Bobra and Hamoda to compute the evaporation and mass transfer coefficient, produced viscosities 100 times greater than the other models so we chose not to plot the ADIOS-2 results in **Figure 47** for the Janeiro et al. viscosity.

We were interested to see what effect changing the evaporation algorithm would have on viscosity so we recomputed evaporation using the empirical equations from Fingas (2013)

that depend only on air temperature. The empirical equation given in Fingas (2013) for Cold Lake Bitumen is

$$f_{evap} = (-0.16 + 0.013T_{air})/t$$

The equation was derived with a constant temperature = 15ºC and the time in minutes. If the temperature were less than 14ºC, the equation would give a negative percent evaporation. Furthermore, as time increases, the fraction evaporated would decrease, which did not make sense to us. Therefore, we abandoned using the empirical equations after this point.

2.1.1 Oil Density

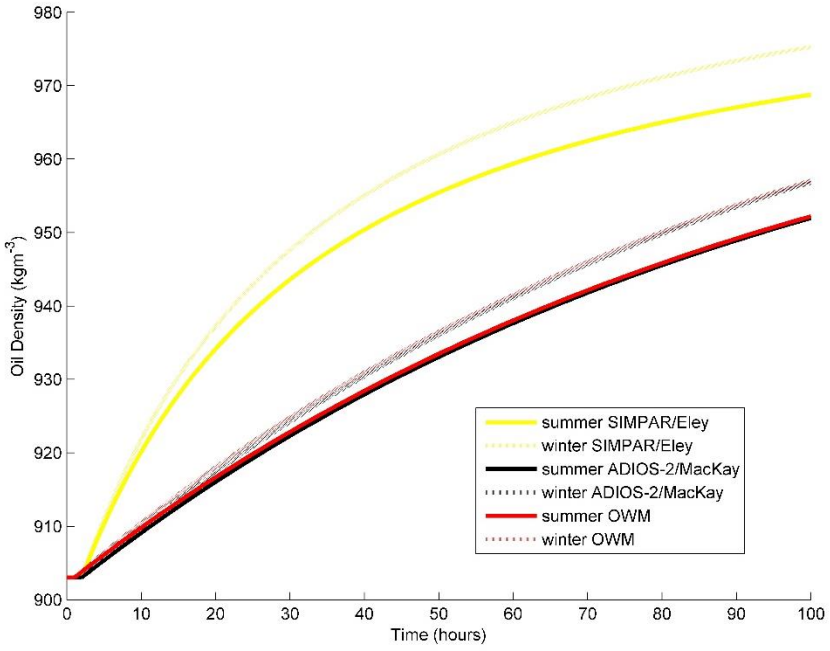

Figure 46 Cold Lake Bitumen density computed for summer and winter using 3 model algorithms with no wind influence. The evaporation computation used variations of the S&M algorithm.

2.1.2 Oil Viscosity

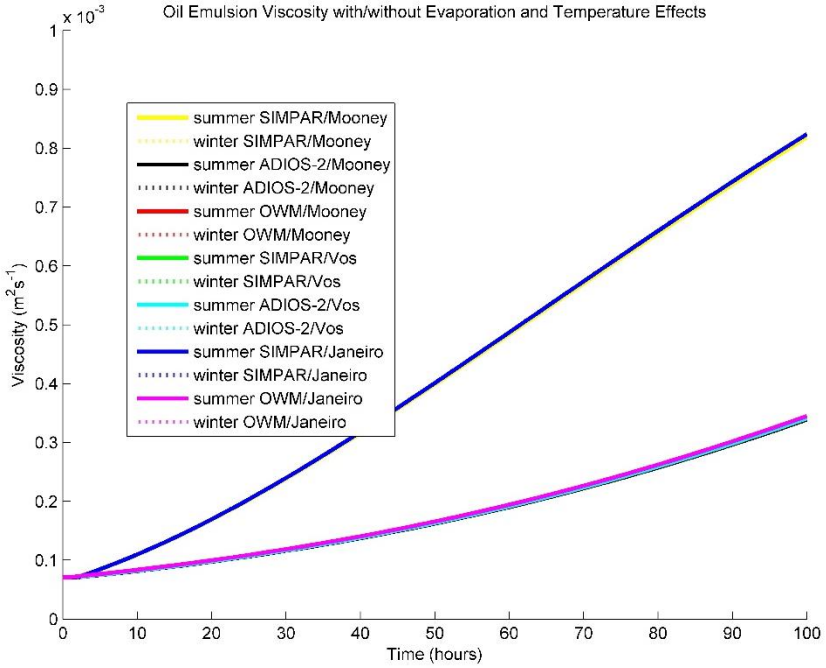

Figure 47 Cold Lake Bitumen viscosity computed for summer and winter using 3 algorithms for the 3 weathering models with no wind influence. The evaporation computation used variations of the S&M algorithm.

2.1.3 Emulsification (Water Content)

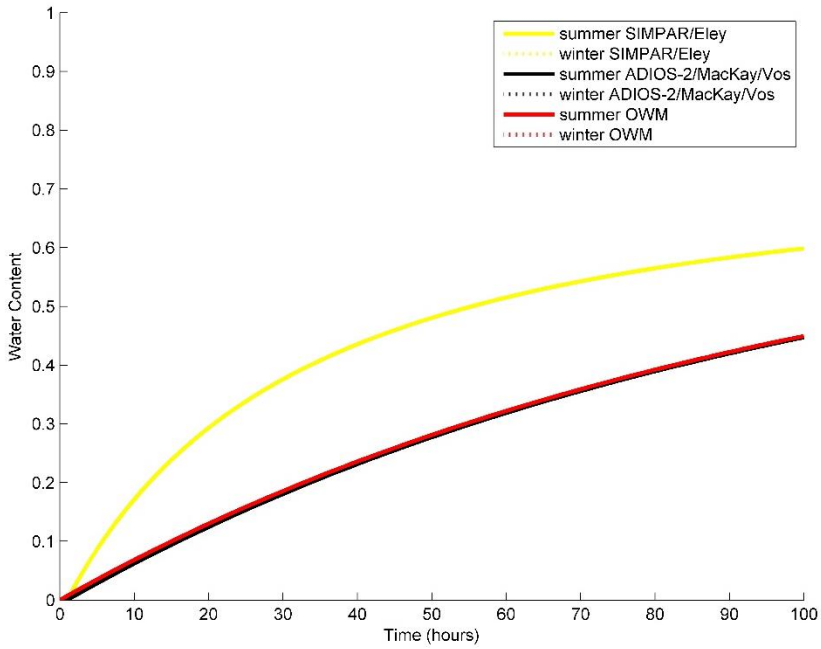

Figure 48 Cold Lake Bitumen water content computed for summer and winter using 3 model algorithms with no wind influence

2.2 CONSTANT WIND SPEED, AIR TEMPERATURE, AND WATER TEMPERATURE AND SALINITY

For this section, we computed parameters of the weathering of the simulated Cold Lake Bitumen spill under constant wind conditions for summer and winter for 100 hrs. The water temperature and salinity were average conditions (Short, 2013). The mean summer and winter air temperatures were from Belore (2010). Plots are presented of summer and winter oil density and oil viscosity, summer and winter water content (emulsification), summer and winter percentage evaporated (evaporation), and summer and winter entrainment rates (dispersion).

In this case, weathering occurred faster in winter than in summer. In both seasons, maximum density and water content was reached within two days. Viscosity increased rapidly for two days then flat-lined in the OWM model, but continued to slowly increase in SIMPAR and ADIOS-2.

We used summer and winter means for air temperature.

2.2.1 With Mean Wind Speed, Mean Air Temperature, and Mean Water Temperature and Salinity

- mean wind speed
  - July: 4.4 ms^{-1}
  - December: 5.5 ms^{-1}
- air temperature
  - summer: 14.24^{o}C
  - winter: 4.30^{o}C
- mean water temperature
  - July: 13.2^{o}C
  - December: 6.8^{o}C
- mean water salinity
  - July: 17.9
  - December: 30.7

2.2.1.1 Oil Density

With a constant wind, the oil density increased more during the winter with the greatest change occurring in less than 20 hours. Belore (2010) also found that MacKay River Heavy bitumen, which has similar properties to Cold Lake bitumen, increased its density faster in winter than in summer at Emilia Island with a constant wind, and the greatest change occurred in less than 24 hours. Short (2013), however, found that Cold Lake bitumen weathered faster in summer than in winter. Short computed an equivalent weathering time of 47 hours for July conditions in Douglas Channel and 72 hours for December conditions. Short defined equivalent weathering time as the time required for the bitumen to reach laboratory conditions (96 hours with 1.5 ms^{-1} wind speed at 15^{o}C).

The rapid increase in density seen in **Figure 49** agrees with results from wave tank experiments by King et al. (2014) who found that Cold Lake diluted bitumen increased

rapidly within the first 24 hours. The Access Western Blend diluted bitumen in King et al.'s tank experiment reached the density of fresh water in 150 hours, but never reached the density of seawater. The Cold Lake diluted bitumen was close to the fresh water density after 300 hours. The Access Western Blend took less time to reach a halfway density in the tank experiment. The Cold Lake diluted bitumen took 24 hours to reach half its final density in the wave tank experiment. In our case, it looks as if the Cold Lake bitumen took just over 10 hours to reach half its final density in summer and just under 10 hours to reach the maximum density in winter. The mean wind speed during King et al.'s experiment was 2.5 ms^{-1}, which is about half the value of the mean wind speeds that we used. The difference in wind speeds is likely why the density increased more rapidly in our test. Our winter density maximum was also higher than our summer maximum.

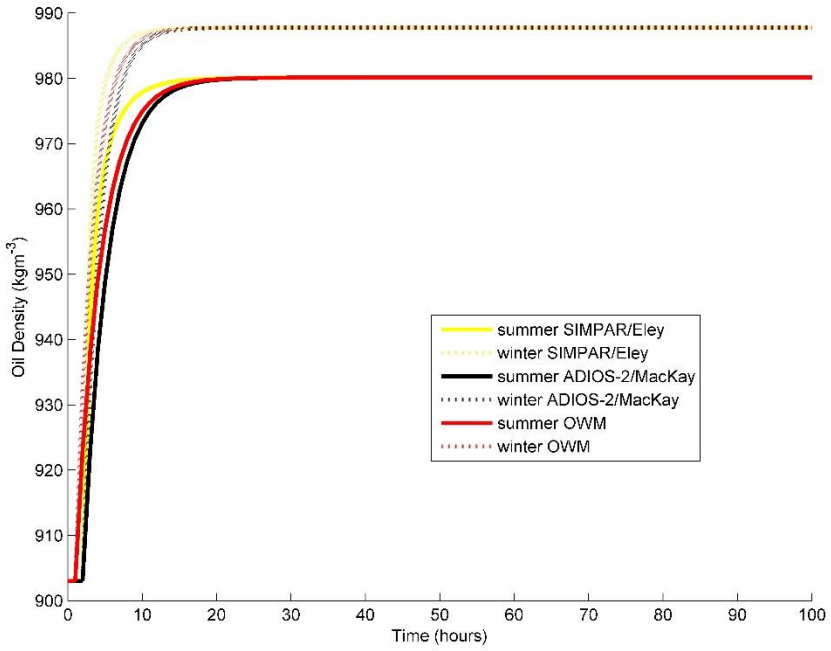

Figure 49 Cold Lake Bitumen density computed for summer and winter using 3 model algorithms with constant summer and winter mean wind speeds and air temperatures

2.2.1.2 Oil Viscosity

As with the oil density, the oil viscosity increased faster in winter than in summer (**Figure 50**). Belore (2010) had a similar result with MacKay River bitumen at Emilia Island. In our computations, the greatest increase in viscosity occurred in less than 20 hours when we computed it with Mooney's algorithm, which is similar to Belore's result for summer. Belore's winter spill had its greatest increase in viscosity occur in less than 12 hours. When temperature and evaporative effects were included in the computation of viscosity, the maximum viscosity reached was much higher with the winter maximum being less than the summer maximum, and viscosity reached its maximum in over 100 hours.

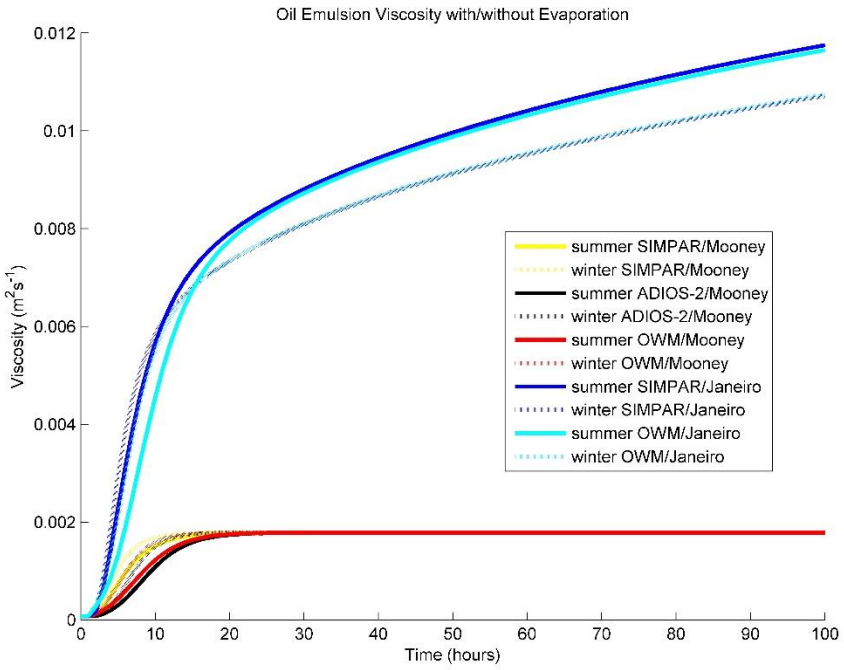

Figure 50 Cold Lake Bitumen viscosity computed for summer and winter using 2 algorithms for the 3 weathering models with constant summer and winter mean wind speeds and air temperatures

2.2.1.3 Emulsification (Water Content)

Water content increased more rapidly in winter than in summer, and it reached its maximum within 20 hours in all cases (**Figure 51**). Belore (2010) also found that water content increased the fastest in winter for MacKay River bitumen, but it reached its maximum in about 12 hours in winter and in 72 hours in summer at Emilia Island.

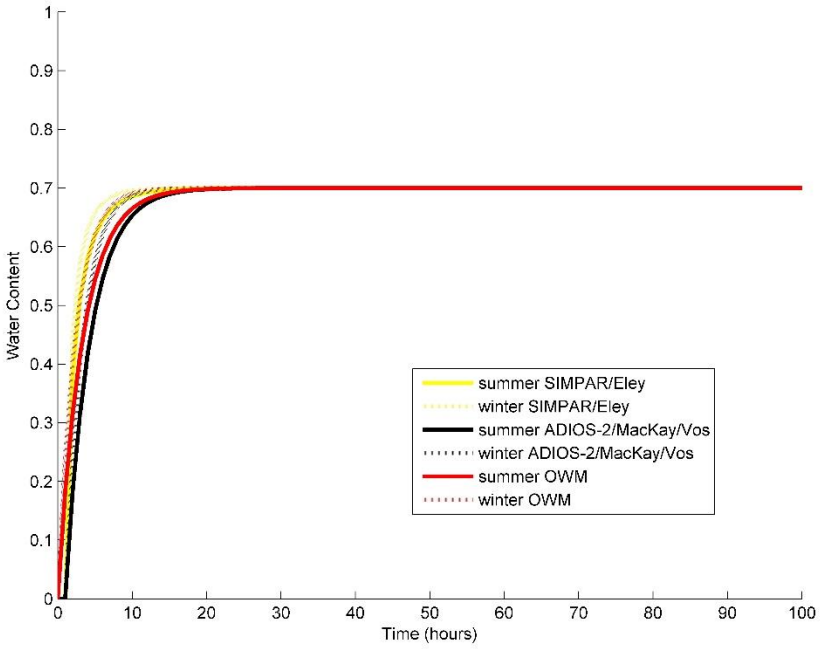

Figure 51 Cold Lake Bitumen water content computed for summer and winter using 3 model algorithms with constant summer and winter mean wind speeds and air temperatures

2.2.1.4 Evaporation

A greater percentage of oil evaporated in summer than in winter, which is a similar result to Belore's (2010) for a MacKay River bitumen spill at Emilia Island. While the most rapid change occurred in less than 12 hours, evaporation continued throughout the 100 hour period but at a much slower rate. The result is also similar to the evaporative loss found in a pan evaporation experiment performed by the Government of Canada (2013). In that experiment, the Cold Lake Bitumen lost 11.7% of its mass within six hours and 15.6% within 24 hours, which is similar to what is shown in **Figure 52** for the SIMPAR and OWM model algorithms that used Short's equation for evaporation. We used the Bobra evaporation equation from Fingas (2011, 2013) for ADIOS-2.

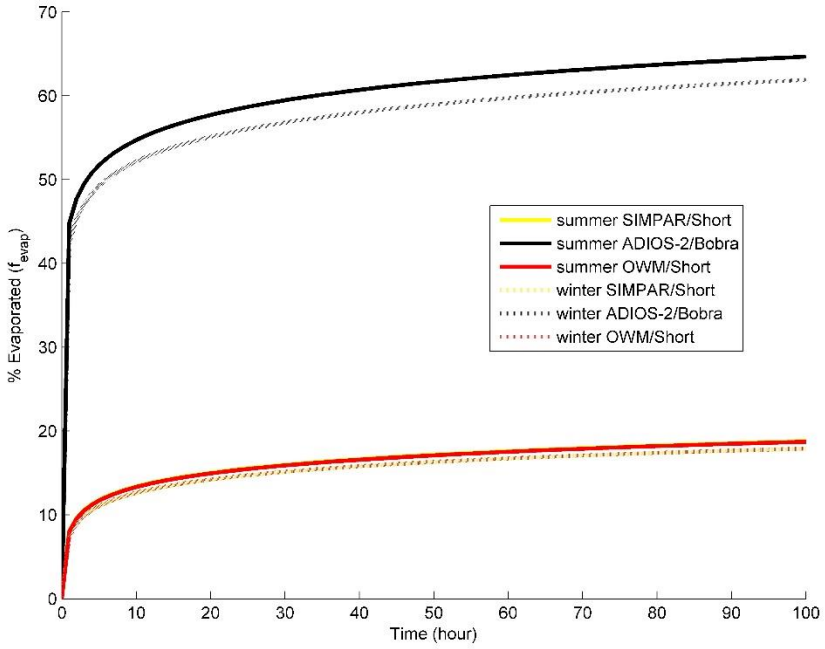

Figure 52 Percent evaporated of Cold Lake Bitumen computed for summer and winter using 2 model algorithms with constant summer and winter mean wind speeds and air temperatures

2.2.1.5 Entrainment Rate

The entrainment rate was higher in winter than in summer. Belore (2010) found that a higher percentage of MacKay River Bitumen dispersed in winter than in summer.

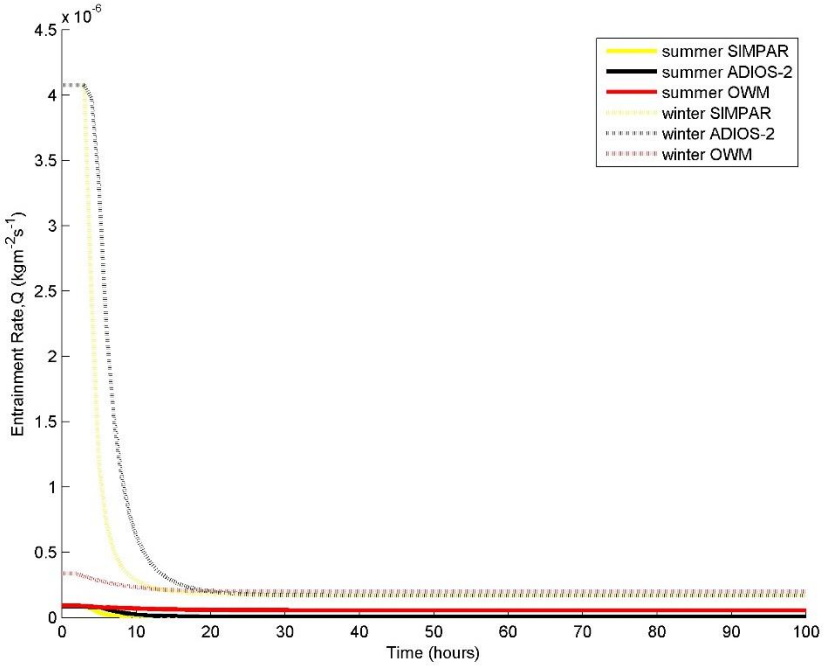

Figure 53 Entrainment rate of Cold Lake Bitumen computed for summer and winter for the 3 models with constant summer and winter mean wind speeds and air temperatures

2.2.2 With Minimum Water Temperature and Salinity and Maximum 1 h Sustained Wind Speed and Mean Temperature

For this section, we computed parameters of the weathering of the simulated Cold Lake Bitumen spill under constant wind conditions for summer and winter for 100 hours using the maximum 1 hour sustained wind speeds from Short (2013). We used minimum water temperature and salinity from Short (2013) and the mean seasonal air temperatures from Belore (2010). Plots are presented of summer and winter oil density, oil viscosity, water content (emulsification), the percentage evaporated (evaporation), and the entrainment rates (dispersion). Short noted that a maximum sustained wind speed of 12 ms^{-1} and minimum water properties in July (11.8^{o}C and 0.3 ppt) would cause Cold Lake Bitumen to sink after only 25 h in Kitimat Arm.

We present a direct comparison of the weathering processes under mean conditions and the processes under extreme conditions in the next section.

- maximum 1 h sustained wind speed
    - July: 12.0 ms^{-1}
    - December: 18.1 ms^{-1}
- air temperature
    - summer: 14.24^{o}C
    - winter: 4.30^{o}C
- minimum water temperature
    - July: 11.2^{o}C
    - December: 6.5^{o}C
- minimum water salinity
    - July: 15.4
    - December: 30.6

2.2.2.1 Oil Density

Under the extreme conditions, the density increased to its maximum in less than 10 hours with a higher maximum density in winter than in summer (**Figure 54**).

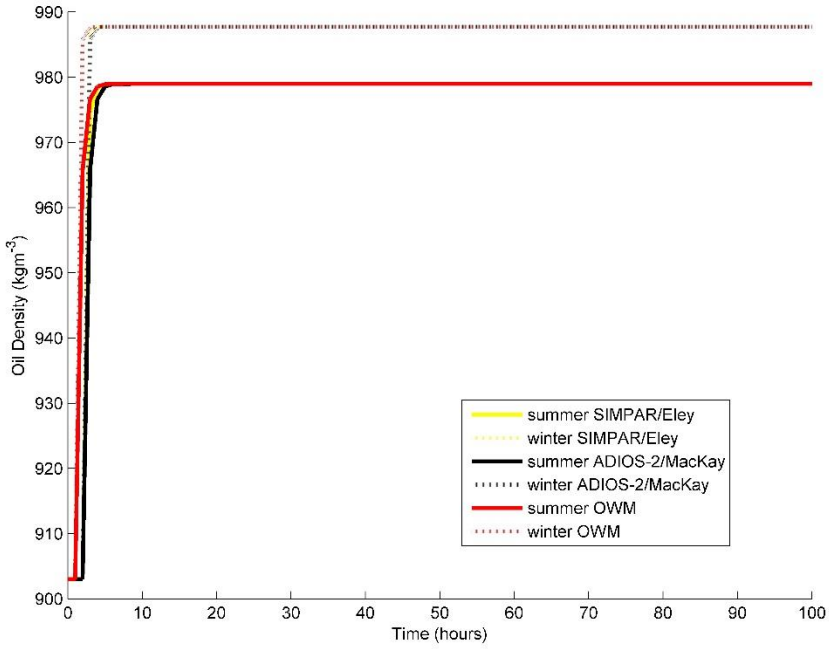

Figure 54 Cold Lake Bitumen density computed for summer and winter using 3 model algorithms with constant summer and winter maximum 1 h sustained wind speeds, constant minimum water temperature and salinity, and constant seasonal mean air temperatures

2.2.2.2 Oil Viscosity

Under the extreme conditions, the viscosity increased at the greatest rate in under 10 hours (**Figure 55**). When temperature and evaporative effects were considered, the viscosity in winter was higher for the OWM model algorithms and lower for the SIMPAR model algorithms.

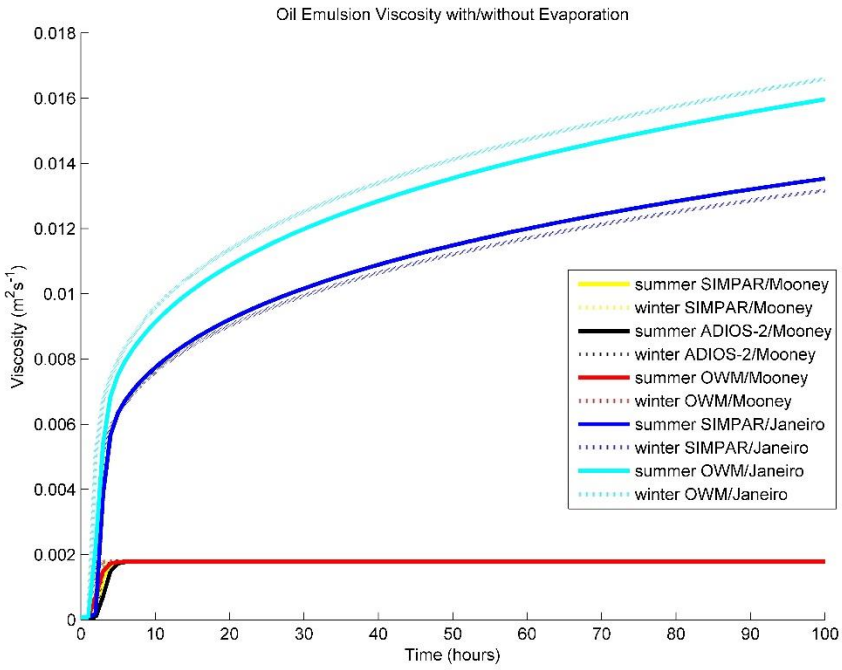

Figure 55 Cold Lake Bitumen viscosity computed for summer and winter using 2 algorithms for the 3 weathering models with constant summer and winter maximum 1 h sustained wind speeds and constant minimum water temperature and salinity, and constant seasonal mean air temperatures

2.2.2.3 Emulsification (Water Content)

Under extreme conditions, maximum water content was reached in less than 10 hours (**Figure 56**). The maximum was reached faster in winter than in summer.

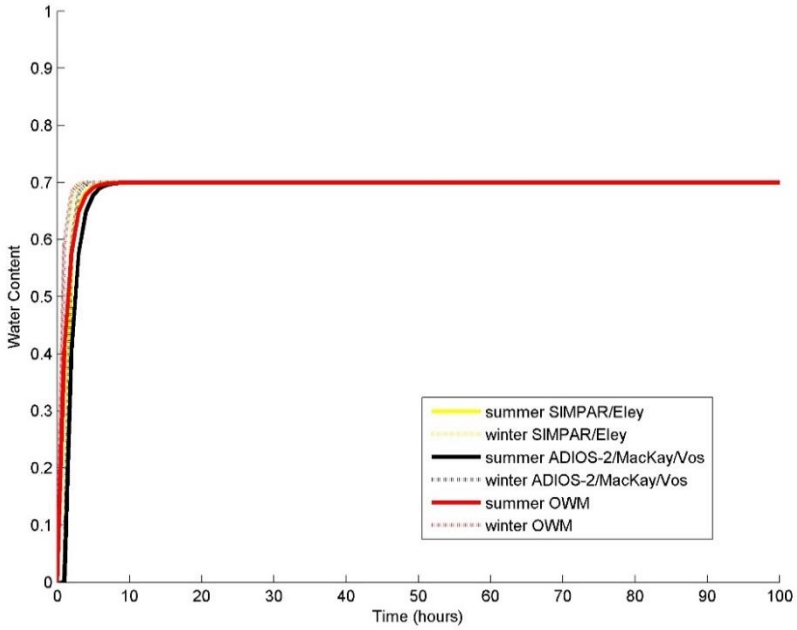

Figure 56 Cold Lake Bitumen water content computed for summer and winter using 3 model algorithms with constant summer and winter maximum 1 h sustained wind speeds and constant minimum water temperature and salinity, and constant seasonal mean air temperatures

2.2.2.4 Evaporation

Under extreme conditions, the greatest fraction of oil evaporated in less than 10 hours (**Figure 57**). Winter evaporation was slightly higher for the OWM model algorithms than for the SIMPAR and ADIOS-2 algorithms. The greatest rate of evaporation in all cases occurred in the first few hours after the spill.

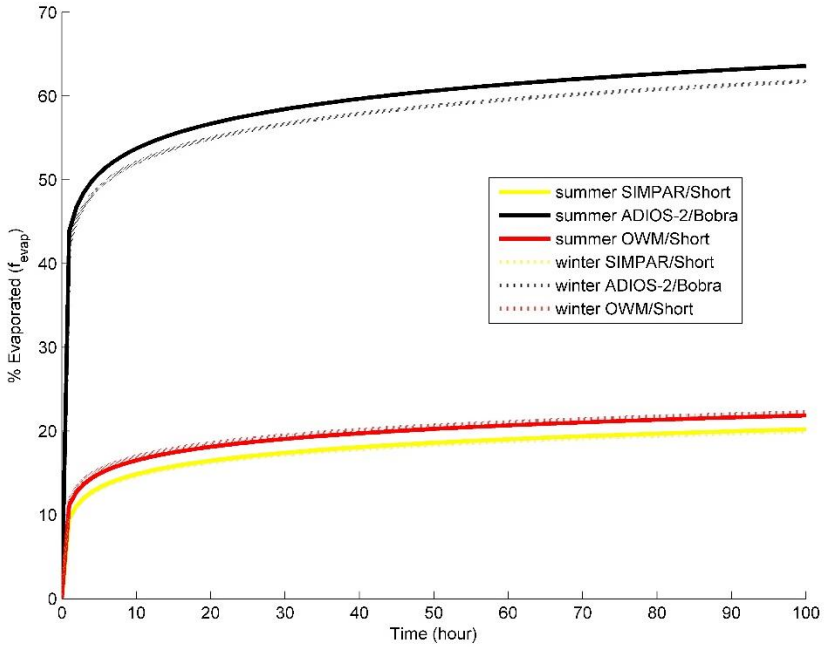

Figure 57 Percent evaporated of Cold Lake Bitumen computed for summer and winter using 3 model algorithms with constant summer and winter maximum 1 h sustained wind speeds and constant minimum water temperature and salinity, and constant seasonal mean air temperatures

2.2.2.5 Entrainment Rate

Under extreme conditions, the greatest change in entrainment rate occurred in less than 10 hours (**Figure 58**). Entrainment in winter was greater than in summer.

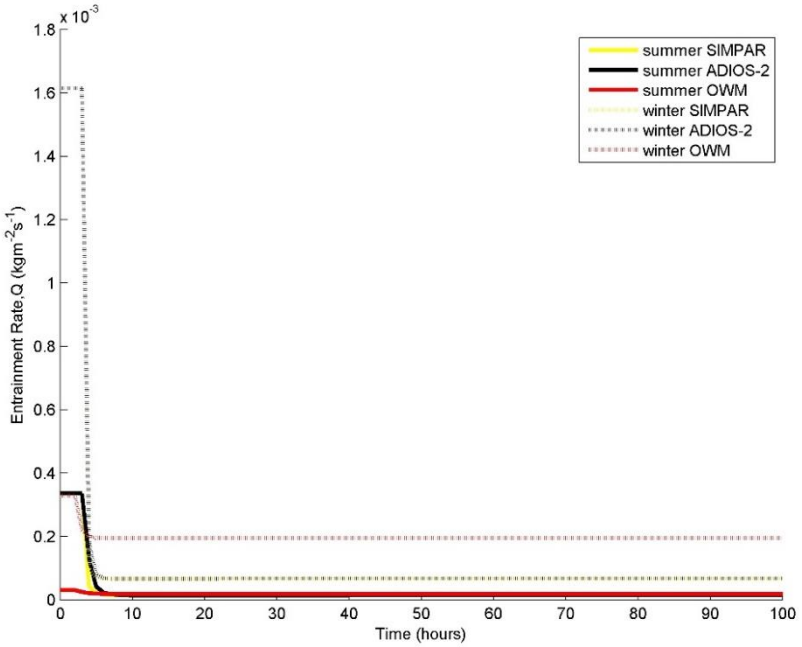

Figure 58 Entrainment rate of Cold Lake Bitumen computed for summer and winter for the 3 models with constant summer and winter maximum 1 h sustained wind speeds and constant minimum water temperature and salinity, and constant seasonal mean air temperatures

2.2.3 Compare Weathering with Mean Values to Weathering under Extreme Conditions

In this section, we present figures of the weathering processes where the results from the computations with mean wind speeds and water properties are presented on the same plots as the results with the maximum wind speeds and minimum water properties for winter and summer. The results for the weathered oil density and viscosity show that the oil weathers faster under the extreme conditions, especially in winter.

2.2.3.1 Oil Density

Figure 59 shows that a greater density is achieved in winter under extreme conditions in less than 10 hours. The extreme conditions produced the greatest rate of change. The maxima produced by the extreme winter conditions are the same as those produced by the mean winter conditions. The same can be said for extreme summer and mean summer conditions. All maxima were reached in less than 20 hours regardless of model or environmental conditions.

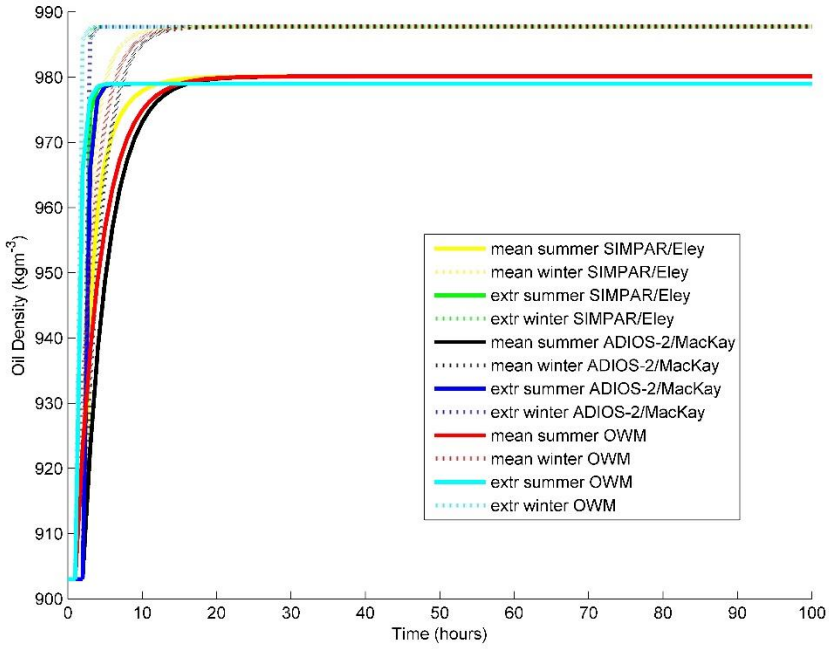

Figure 59 Cold Lake Bitumen density computed for summer and winter using 3 model algorithms with constant summer and winter maximum 1 h sustained wind speeds and constant minimum water temperature and salinity compared to density computed with mean wind speeds and water properties

2.2.3.2 Oil Viscosity

Figure 60 shows that the greatest viscosity was reached under extreme conditions in both models, SIMPAR and OWM. The greatest rate of change occurred in less than 10 hours for both models under extreme conditions and in under 12 hours for the mean conditions. The extreme conditions also produced a faster rate of change. Summer produced greater viscosities than winter except for the OWM algorithms under extreme conditions.

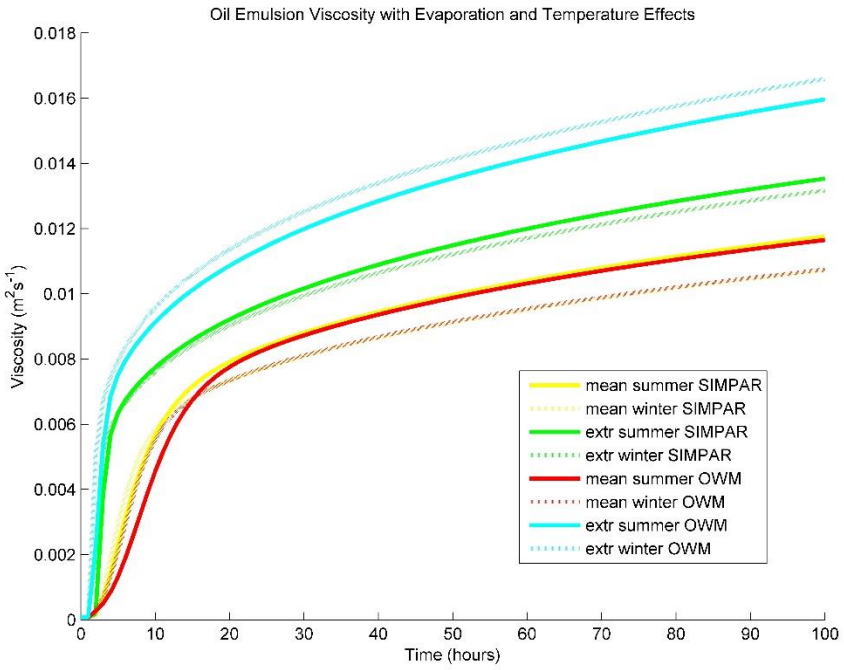

Figure 60 Cold Lake Bitumen viscosity computed with Janeiro et al.'s (2008) viscosity formula using summer and winter constant maximum 1 h sustained wind speeds and minimum water properties compared to viscosity computed with mean wind speeds and water properties

2.2.3.3 Emulsification (Water Content)

Maximum water content was achieved quicker under the extreme conditions than under the mean conditions (**Figure 61**). The extreme conditions produced the maximum water content in under 6 hours, and the mean conditions produced the maximum in under 20 hours. Winter conditions produced faster water uptake than summer conditions.

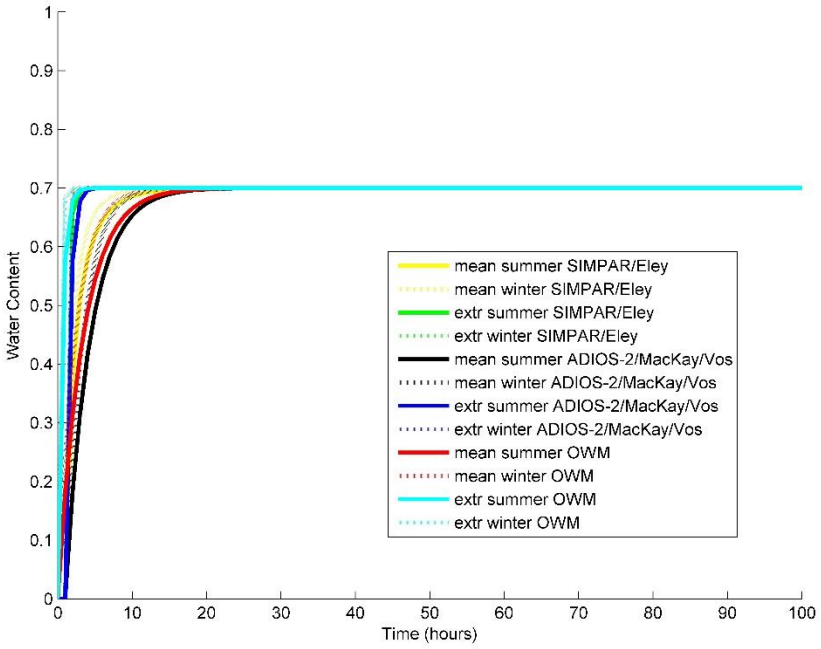

Figure 61 Cold Lake Bitumen water content computed with 3 different algorithms for the 3 models using summer and winter constant maximum 1 h sustained wind speeds and minimum water properties compared to viscosity computed with mean wind speeds and water properties

2.2.3.4 Evaporation

For two of the models, the fraction evaporated occurred most rapidly under extreme conditions than under mean conditions with a greater percentage being evaporated under the extreme conditions (**Figure 62**). The two models were SIMPAR and OWM. For the ADIOS-2 algorithm, the mean summer conditions produced a greater fraction evaporated than the extreme summer conditions. In addition, the extreme winter conditions produced a slightly greater fraction evaporated than the extreme summer conditions for the OWM algorithms. However, the seasonal differences were small in most cases. In all cases, the most rapid evaporation occurred in less than 5 hours.

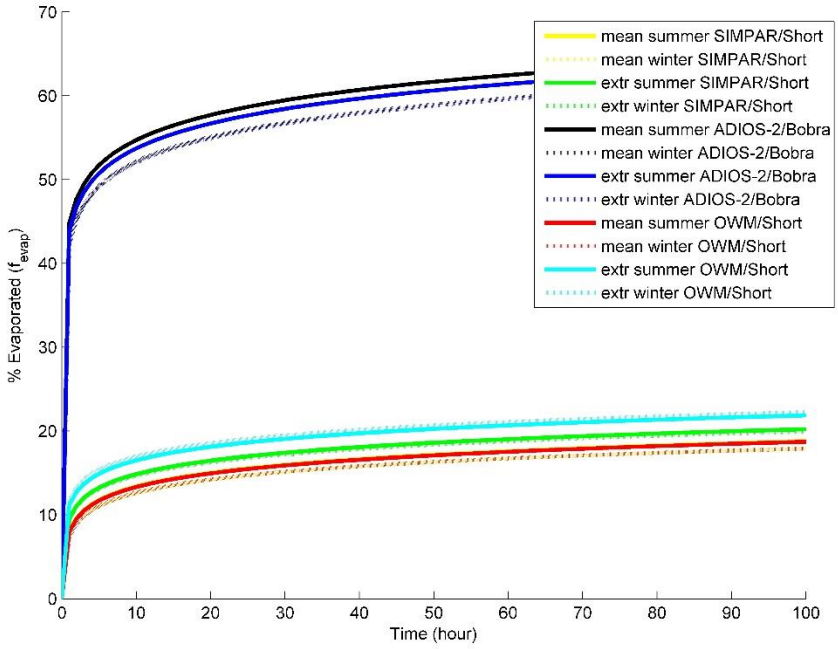

Figure 62 Percentage of evaporated Cold Lake Bitumen computed with 2 different algorithms for the 3 models using summer and winter constant maximum 1 h sustained wind speeds and minimum water properties compared to viscosity computed with mean wind speeds and water properties

2.3 VARIABLE WIND SPEED, CONSTANT AIR TEMPERATURE AND CONSTANT WATER TEMPERATURE AND SALINITY

In this section, we tested the oil weathering algorithms with variable wind speed, but we used constant mean air and water temperatures and constant mean water salinity.

For the variable wind speed, we used hourly wind speed data measured at Emilia Island (Emilia Rock station) (**Figure 63** and **Figure 64**) for July 2013 and January 2014. Wind data were measured by a GEM meteorological station at Emilia Island as reported in Stronach et al., (2010). The figures display all the data that were measured: wind speed, sea surface temperature (SST), and surface air temperature (SAT). The data were measured at a GEM meteorological station, and they were used for the Enbridge Northern Gateway Project as described in Stronach et al. (2010).

Stronach et al. reported that the annual mean wind speed at Emilia Rock was 3.73 ms^{-1}. The authors noted that the January mean wind speed for this station was 3.51 ms^{-1} and the December mean was 3.53 ms^{-1}, which are slightly lower than Short's December mean (5.5 ms^{-1}) that we used earlier as representative for Douglas Channel's mean winter wind speed. Stronach et al. reported the mean wind speed for July as 4.52 ms^{-1}, which is similar to what Short noted. Stronach et al. described that winds from the north were stronger and more frequent in the winter, and "inflow" winds from the south and southwest were

common in the summer. The wind direction in the confined channel space of Douglas Channel influences where spilled oil will land on shore (Stronach, 2011).

The mean daily air temperature measured at Emilia Rock for January was 0.3ºC and for July it was 14.7ºC (Stronach et al., 2010). For our 100 hour periods, the mean winter air temperature was 2.23ºC, and the mean summer air temperature was 15.82ºC. Because of the small differences in the air temperatures from the two sources, we believed that the mean from the first 100 hrs of data was representative of mean seasonal conditions. We expected the effects from the 100- hour mean air temperatures to be the same as in the first two tests.

Belore (2010) reported that the mean SST in winter at Emilia Island was 6.39ºC in winter and 13.27ºC in summer. For our 100-hour periods, the mean winter SST was 4.76ºC, and the mean summer SST was 14.19ºC. Because of the small differences in the SST from the two sources, we believed that the mean from the first 100 hrs of data was representative of winter conditions. We expected the effects from the 100- hour mean air temperatures to be the same as in the first two tests.

This section describes the application of 100 hours of variable wind speed data, mean air temperature and mean SST data from Emilia Island to the weathering processes. In this particular case, we used the same salinity data measured by Fissel et al. (2010) at the near-surface depth, 1.5 m. We report 100 hours of weathering for oil density, oil viscosity, water content, percentage evaporated, and the entrainment rate.

2.3.1 Meteorological and SST Data from Emilia Island

Figure 63 and **Figure 64** present the hourly meteorological record from Emilia Island in 2012 and 2014.

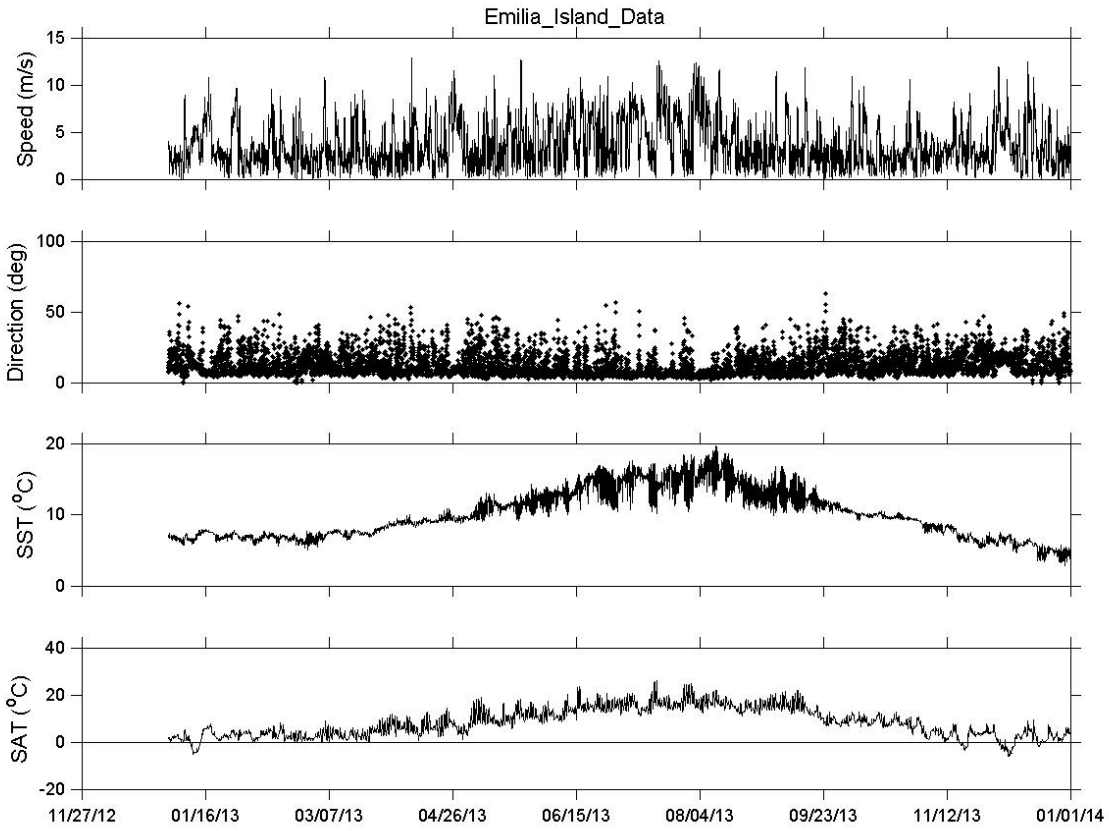

Figure 63 Hourly meteorological record from Emilia Island from late 2012 to end of 2013

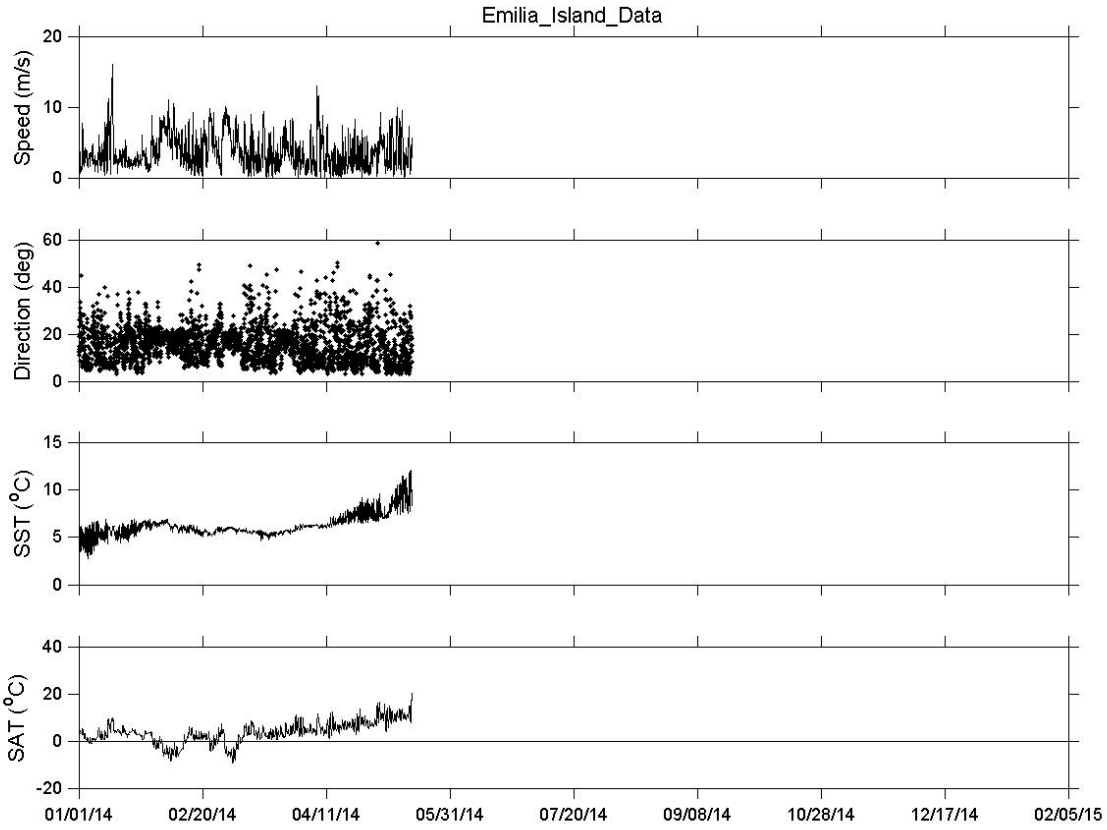
Emilia_Island_Data
Speed (m/s)
20
10
0
Direction (deg)
60
40
20
0
SST (°C)
15
10
5
0
SAT (°C)
40
20
0
-20
01/01/14
02/20/14
04/11/14
05/31/14
07/20/14
09/08/14
10/28/14
12/17/14
02/05/15

Figure 64 Hourly meteorological record from Emilia Island for early 2014

We used the first 100 hours of the hourly meteorological data from July 2013 to represent typical summer conditions (

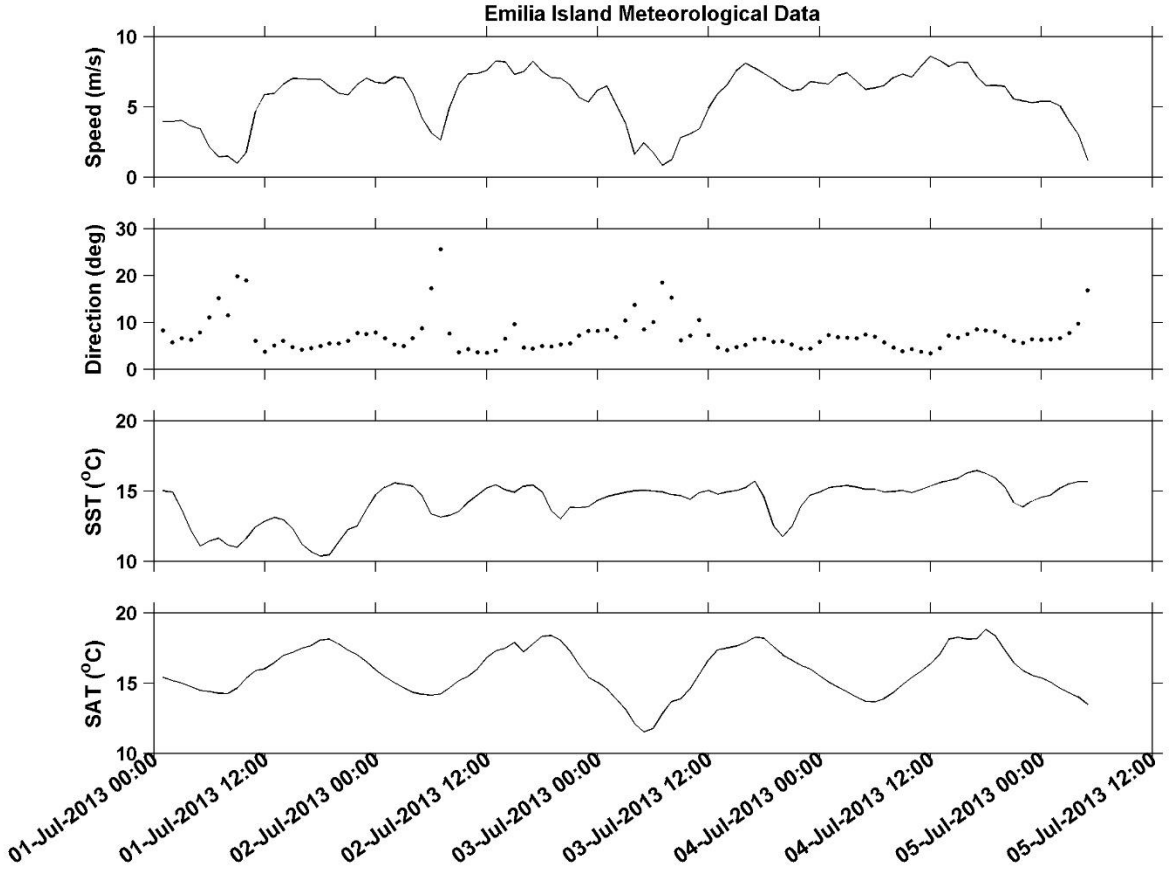

Figure 65), and we used the first 100 hours of the hourly record from January 2014 as representative of typical winter conditions (**Figure 66**).

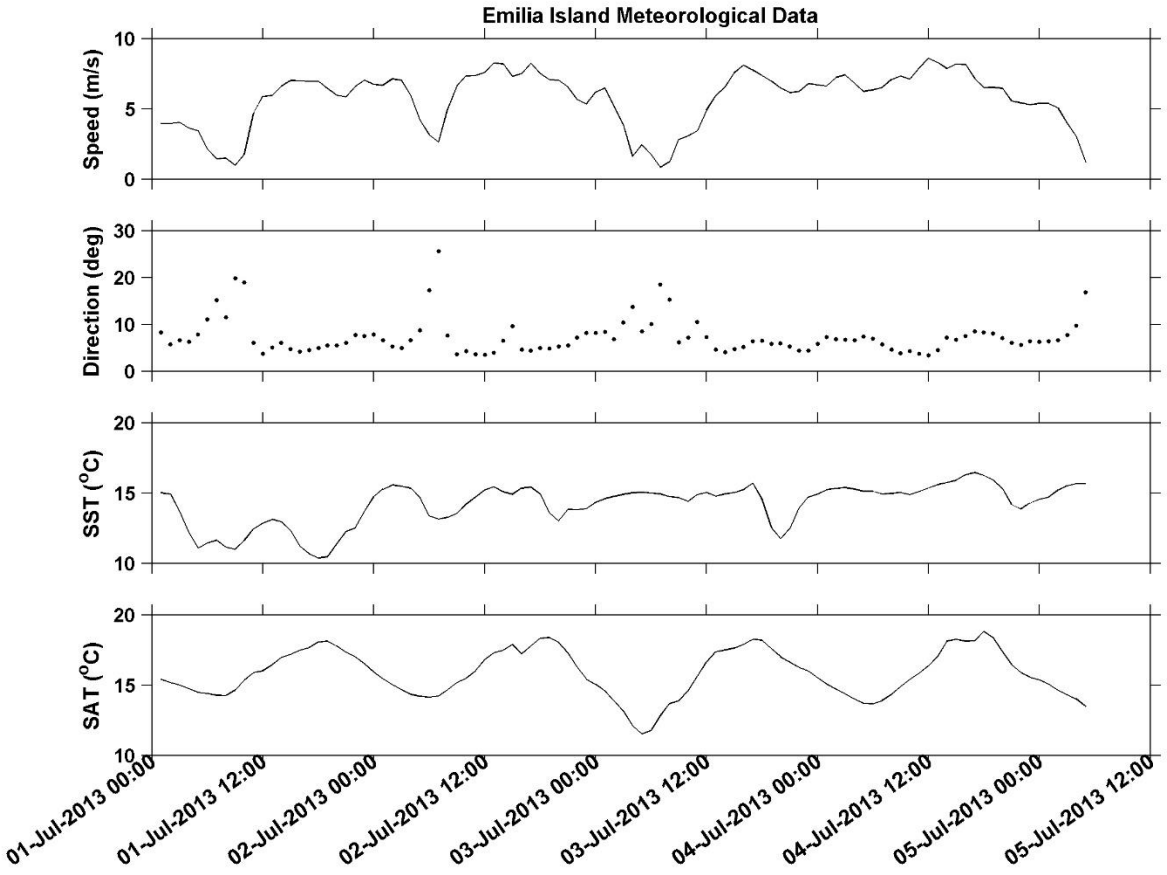

Figure 65 Hourly meteorological record from Emilia Island for the first 100 hours of July 2013

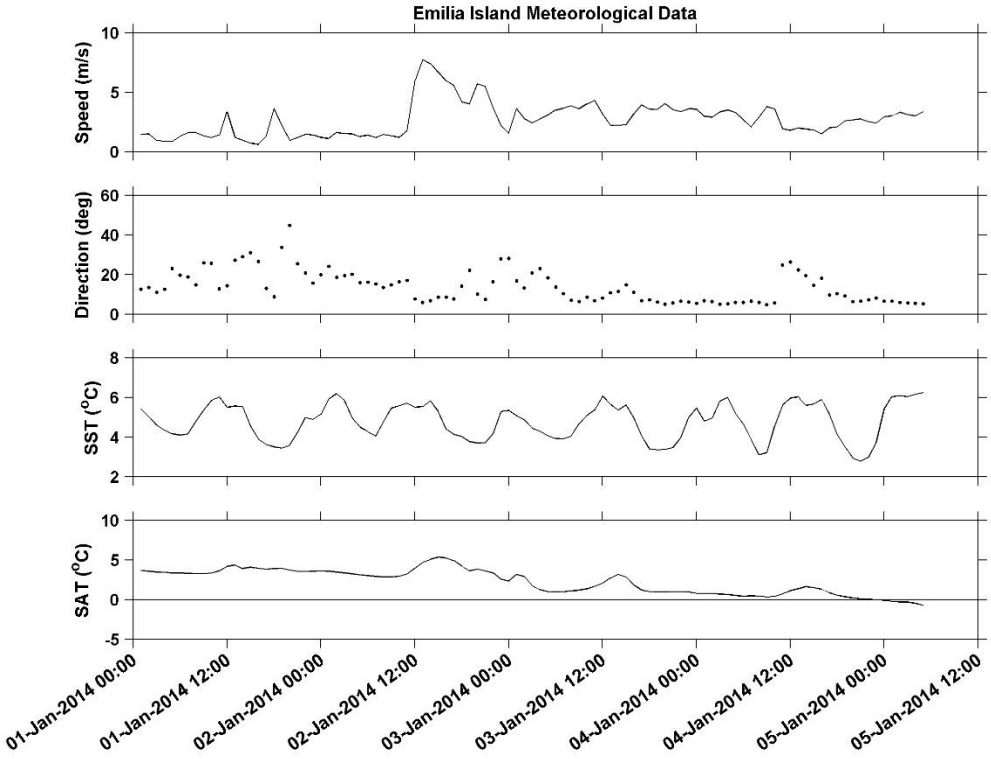

Figure 66 Hourly meteorological record from Emilia Island for the first 100 hours of January 2014

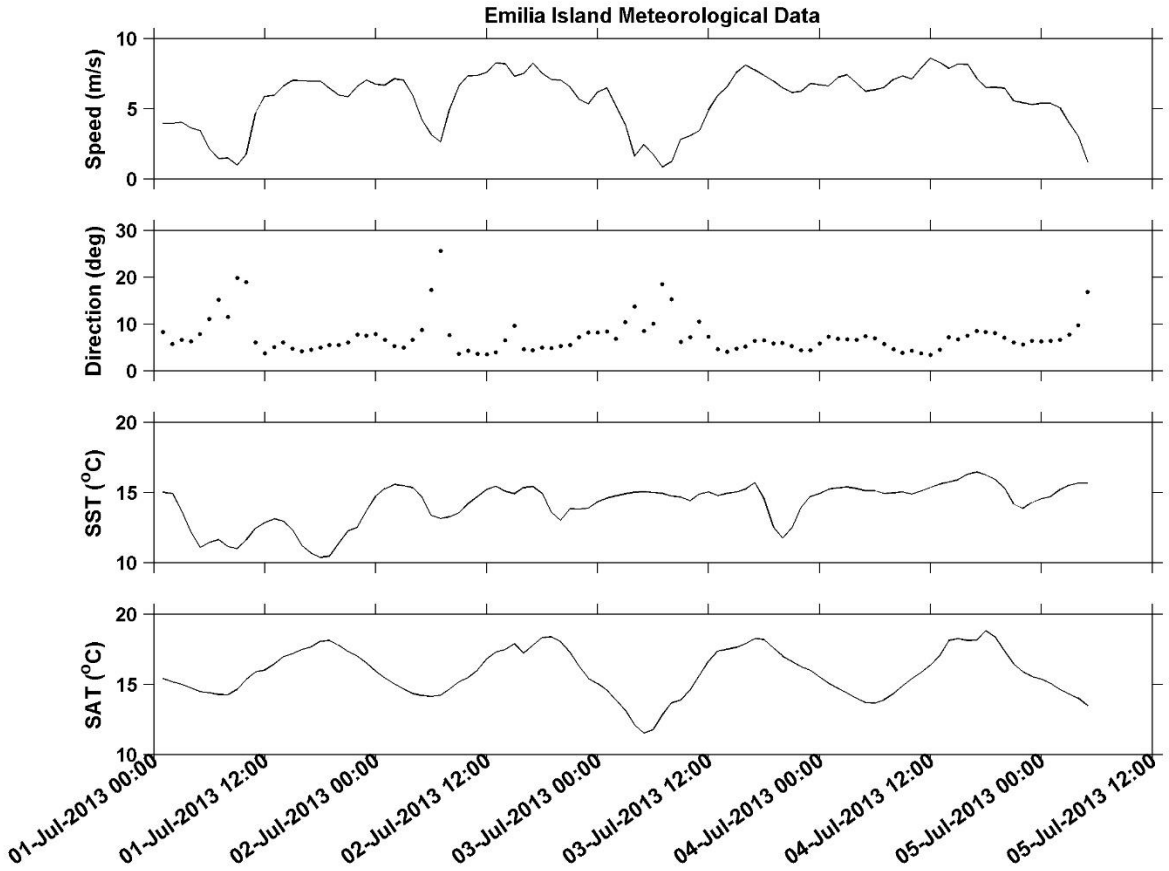

Figure 65 Hourly meteorological record from Emilia Island for the first 100 hours of July 2013

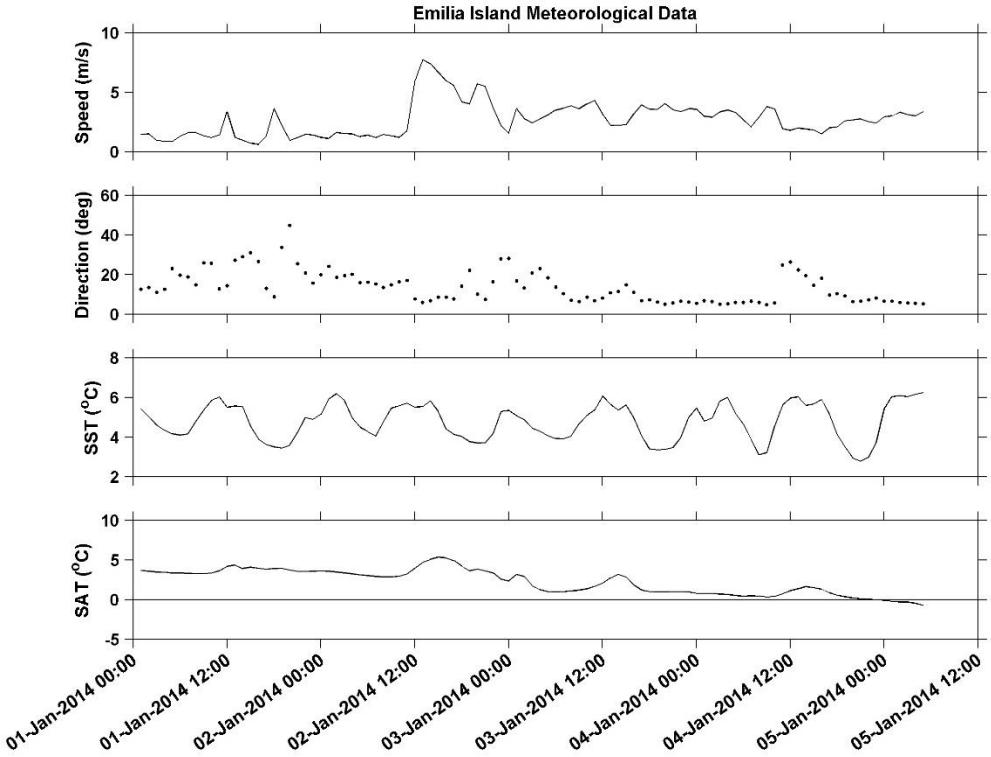

Figure 66 Hourly meteorological record from Emilia Island for the first 100 hours of January 2014

2.3.2 Oil Density

Oil density increased faster in summer than in winter using the variable wind and constant mean air and water temperature and constant mean salinity (**Figure 67**). Most of the change occurred in less than 24 hours in summer and in less than 48 hours in winter.

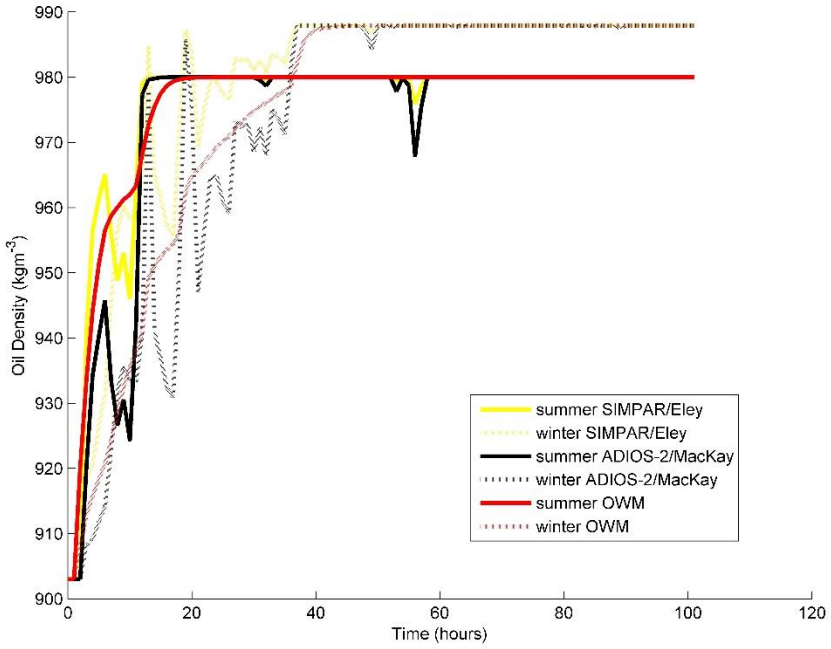

Figure 67 Cold Lake Bitumen density computed for summer and winter using 3 model algorithms with variable summer and winter mean wind speed and constant seasonal mean air temperature, SST, and salinity

2.3.3 Oil Viscosity

We computed the oil viscosity using the evaporation algorithms associated with each model. **Figure 68** shows the change in the oil viscosity over 100 hours. The viscosity increased faster in summer than in winter with a variable wind speed. In both seasons, the greatest change occurred in less than 40 hours, but in summer the greatest change in viscosity occurred in less than 20 hours. Summer weathering achieved a higher viscosity than winter weathering.

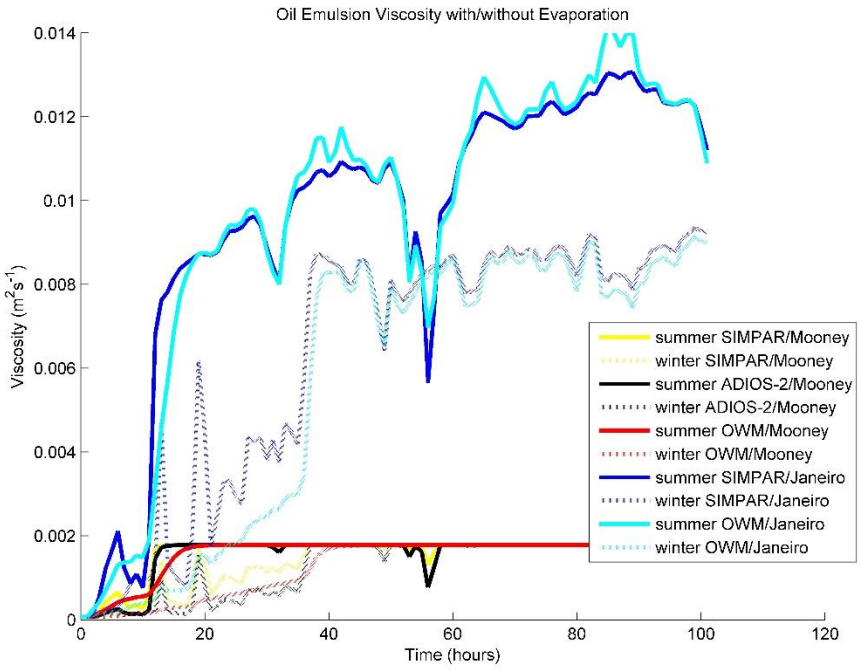

Figure 68 Cold Lake Bitumen viscosity computed for summer and winter using 2 algorithms for the 3 weathering models with variable summer and winter mean wind speed and constant seasonal mean air temperature, SST, and salinity

2.3.4 Emulsification (Water Content)

Water content reached its maximum faster in summer than in winter with a variable wind speed (**Figure 69**). The greatest rate of change was in summer in less than 20 hours. In winter, it took about 40 hours to reach the maximum water content.

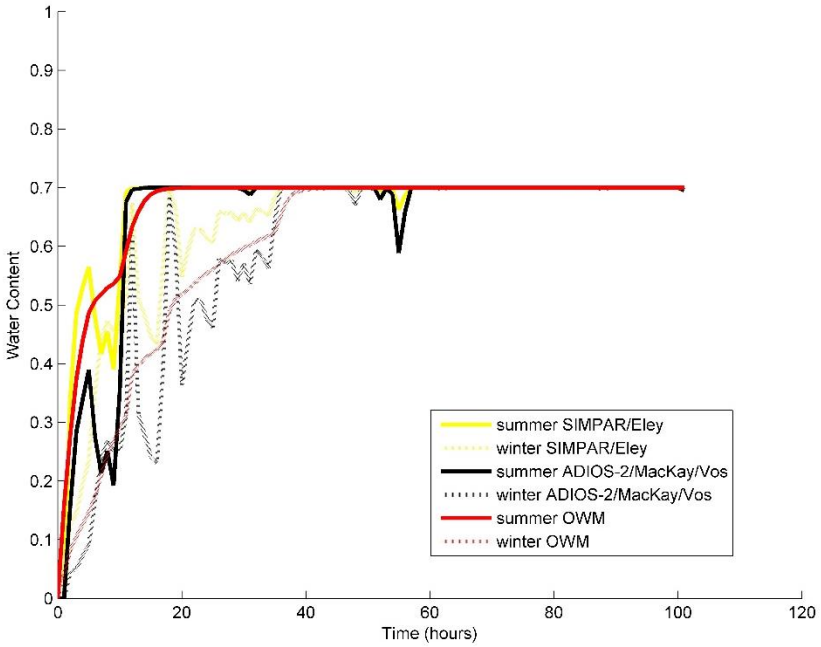

Figure 69 Cold Lake Bitumen water content computed for summer and winter using 3 model algorithms with variable summer and winter mean wind speed and constant seasonal mean air temperature, SST, and salinity

2.3.5 Evaporation

The fraction evaporated was greater in summer than in winter under variable wind speeds. The greatest change occurred in less than 12 hours in all the models regardless of the evaporation algorithm used (**Figure 70**).

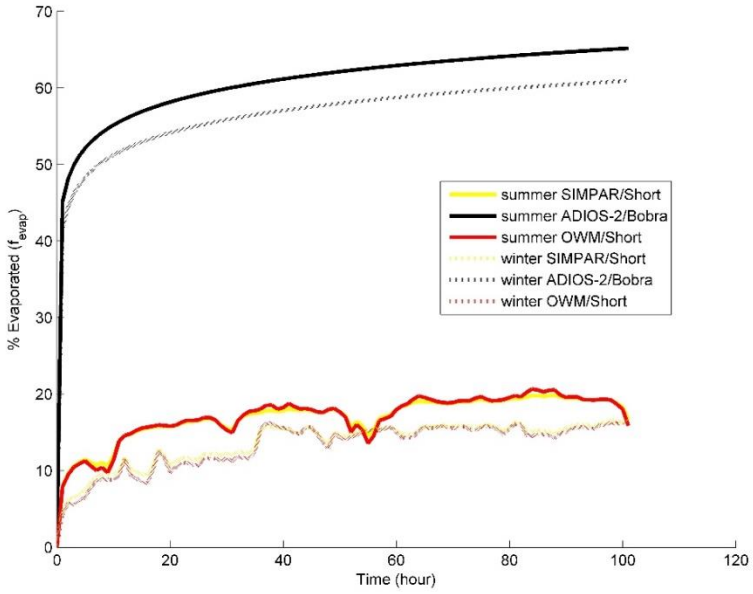

Figure 70 Percent evaporated of Cold Lake Bitumen computed for summer and winter using 2 model algorithms with variable summer and winter mean wind speed and constant seasonal mean air temperature, SST, and salinity

2.3.6 Entrainment Rate

With the varying wind speed, the entrainment rate no longer decreased steadily. This makes sense because the viscosity varies so much now. If we ignored the variability in the entrainment rate, **Figure 71** shows that the summer signal dominates the plot.

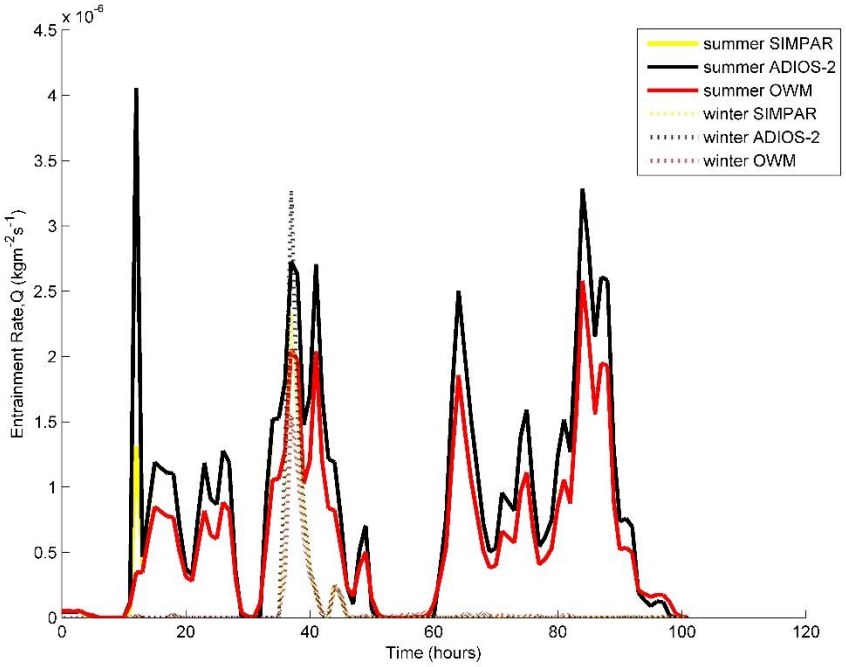

Figure 71 Entrainment rate of Cold Lake Bitumen computed for summer and winter using 3 model algorithms with variable summer and winter mean wind speed and constant seasonal mean air temperature, SST, and salinity

2.4 VARIABLE WIND SPEED AND AIR TEMPERATURE AND VARIABLE WATER PROPERTIES

2.4.1 Water Properties in Douglas Channel

We received hourly water temperature and salinity data from the Institute of Ocean Sciences (Fisheries and Oceans Canada) (**Figure 72** and **Figure 73**). These data are described in detail by Wright et al. (2015).

The meteorological data from Emilia Island also had SST values. We compared the meteorological SST to the measured data in **Figure 74** for summer and in **Figure 75** for winter. The Douglas Channel July mean water temperature reported in Short was 13.2^{o}C at 1.5 m and it was 6.8^{o}C in December. Clearly, the measured temperature data for summer was too cold at 16 m depth to be representative of summer SST when compared to Short's summer mean. For winter, the measured temperature data at 16 m depth was

only slightly colder than the seasonal SST. Belore (2010) reported the mean water temperature in winter as 6.39^{o}C. We computed the winter mean SST for the first 100 hours of January 2014 from the measured Douglas Channel data at 16 m depth to be 6.81^{o}C. We computed the summer mean SST for the first 100 hours of July 2013 data from the measured Douglas Channel data at 16 m depth to be 8.08^{o}C. The mean SST from the 100 hours of meteorological data in in winter was 4.75^{o}C, and the mean meteorological SST in summer was 14.17^{o}C. Because the mean SST that was measured at 16 m was much cooler than the mean July SST reported in Short, and cooler than the mean computed from the meteorological data, we used the 100 hours of meteorological SST for our computations in this section.

The measured winter salinity at 16 m was slightly lower than the mean salinity at 1.5 m reported in Short for December (30.7). The measured summer salinity at 16 m was closer to the winter mean than Short's reported July surface mean of 17.9. We computed the winter mean for the first 100 hours of January 2014 data from the measured Douglas Channel data at 16 m to be 29.24 ppt. The mean summer salinity for the first 100 hours of July 2013 data from the measured Douglas Channel data at 16 m was 30.56 ppt. Even though the *in-situ* salinity was not representative of the seasonal salinities when compared to Short's values, we had no other source of salinity data, and we used the data that were measured at 16 m. We only used the variable salinity to compute seawater density, kinematic water viscosity, and to compute the mass transfer coefficient (Equation 31 in Fingas, 2013) for the Bobra algorithm that computes evaporated fraction (Fingas, 2013) in the ADIOS-2 model computation. We have not been reporting the results produced from that ADIOS-2 evaporation algorithm because the values were not consistent with those from the other model algorithms so that mass transfer coefficient computation was not crucial for this report.

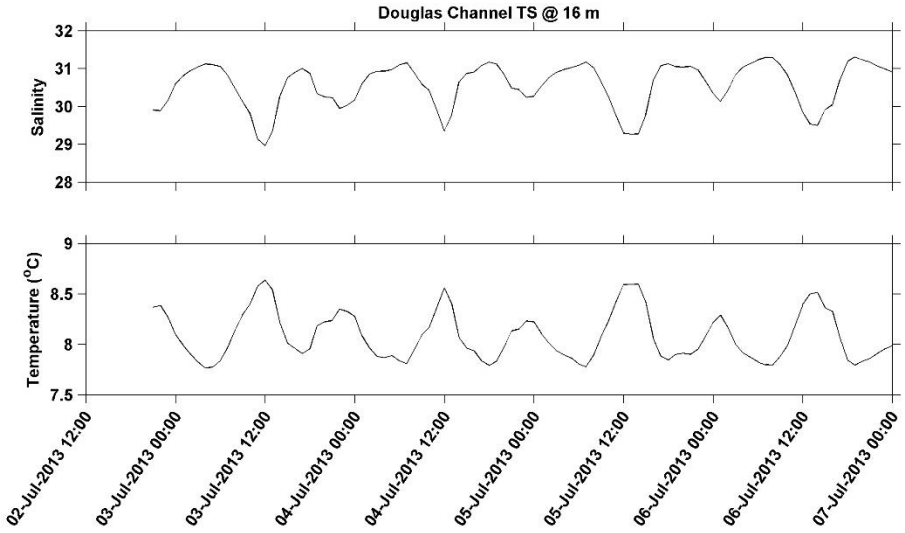

Figure 72 The first 100 hours of July 2013 water temperature and salinity data that were recorded in Douglas Channel at 16 m

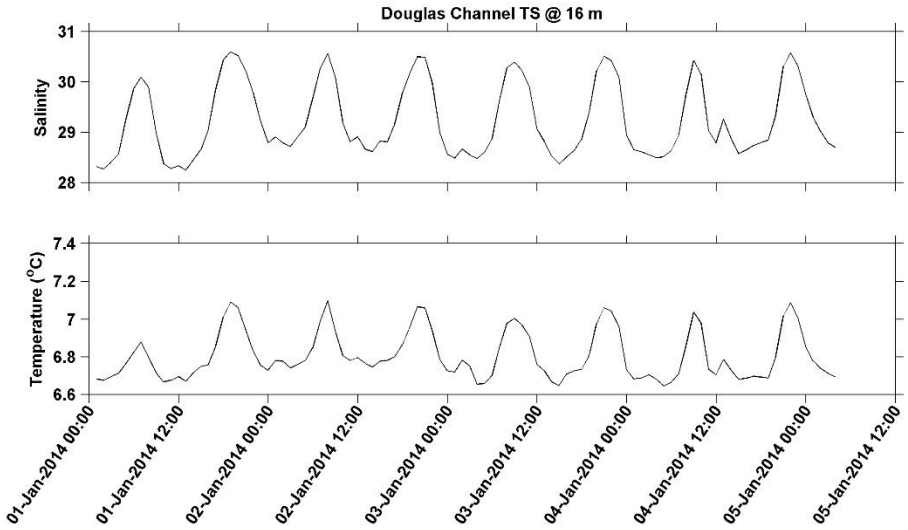

Figure 73 The first 100 hours of January 2014 water temperature and salinity data that were recorded in Douglas Channel at 16 m

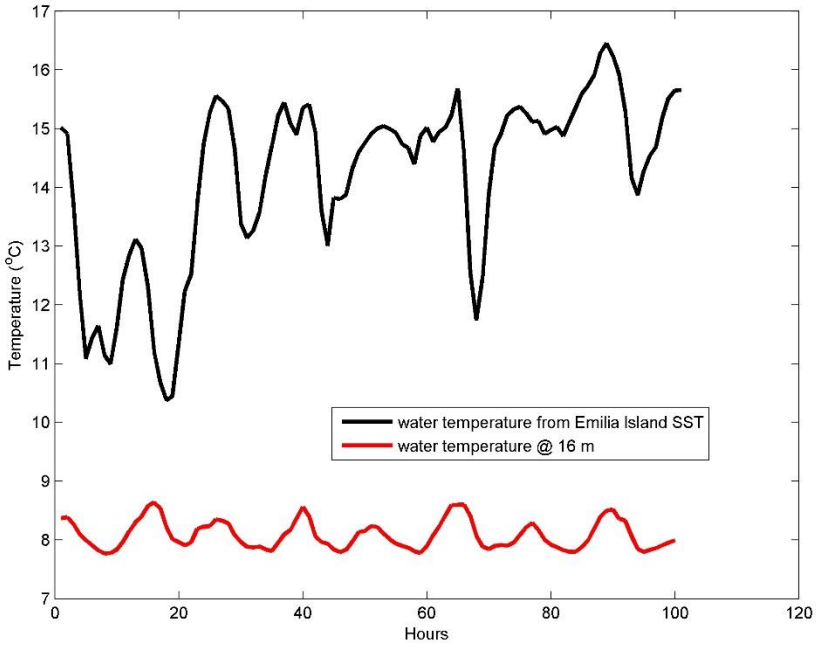

Figure 74 Summer meteorological SST data and water temperature data measured at 16 m for the first 100 hours of July 2013

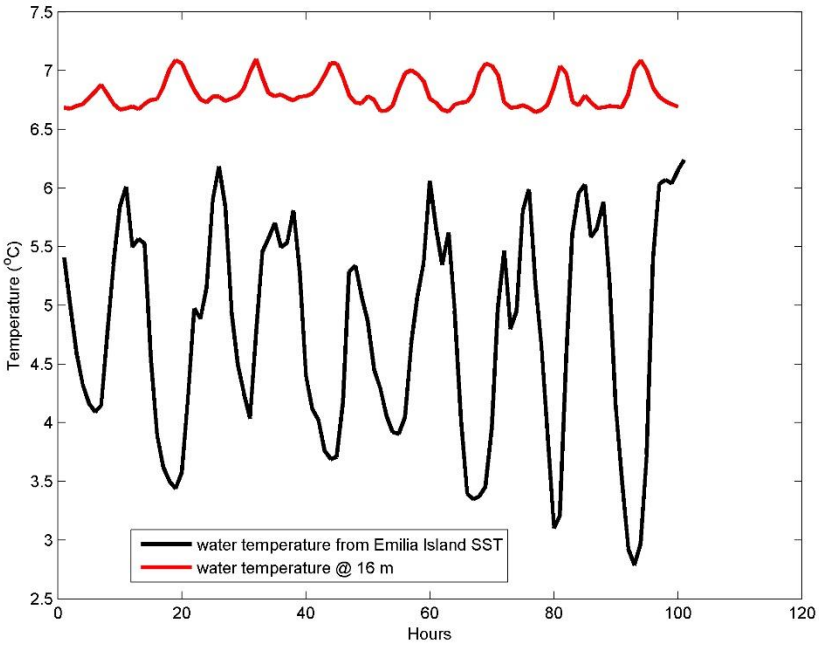

Figure 75 Winter meteorological SST data and water temperature data measured at 16 m for the first 100 hours of January 2014

2.4.2 Oil Density

Oil density in summer increased at a faster rate than in winter (**Figure 76**). The summer maximum density was reached in less than 24 hours, and the winter maximum was reached in less than 48 hours.

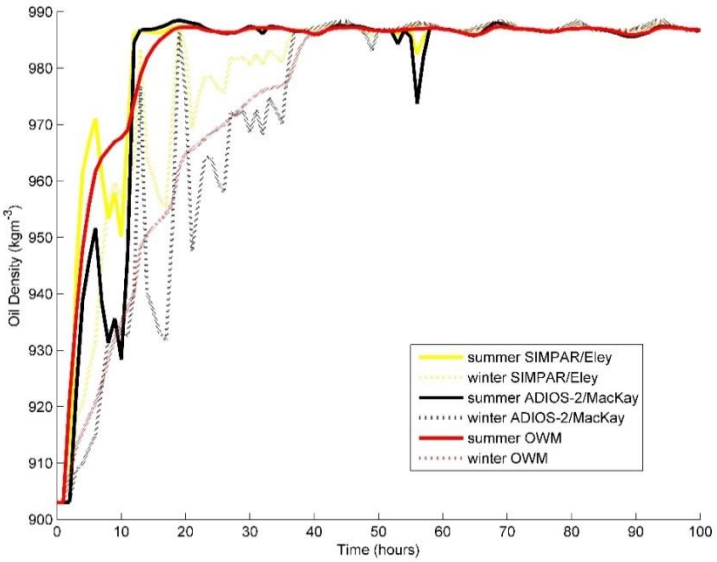

Figure 76 Cold Lake Bitumen density computed for summer and winter using 3 model algorithms with variable summer and winter mean wind speed and air temperature and variable water temperature and salinity

2.4.3 Oil Viscosity

In summer, the viscosity increased at its greatest rate in less than 20 hours, and in winter it increased at its greatest rate in less than 40 hours (**Figure 77**).

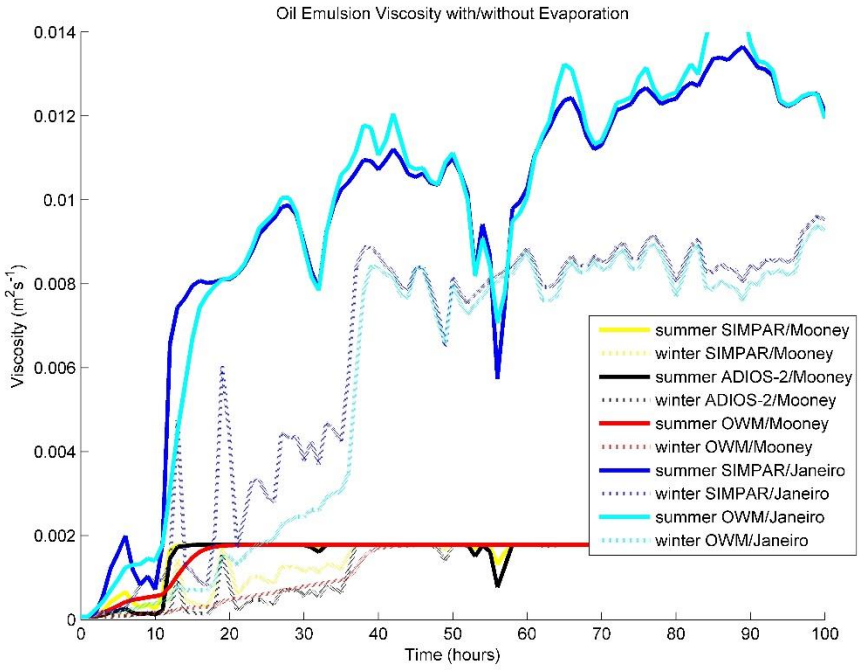

Figure 77 Cold Lake Bitumen viscosity computed for summer and winter using 2 model algorithms for the 3 weathering models with variable summer and winter mean wind speed and air temperature and variable water temperature and salinity

2.4.4 Emulsification (Water Content)

The water content reached its maximum value faster in summer than in winter (**Figure 78**). The greatest change occurred in less than 12 hours in summer, and it occurred in less than 40 hours in winter.

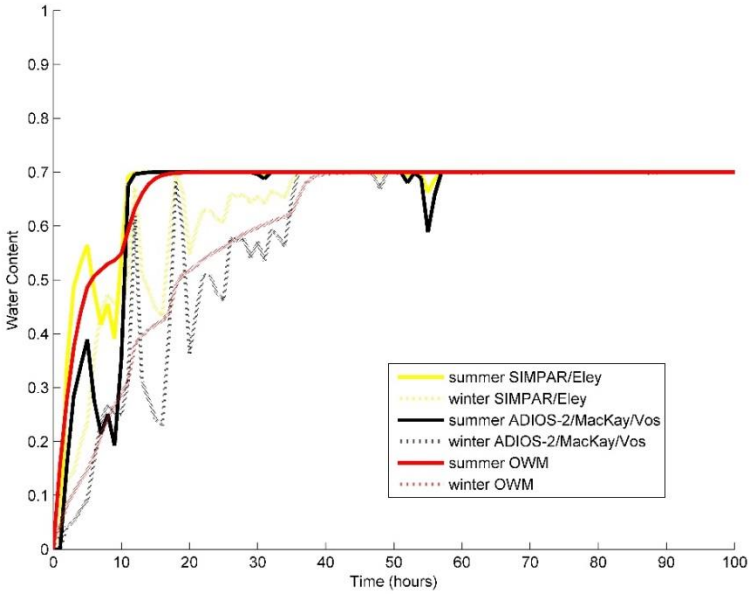

Figure 78 Cold Lake Bitumen water content computed for summer and winter using 3 model algorithms with variable summer and winter mean wind speed and air temperature and variable water temperature and salinity

2.4.5 Evaporation

The fastest change in evaporation occurred in less than 6 hours in summer and winter (**Figure 79**). The fraction evaporated continued to increase steadily with a greater fraction of oil being evaporated in summer than in winter.

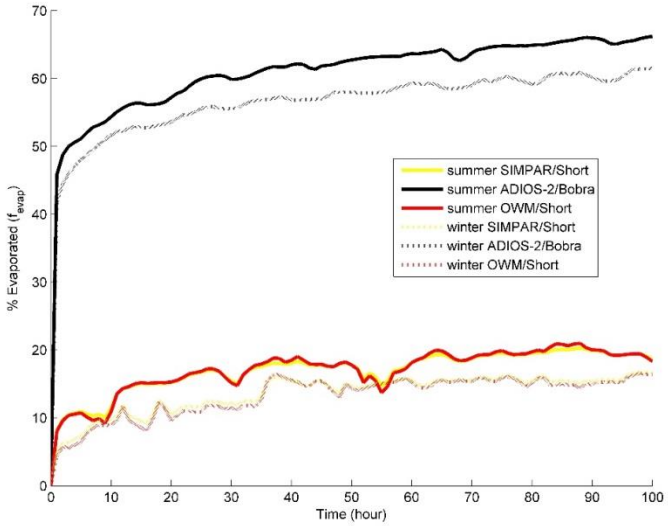

Figure 79 Cold Lake Bitumen percentage evaporated computed for summer and winter using 2 model algorithms for the 3 weathering models with variable summer and winter mean wind speed and air temperature and variable water temperature and salinity

2.4.6 Entrainment

The entrainment rates that we computed under summer conditions dominated the entrainment rates computed using winter conditions (**Figure 80**). The varying wind speed rather than the varying oil viscosity dominated the signals.

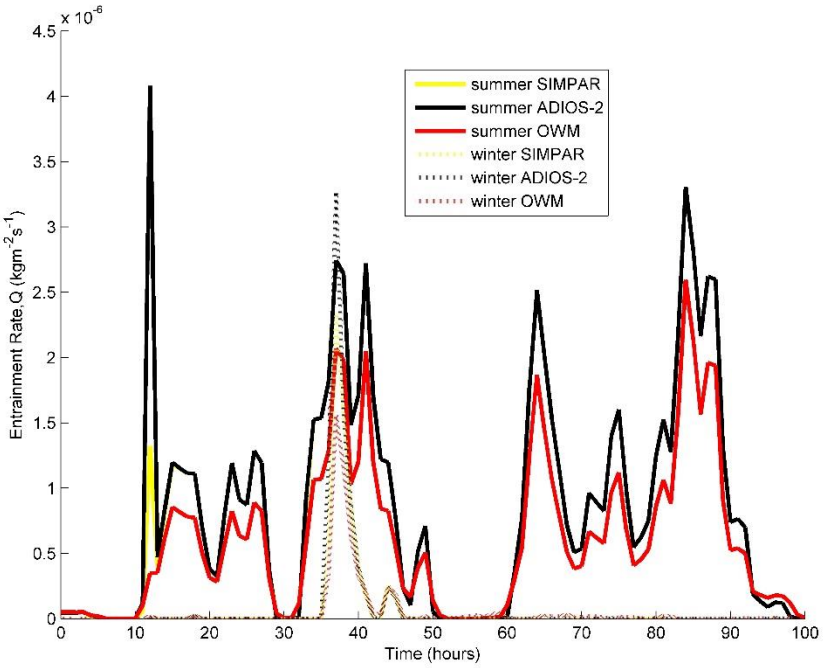

Figure 80 Cold Lake Bitumen entrainment rate computed for summer and winter for the 3 weathering models with variable summer and winter mean wind speed and air temperature and variable water temperature and salinity

2.5 SUMMARY OF PART 2

In this section, we summarize a few points that we discovered using our Matlab® functions to describe the weathering of Cold Lake diluted bitumen in Douglas Channel using “real” input data. We used mean water temperature and salinity data from Fissel et al. (2010), as reported by Short (2013), and variable salinity that we received from the Institute of Ocean Sciences (C. Hannah). Wind data were measured by a GEM meteorological station at Emilia Island as reported in Stronach et al., (2010). We compared weathering conditions in summer to those in winter for Douglas Channel in the absence of wind, with a constant wind, with a variable wind, and with a variable wind and variable water properties.

Using real data for a hypothetical oil spill highlighted the sensitivity of the three model algorithms, and algorithms that we found in literature, to wind speed, air temperature, salinity, and sea surface temperature. For example, oil viscosity was sensitive to the evaporation algorithm used in SIMPAR and ADIOS-2 as well as to the wind. The oil density reflected the changes in water content more than the changes in SST, showing

its sensitivity to a varying wind speed. The oil density was most sensitive to wind when computed with water content from by SIMPAR and ADIOS-2 algorithms. Variable wind speed also affected how strong the seasonal response was to the weathering process; with a constant wind, the weathering was more aggressive in winter, but with a variable wind speed and air temperature, weathering in summer became more aggressive. Varying the salinity and water temperature did not have as great an effect as varying the wind, even though the salinity that we used was subsurface. This implies that a mean value for surface water temperature and salinity would be sufficient. The time scale of rapid change in weathering properties suggests that a mean wind speed (and air temperature) value over 6-12 hours might be enough to study short-term weathering.

2.5.1 No Wind

In the absence of wind, and with seasonal mean water properties, the oil density increased towards a higher density in winter than in summer. However, there was no seasonal difference in the viscosity and water content in summer and winter. The computation of viscosity was sensitive to a change in how evaporation was computed. When the algorithm for computing evaporation was changed to one that accounted for salinity and API in the mass transfer coefficient, increasing viscosity values were higher in summer than in winter.

2.5.2 Constant Wind

When we used a constant seasonal mean wind speed to compute the weathering changes, we found that the oil density and viscosity increased more rapidly in winter than in summer, and there was slightly greater evaporation in summer than in winter. In either season, the halfway point to the maximum density was reached within 12 hours, and most of the viscosity changes occurred in less than 24 hours. The halfway point of the maximum water content was also reached within 12 hours, and, in most cases, 15% of the mass had evaporated within 24 hours. These results are slightly faster than what has been seen in tank experiments (King et al., 2014), and qualitatively agree with what Belore (2010) found for MacKay River diluted bitumen. The entrainment rate decreased the most within 12 hours as well.

Under extreme conditions, the speed of weathering increased in all cases. Winter changes still dominated the summer changes for density, viscosity, water content, and entrainment, but, under extreme conditions, evaporation in winter was slightly greater than in summer for some models and equal for other models.

2.5.3 Variable Wind

Under varying wind speeds and air temperature, the summer oil density reached its maximum faster (<20 hours) than the winter oil density (<40 hours). Oil viscosity increased at its greatest rate in less than 20 hours in summer and in less than 40 hours in winter. Water content reached its maximum in less than 20 hours in summer and in less than 40 hours in winter. The greatest evaporative loss was almost immediate with more mass lost in summer than in winter.

2.5.4 Variable Wind and Water Properties

With variable wind speeds, air temperature, water temperature and salinity, the results were almost indistinguishable from the weathering with varying atmospheric conditions and constant mean water properties.

The maximum density was reached in summer faster than it was reached in winter in both cases, but the maximum summer density was equal to the maximum winter density when water properties varied. The varying water properties did not seem to make any difference to the oil viscosity, water content, or evaporation.

Using variable wind, air, and water properties affected the magnitude of the final oil density and oil viscosity, but the timing of the greatest change remained the same. This could be a good thing because the weathering equations were developed empirically in the laboratory with constant wind and water properties. The insensitivity of the timing of the greatest change also means that the timing of spill response could be based on constant values. However, differences in the timing of the largest change that occurred under extreme conditions vs. mean conditions means that consideration of the “type” of conditions is important. The timing of the weathering processes is critical. Stronach (2011) noted from model results that oil could reach the north shore of Douglas Channel within eight hours of a spill at Emilia Island under winter conditions, and that, after 24 hours, some oil could become stranded on shore while more oil would move farther south for the next 15 hours. From his model, no oil was at the surface after 57 hours.

When looking at seasonal differences, under constant wind conditions, winter dominated the weathering with density and viscosity responding to winter conditions with higher maximum values, and the time needed to reach the maximum water content being shorter in winter than summer. The fraction evaporated in winter, however, was less than that in summer. Furthermore, under variable environmental conditions, summer density and viscosity dominated the weathering.

3 ACKNOWLEDGEMENTS

This research was supported by World Class Tank Safety System Program of Federal Government of Canada. We thank M. Mo from ECCC for providing air forcing data. We also thank A. Drozdowski, C. O'Laughlin at the Bedford Institute of Oceanography for their comments on the draft manuscript.

4 REFERENCES

Amorocho, J. and J. J. Devries, 1980, “A new evaluation of the wind stress coefficient over water surfaces”, *J. Geophys. Res.*, **85**(C1): 433-442

Belore, R., 2010, Properties and fate of hydrocarbons associated with hypothetical spills at the marine terminal and in the confined channel assessment area, Technical Data Report, SL Ross Environmental Research Ltd., Ottawa, Ontario, 132 p, http://www.ceaa-acee.gc.ca/050/documents_staticpost/cearref21799/2430/Properties_and_Fate_from_Spills_-_Confined_Channel.pdf (accessed 08 March 2013)

Buchanan, I. and N. Hurford, 1988, “Methods for predicting the physical changes in oil spilt at sea”, *Oil and Chemical Pollution*, **4**: 311-328

CSIRO, www.cmar.csiro.au/datacentre/ext_docs/seawater.htm (accessed 18 November 2015)

De Dominicis, M., N. Pinardi, G. Zodiatis, and R. Lardner, 2013a, “MEDSLIK-II, a Lagrangian marine surface oil spill model for short-term forecasting – Part 1: Theory”, *Geosci. Model Dev.*, **6**: 1851-1869, doi: 10.5194gmd-6-1851-2013

De Dominicis, M., N. Pinardi, G. Zodiatis, and R. Archetti, 2013b, “MEDSLIK-II, a Lagrangian marine surface oil spill model for short-term forecasting – Part 2: Numerical simulations and validations”, *Geosci. Model Dev.*, **6**: 1871-1888, doi: 10.5194gmd-6-1871-2013

Delvigne, G. A. L., 1993, “Natural dispersion of oil by different sources of turbulence”, International Oil Spill Conference Proceedings: March 1993, Vol. 1993, No. 1, pp. 415-419

Delvigne, G. A. L. and C. E. Sweeney, 1988, “Natural Dispersion of Oil”, *Oil and Chemical Pollution*, **4**: 281-310

Eley, D. D., M. J. Hey, and J. D. Symonds, 1988, “Emulsions of water in Asphaltene-Containing Oils 1. Droplet size distribution and emulsification rates”, *Colloid and Surfaces*, **32**: 87-101

Fay, J. and D. Hoult, 1971, Physical Processes in the Spread of Oil on a Water Surface, Report DOT-CG-01 381-A. Washington, DC, US Coast Guard

Fingas, M. F., 1995, “A literature review of the physics and predictive modelling of oil spill evaporation”, *J. of Hazardous Materials*, **42**: 157-175

Fingas, M. F., 2011, “Evaporation Modeling”, in Oil Spill Science and Technology, Elsevier, pp. 1149, doi: 10.1016/B987-1-85617-943-0.10008-5

Fingas, M. F., 2013, “Modeling oil and petroleum evaporation, *J. of Petroleum Science Research*, **2**(3): 104-115

Fissel, D. B., K. Borg, D. D. Lemon, and J. R. Birch, 2010, Technical Data Report Marine Physical Environment Enbridge Northern Gateway Project, ASL Environmental Sciences, Sidney, British Columbia

Government of Canada, 2013, Properties, Composition and Marine Spill Behaviour, Fate and Transport of To Diluted Bitumen Products from the Canadian Oil Sands, Federal Government Technical Report: Environment Canada, Fisheries and Oceans Canada, Natural Resources Canada, November 30, 2013, 87 p, http://www.ec.gc.ca/scitech/6A2D63E5-4137-440B-8BB3-E38ECED9B02F/1633_Dilbit%20Technical%20Report_e_v2%20FINAL-s.pdf (accessed 08 March 2016)

Guo, W. J. and Y. X. Wang, 2009, “A numerical oil spill model based on a hybrid method”, *Marine Pollution Bull.*, **58**: 726-734

Hamoda, M. F., S. E. M. Hamam, and H. I. Shaban, 1989, “Volatization of Crude Oil from Saline Water”, *Oil and Chemical Pollution*, **5**: 321-331

Holthuijsen, L. H. and T. H. C. Herbers, 1986, “Statistics of breaking waves as whitecaps in the open sea”, *J. Phys. Ocean.*, **16**: 290-297

Janeiro, J., E. Fernandes, F. Martins, and R. Fernandes, 2008, “Wind and freshwater influence over hydrocarbon dispersal on Patos Lagoon, Brazil”, *Marine Pollution Bulletin*, **56**: 650-665

Jones, R. K., 1997, “A simplified pseudo-component oil evaporation model”, Proceedings of the Twentieth Arctic and Marine Oilspill (*sic*) Program (AMOP) Technical Seminar, Environment Canada Emergencies Science Division, Ottawa, Canada: 43-61

King, T. L., B. Robinson, M. Boufadel, and K. Lee, 2014, “Flume tank studies to elucidate the fate and behavior of diluted bitumen spilled at sea, *Marine Pollution Bulletin*, **83**: 32-37

Lehr, W. J., 2001, “Review of modeling procedures for oil spill weathering behavior”, *Adv. Ecol. Sci.,* **9**: 51-90

Lehr, W., R. Jones, M. Evans, D. Simecek-Beatty, and R. Overstreet, 2002, “Revisions of the ADIOS oil spill model”, *Env. Modelling and Software*, **17**: 191-199

Mackay, D. and R. S. Matsugu, 1973, “Evaporation rates of liquid hydrocarbon spills on land and water”, *Can. J. Chem. Eng.*, **51**: 434-439

MacKay, D., I. Buist, R. Mascarenhas, and S. Petersen, 1980, Oil Spill Processes and Models, Environmental Protection Service, Canada, Report EE-8

MacKay, D., W. Stiver, and P. A. Tebeau, 1983, “Testing of crude oils and petroleum products for environmental purposes, in Proceedings of the 1983 Oil Spill Conference, American Petroleum Institute, Washington, DC, pp: 331-337

Milgram, J. H. R. G. Donnelly, R. J. van Houten, and J. M. Camperman, 1978, “Effects of Oil Slick Properties on the Dispersion of Floating Oil into the Sea”, U. S. Dept. of Transportation, Washington DC

Mishra, A. K. and G. S. Kumar, 2015, “Weathering of oil spill: modeling and analysis”, *Aquatic Procedia*, **4**: 435-442

Mooney, M., 1951, “The viscosity of a concentrated suspension of spherical particles”, *J. Colloid. Sci.*, **6**(2): 162-170

Monahan, E. C. and I. O’Muircheartiagh, 1980, “Optimal power-law description of oceanic whitecap coverage dependence on wind speed”, *J. Phys. Ocean.*, **10**: 2094-2099

Payne, J. R., B. E. Kierstein, J. R. Clayton, Jr., C. Clary, R. Redding, D. McNabb, Jr., and G. Farmer, 1977, Final Report: Integration of Suspended Particulate Matter and Oil Transportation Study, Contract No. 14-12-0001-030146, September 15, 1987, Science Applications International Corporation, San Diego, CA, USA

Perry’s Chemical Engineering Handbook, Sixth Edition, 1973, McGraw-Hill Inc.

Reed, M., 1989, “The physical fates Component of the Natural Resource Damage Assessment Model System”, *Oil and Chemical Pollution*, **5**: 99-123

Reed, M., 2001, Technical Description of the Dose-Related Exposure Assessment Model DREAM. SINTEF Report STF66 F 24-09-2001, 77 p.

Reijnhart, R. and R. Rose, 1982, “Evaporation of crude oil at sea”, *Water Res.*, **16**(8): 1319-1325, doi: 10.1016/0043-1354(82)90210-X

Schneider, D. F., 1998, “Select the Right Hydrocarbon Molecular Weight Correlation”, white paper, Stratus Engineering, Inc. League City, Texas, 20 p. (accessed 10 August 2015)

Shaw, D. G., 1977, Hydrocarbons in the Water Column, In: Fates and effects of Petroleum Hydrocarbons in Marine Ecosystems and Organisms, D. A. Wolfe (ed.)

Short, J. W., 2013, “Susceptibility of diluted bitumen products from the Alberta Tar Sands to sinking in water”, white paper, JWS Consulting LLC, Juneau, Alaska

SINTEF, 2005, “SINTEF Oil Weathering Model User’s Manual Version 3.0”, http://www.boem.gov/BOEM-Newsroom/Library/Publications/2005/2005_020_appD.aspx (accessed 10 August 2015)

Stiver, W. and D. MacKay, 1984, “Evaporation rate of spills of hydrocarbon and petroleum mixtures”, *Environ. Sci. Technol.*, **18**: 834-840

Stronach, J., 2011, Hydrocarbon Mass Balance Estimates: Inputs for Spill Response Planning, Technical Data Report October 2010, Hay and Company Consultants, Vancouver, British Columbia, 92 p, http://www.ceaa.gc.ca/050/documents_staticpost/cearref_21799/2561/hydrocarbon.pdf (accessed 08 March 2016)

Stronach, J., E. Wang, B. Draho, and T. Miguez, 2010, “Wind observations in Douglas Channel, Squally Channel, and Caamaño Sound”, Technical Data Report October 2010, Hay and Company Consultants, Vancouver, British Columbia, 162 p, http://www.ceaa.gc.ca/050/documents_staticpost/cearref_21799/2431/Wind_1of3.pdf (accessed 08 March 2016)

Vos, R. J., 2005, “Comparison of 5 oil-weathering models”, white paper: Werkdocument RIKZ/ZD/2005.011W, Minitsterie van Verkeer en Waterstaat, Rijkswaterstaat, The Netherlands

Wang, S. D., Y. M. Shen, and Z. H. Zheng, 2005, “Two-dimensional numerical simulation for transport and fate of oil spills in seas”, *Ocean Engineering*, **32**(2005): 1556-1571

Wright, C. A., S. Vagle, C. Hannah, and S. J. Johannessen, 2015. Physical, chemical, and biological oceanographic data collected in Douglas Channel and the approaches to Kitimat, June 2013 – July 2014, Can. Data Report Hydrog. Ocean Sci. 196: viii+66 pp., http://www.dfo-mpo.gc.ca/Library/359327_pt1.pdf; http://www.dfo-mpo.gc.ca/Library/359327_pt2.pdf; http://www.dfo-mpo.gc.ca/Library/359327_pt3.pdf

Zanier, G., A. Petronio, F. Roman, and V. Armenio, 2014, “High resolution oil spill model for harbour and coastal areas”, 3rd IAHR Europe Congress, Book of Proceedings, 2014, Porto-Portugal.

5 APPENDIX

Table 1 Table of equations for each weathering process

Weathering Process	Model(s)	Source/Based on	Equation
Initial Release/ Spreading	SIMPAR ADIOS-2	Fay and Hoult (1971)	$R = \frac{k_2^2}{k_1}\left(\frac{V_{oil}^5 g(\rho_w - \rho_{oil})/\rho_w}{v_w^2}\right)^{1/12}$
	OWM DREAM	Reed (2001)	$X = \left[\frac{3}{2}\frac{V_{oil}^2 \rho_{oil} g'}{B^2}\right]^{\frac{2}{5}} (\rho_w \mu_w)^{\frac{-1}{5}} U_{H2O}^{\frac{-3}{5}}$
			$\mu_w = v_w \rho_w$
			$g' = g(\rho_w - \rho_{oil})/\rho_w$
Dispersion	SIMPAR ADIOS-2	Vos (2005)	$Q = \frac{dmax^{1.7}}{1.7} \times C_0 D_{ba}^{0.57} F_{wc} S_{cov}$ $D_{ba} = 0.0034 \rho_w \, g \left(\frac{H_0}{\sqrt{2}}\right)^2$ $H_0 = \frac{0.243 \, U_w^2}{g}$
		Holthuijsen and Herbers (1986)	$F_{wc} = \frac{0.032 \max(U_w - 5.0; 0.0)}{T_w}$
	OWM DREAM	Delvigne and Sweeney (1988) Delvigne (1993)	$Q(d) = C_0 D_{ba}^{0.57} d_o^{0.7} \Delta d S_{cov} F_{wc}$
		Monahan and O'Muircheartaigh (1980)	$F_{wc} = 3 \times 10^{-6} \, U_w^{3.5}$
Evaporation (semi-empirical distillation theory)	SIMPAR OWM	Short (2013) Stiver and MacKay (1984)	$f_{evap} = \ln\left[1 + \left(\frac{12191}{T_{oil}}\right)\theta e^{8.2 - \left(\frac{5239}{T_{oil}}\right)}\right] / \left(\frac{12191}{T_{oil}}\right)$
			$K = 0.0015 U_w^{0.78}$
			$K(t) = C_d U_w(t)$ in OWM
			$C_d = \left(\frac{U_w^*}{U_w(t)}\right)^2$ in OWM
			$U_w^* = \begin{cases} CU_w(t) & for \quad U_w(t) < u_1 \\ Cu_1 + (Du_2 - Cu_1)\frac{U_w(t) - u_1}{u_2 - u_1} & for \; u_1 \le U_w(t) \le u_2 \\ DU(t) & for \quad U_w(t) > u_2 \end{cases}$
	ADIOS-2	Bobra (1992)/Fingas(2011, 2013) Stiver and MacKay (1984)	$f_{evap} = \ln\left[1 + B\left(\frac{T_G}{T_{oil}}\right)\theta e^{A - B\left(\frac{T_0}{Toil}\right)}\right]\left(\frac{T_{oil}}{BT_G}\right)$
			$K = 1.68 \times 10^{-5} API^{1.253} T^{1.80} S^{0.1441}$
	from the literature	Buchanan and Hurford (1988) Stiver and MacKay (1984)	$f_{evap} = \frac{15}{C_2} ln\left[\frac{C_2 U_w^{0.78} t}{6000h} exp\left(16.6 - \frac{C_1}{15}\right) + 1\right]$
Evaporation Empirical Equations	from the literature	Fingas (2013)	Ekofisk $f_{evap} = [4.92 + 0.045T]\ln(t)$ Troll $f_{evap} = [2.26 + 0.045T]\ln(t)$ Cold Lake Bitumen $f_{evap} = [-0.16 + 0.013T]/\mathrm{t}$

Weathering Process	Model(s)	Source/Based on	Equation
Emulsification	SIMPAR	Eley (1988) Vos (2005)	$y = \frac{x}{(6+x)}$
			$x = x_{max}(1 - e^{-k_s t})$
			$x_{max} = \frac{6y_{max}}{(1-y_{max})}$
			$k_y = \frac{k_0}{y_{max}}(U_w + 1)^2$
	ADIOS-2	MacKay et al. (1980) Vos (2005) Reed (1989)	$y = y_{max}(1 - e^{-k_y t})$
			$k_y = \frac{k_0}{y_{max}}(U_w + 1)^2$
			$k_0 = 1x10^{-6}\ s^{-1}$
	OWM	SINTEF (2005) Vos (2005) MacKay et al. (1980)	$y(t + \Delta t) = y_{max}(t) - [y_{max}(t) - y(t)]0.5^{\frac{\Delta t}{t_{1/2}}}$
			$t_{1/2} = 2.43\ x\ 10^5\ when\ U_w = 0$ $t_{1/2} = \frac{ln2}{k_y}$
			$k_y = \frac{k_0}{y_{max}}(U_w + 1)^2$
Oil Density	SIMPAR ADIOS-2 OWM	Vos (2005)	$\rho_{oil}(y, T_{oil}) = y\rho_w + (1-y)\rho_0(0, T_{ref})[1 - c_1(T_{oil} - T_{ref})(1 + c_2 f_{evap})]$
Oil Viscosity	from the literature	Mooney (1951) Vos (2005)	$\nu(t) = \nu_0 \exp(\frac{ay(t)}{1-by(t)})$
	from the literature	Guo and Wang (2009)	$\nu(t) = \nu_0 \exp(K_c f_{evap}) \exp(\frac{ay(t)}{1-by(t)})$
	SIMPAR ADIOS-2	Vos (2005)	$\nu(t) = \nu_0 \exp(c_b(f_{evap}(0) - f_{evap}(t))) \exp(\frac{ay(t)}{1-by(t)}) \exp(\frac{c_T}{T_{oil}} - \frac{c_T}{T_0})$
	OWM	Vos (2005)	$\nu(t) = \nu_0 \exp(c_b(f_{evap}(0) - f_{evap}(t))) \exp(\frac{ay(t)}{100+by(t)}) \exp(\frac{c_T}{T_{oil}} - \frac{c_T}{T_0})$
	from the literature	Janeiro et al. (2008)	$\nu(t) = \nu_0 \exp(c_e f_{evap}(t)) \exp(\frac{ay(t)}{1-by(t)}) \exp(\frac{c_T}{T_{oil}} - \frac{c_T}{T_0})$

Table 2 Table of equation variables for each weathering process

Weathering Process	Variable	Definition/Value
Initial Release/ Spreading	R	computed spill radius
	V_{oil}	volume of spilled oil
	k_1	1.15
	k_2	1.45
	ρ_w	computed density of water
	ρ_{oil}	density of oil
	ν_w	computed kinematic viscosity of water
	g	9.80665 ms^{-2}
	X	length scale of spilled oil
	B	channel width
	U_{H2O}	water current speed
Dispersion	Q	entrained mass of water droplets
	d_{max}	maximum oil droplet diameter SIMPAR & ADIOS-2: d_{max} = 70 µm; OWM: $d_{max} = max(d_0)$
	d_o	oil droplet diameter OWM: $d_o = \frac{c\nu^{0.34}}{\sqrt{e}}$; $C=1000; e = 1000$
	Δd	interval that surrounds d_o per unit surface area per breaking event
	U_w	wind speed
	C_0	proportionality constant SIMPAR & ADIOS-2: $\nu <$ 125; $C_0 = 1827\nu^{0.04658}$ and if $\nu >$ 125; $C_0=1827\nu^{-1.1951}$ where ν is in cSt OWM: $C_0 = 4450\nu^{0.4}$
	T_w	wave period
	F_{wc}	fraction of sea surface hit by breaking waves
	S_{cov}	sea coverage factor of the oil spill
	D_{ba}	dissipative wave energy
Evaporation	f_{evap}	fraction evaporated
	C_d	air/sea drag coefficient
	K	mass transfer coefficient
	$Area$	surface area of the spill
	u_1	7; to define C_d in OWM
	u_2	20; to define C_d in OWM
	C	0.0323; to define C_d in OWM
	D	0.474; to define C_d in OWM
	A	4.8
	B	10.3
	API	API of the spilled oil
	T	sea surface temperature (SST)
	S	sea surface salinity
	C_1	10.3
	C_2	6.3
	T_{oil}, T_{air}	temperature of the oil (=SST); air temperature
	V_0	volume of initial spill
	T_0	Janeiro et al. (2008): $T_0 = 532.98 - 3.1295 \times API$
	T_g	Janeiro et al. (2008): $T_g = 985.62 - 13.597 \times API$

Weathering Process	Variable	Definition/Value
Emulsification	y	water content
	y_{max}	maximum water content: $y_{max} = 0.7$
	k_y	emulsification rate
	k_0	the emulsification rate for $y_{max}=1$ and zero wind: $k_0 = 2 \times 10^{-6}$
	$t_{1/2}$	half saturation time
	$U_{(t)}$	wind speed
Oil Density	c_1	SIMPAR and OWM: $c_1 = 0$ ADIOS-2: $c_1 = 8 \times 10^{-4}$
	c_2	SIMPAR and OWM: ADIOS-2: $c_2 = 0.18$
	T_{ref}	reference oil temperature: T_{ref} = SST at t= 0
Oil Viscosity	a	in Vos, SIMPAR and ADIOS-2: $a=2.5$ in Vos, OWM: $a=5$
	b	in Vos, SIMPAR and ADIOS-2: $b=0.654$ in Vos, OWM: $b=-2$
	c_T	5
	c_b	5
	ν_0	reference oil viscosity at t = 0
	c_e	If $\nu_0 > 38$, then $c_e=10$. Otherwise, $c_e = -0.0059\nu_0^2 + 0.4461\nu_0 + 1.413$
	K_c	4